COMPREHENSIVE DEFINITION OF SER/THR/TYR PHOSPHORYLATION IN MYCOBACTERIA: TOWARDS UNDERSTANDING REPROGRAMMING OF NORMAL MACROPHAGE FUNCTION BY PATHOGENIC MYCOBACTERIA

Kehilwe Confidence Nakedi

This thesis is submitted in fulfilment of the requirements for the degree of Doctor of Philosophy

Division of Chemical and Systems Biology

Department of Integrated Biomedical Sciences

University of Cape Town

June 2018

Supervisors: Professor Jonathan M Blackburn and Dr Nelson Da Cruz Soares

DECLARATION

I, Kehilwe C Nakedi, hereby declare that the work on which this dissertation/thesis is based is my original work (except where acknowledgements indicate otherwise) and that neither the whole work nor any part of it has been, is being, or is to be submitted for another degree in this or any other university.

I empower the university to reproduce for the purpose of research either the whole or any portion of the contents in any manner whatsoever.

Signature: ……Signed by candidate.

Date: …21 June 2018…….

Kehilwe Confidence Nakedi (B.sc, Bsc (Med) Hons, M. Med.Sc)

I dedicate this degree to my family. Thank you for understanding and supporting me in the pursuit of my dreams, even when that meant putting your plans on hold.

In Christ alone, I have found a source of peace.
Let my life be testament of God’s love and mercy

ACKNOWLEDGEMENTS

Professor Jonathan M Blackburn. My sincerest gratitude for taking a chance on me, coming from a completely different background and learning a new skill. I didn't know I could do it, most of the time I felt like I couldn't, but your door has always been opened, and it takes you only 5 seconds to come up with a solution to a problem I've been struggling with for days. But not only that, you also put people around me to help me on this new path. For that I'm grateful. Your wealth of knowledge always leaves me amazed. I can only hope to be half the scientist you are, and that would still be brilliant. Prof the way you come up with ideas on the spot is so beautiful to watch, also not so much because every time I leave our meeting I have another side project that you've convinced me it will take only a week to complete and I'd walk out feeling like it should be easy….. until I get to my desk. I cherish the fruitful discussions we've had, not only around my work, but from politics to life in general and you entertaining my very naïve thoughts. It has been such an honor to learn from you and watch you work. Thank you so much.

Dr Nelson Da Cruz Soares, words fail me. There are no words in the English dictionary that could express my gratitude to you. I don't even know how to start because it might just be a thesis on its own. Nelson I'm trying but all I can say right now is thank you. Thank you for being you. Thank you for your calmness and patience with me even when I didn't deserve it. There are so many things I'm grateful for and I feel privileged to have been your student. You have had a front row seat to all my emotional rollercoaster and meltdowns, and you calmly rationalized everything and came up with a plan to move forward. I am sincerely grateful for your supervision. You encouraged me when I needed it and also allowed me to be an independent thinker (I know you say I never listen to you), but its because of your supervision that I am able to be an independent scientist. I'm sincerely grateful.

The Blackburn Lab colleagues. Thank you for fruitful discussions. A special thank you to Dr Andrew Nel. Thank you, Andrew, for holding my hand and those late-night texts trying to optimise methods for my samples. Thank you for knowing where everything is in the lab. I am sincerely grateful. Alexander Giddey, they don't make 'em like you anymore and you know how grateful I am for your friendship and being such a good sounding board. I seriously don't think I would've survived in that lab without the both of you.

My village: It takes a village to complete this journey sane. Firstly, my prayer warriors. Karabo Kekana and Michelle Bristow, thank you ladies for praying with me and for me. Karabo, even when I wasn't the best of friend you would always check up on me and pray and encourage me. Your friendship and support means a lot to me and will cherish it always. Michelle, you've been holding my hand throughout my spiritual journey since our days in Durban. I thank you for always being there for me when I called you overwhelmed and you'd say just come over and a prayer and a glass or two of wine later I'm back to normal. My sincerest

gratitude. Secondly: The Doctors. In you ladies, I found sisters. Dr Aletta Rapuleng, 18 years later and you are still my person, my best friend. Dr Itu Tloubatla thank you friend for all those late-night calls and everything in between. Thank you, ladies, for the love, patience, unconditional support and riding this journey with me. And lastly my lab friends Sue and Zandi. You both know how much your friendship and support mean to me. Thank you.

SUMMARY / ABSTRACT

Mycobacterium tuberculosis, the causative agent for the disease Tuberculosis, is a serious public health problem that is responsible for 1.6 million deaths each year. The WHO's recent report on Tuberculosis estimates that a third of the world's population is latently infected with the bacteria, and, of those, 10% will progress to active disease. *M. tuberculosis* is a successful pathogen mainly due to its ability to adapt and survive in changing environments. It can survive a dormant state with limited metabolic activity during latent infection, while also being able to escape the macrophage and disseminate into active disease. Efforts to eradicate the disease must be based on understanding the biology of this organism, and the mechanisms it uses to infect, colonize, and evade the immune system. Understanding the behaviour of pathogenic mycobacteria in the macrophage is also important to the discovery of new drug targets. In this thesis, we employed state of the art mass spectrometry techniques, which allowed us to unpack the biology of this bacterium in different growth environments and expand our understanding of the mechanisms it employs to adapt and survive. We investigated protein regulation by the process of phosphorylation, through sensory kinases, which add a phosphate group to a protein of interest, thereby regulating its function. First, we interrogated the phosphoproteomic landscape between *M. bovis* BCG and *M. smegmatis* to explain how differential protein regulation results in the differences between slow and fast growth of mycobacteria. Second, we focused on Protein Kinase G (PknG), which plays an important role in bacterial survival by blocking phagosome/lysosome fusion. We identified the *in vivo* physiological substrates of this kinase in actively growing *M.bovis* BCG culture. Our results revealed that this kinase is a regulator of protein synthesis. We then examined the mechanisms of survival in murine RAW 246.7 macrophages mediated by PknG, using *M. bovis* BCG reference strain and PknG knock-out mutant. Our results indicated strong evidence that pathogenic

mycobacteria disrupt the macrophagic cytoskeleton, through phosphorylation of proteins that are involved in cytoskeleton rearrangement. These results explain the strategies that pathogenic mycobacteria employ mediated by PknG to block phagosome-lysosome fusion and evade the host immune system and survive for prolonged periods in the macrophages.

The findings of this thesis contribute to our understanding of the physiology of pathogenic mycobacteria and their interaction with the host.

Publications of this work:

Nakedi, K. C., Nel, A. J. M., Garnett, S., Blackburn, J. M., and Soares, N. C. (2015). Comparative Ser/Thr/Tyr phosphoproteomics between two mycobacterial species: the fast-growing *Mycobacterium smegmatis* and the slow growing *Mycobacterium bovis* BCG. *Front. Microbiol*. 6:237. doi: 10.3389/fmicb.2015.00237

Nakedi, K. C., Calder, B., Banerjee, M., Giddey, A., Nel, AJM., Garnett, S., Blackburn, J. M., and Soares, N. C. (2018). Identification of novel physiological substrates of Mycobacterium Bovis BCG Protein Kinase G (PknG) by label-free quantitative phosphoproteomics. *Mol Cell Proteomics*, doi:10.1074/mcp.RA118.000705

Conference presentations:

Poster Presentation: Post-translational Modifications, Tübingen, Germany 2014

Poster Presentation: Gordon Research Conferences: TB Drug Discovery, Barcelona, Spain 2015

Poster Presentation: H3D Drug Discovery Conference, Western Cape, South Africa

Oral and Poster Presentation: International Conference of Analytical Proteomics (ICAP), Lisbon Portugal 2017

Grants to support this work:

NRF Grants: 98963 and 95984

NRF Innovative PhD Scholarship

UCT/CSIR PhD Scholarship

IBMS Departmental PhD Bursary

TABLE OF CONTENTS

1. MYCOBACTERIAL KINASES: STRUCTURE, FUNCTIONS AND SUBSTRATES…1
1.1 Signaling biology…1
1.2 Eukaryotic signalling…2
1.3 Mycobacterium tuberculosis' kinases…3
1.4 Classes of STPKs…4
1.5 Structural studies of PknG…8
1.6 Mass spectrometry as a platform to study phosphorylation and identification of kinase substrates…10
1.6.1 Top-down phosphoproteomics…10
1.6.2 Bottom-up phosphoproteomics…11
1.6.3 Phosphopeptide enrichment techniques…14
1.6.4 Database search engines and Quantification of phosphopeptides…16
1.7 Statistical analysis of phosphoproteomic data…18
1.8 Targeted mass spectrometry in phosphoproteomics…19
1.9 Objectives of the thesis…22
2. MATERIALS AND METHODS…23
2.1 Bacterial strains…23
2.1.1 Culture conditions of bacterial strains…23
2.1.2 Harvesting of bacterial strains…23
2.1.3 Bacterial lysis…24
2.2 Eukaryotic cells culture…24
2.2.1 Culture conditions of RAW 247.6 macrophages…24
2.2.2 Splitting of macrophages…24
2.2.3 Checking for mycoplasma infection of macrophages…25
2.2.4 Infection of Macrophages with *M. bovis* BCG…25
2.2.5 Harvesting and lysis of eukaryotic cells…25
2.3 Biochemical methods…26
2.3.1 Chloroform-methanol precipitation…26
2.3.2 Protein quantification…26
2.3.3 In-solution digestion…27
2.3.4 Peptide clean-up…27
2.3.5 Phosphopeptide enrichment…27
2.3.6 LC-MS/MS…28
2.3.7 Targeted Mass Spectrometry (PRM)…29

2.3.8 Kinase-substrate interactions....29

3. COMPARATIVE SER/THR/TYR PHOSPHOPROTEOMICS BETWEEN TWO MYCOBACTERIAL SPECIES: THE FAST-GROWING *MYCOBACTERIUM SMEGMATIS* AND THE SLOW GROWING *MYCOBACTERIUM BOVIS* BCG....31

3.1 Introduction....33

3.2 Aims:....34

3.3 Results:....35

3.3.1 Data quality....35

3.3.2 Phosphorylation frequency between two mycobacterial species....38

3.3.3 Tyrosine phosphorylation in mycobacteria....39

3.3.4 Functional characterization and localization of phosphoproteins....41

3.3.5 Sequence alignment of all identified phosphopeptides....45

3.4 Discussion....46

3.5 Conclusion and perspectives....52

4. IDENTIFICATION OF PHYSIOLOGICAL SUBSTRATES OF *M. BOVIS* BCG PROTEIN KINASE G (PKNG) IN ACTIVELY GROWING CULTURE BY LABEL-FREE MASS-SPECTROMETRY BASED PHOSPHOPROTEOMICS....53

4.1 Introduction....54

4.2 Aims:....55

4.3 Results....56

4.3.1 Growth monitoring of bacterial strains....56

4.3.2 Identification of physiological substrates for PknG....58

4.3.3 Global phosphorylation changes resulting from PknG gene knock-out 60

4.3.4 Validation of candidate substrates by Targeted Mass Spectrometry. 66

4.3.5 Kinase-substrate Interactions....67

4.3.6 Functional and spatial relationships of candidate substrates....70

4.4 Discussion....72

4.5 Conclusions....76

5. IDENTIFICATION OF THE HOST MACROPHAGE SUBSTRATES PHOSPHORYLATED BY *M. BOVIS* BCG PROTEIN KINASE G (PKNG): REPROGRAMMING NORMAL MACROPHAGE FUNCTIONS....77

5.1 Introduction....78

5.2 Aims:....79

5.3 Results:....80

5.3.1 Experimental design....80

5.3.2 Phosphoproteomic changes in the host’s macrophages mediated by PknG 82

5.3.3 Functional annotation of host's proteins under the regulation of PknG 89
5.3.4 Network analysis and visualization of candidate substrates of PknG 90
5.4 Discussion 92
5.5 Conclusions and future perspectives 102
6. THESIS SUMMARY AND GENERAL CONCLUSIONS 104
7. REFRENCES 106
8. APPENDICES 140

LIST OF FIGURES:

FIGURE 1-1. SEQUENCE ALIGNMENT OF M. TUBERCULOSIS STPKS PERFORMED BY AV-GAY'S TEAM USING CLUSTAL W. THE FIGURE SHOWS THE CONSERVED RESIDUES WITHIN THE CATALYTIC SITE (BETWEEN 156 AND 202 RESIDUES) OF THESE KINASES [22] .IN THE BOTTOM PANEL, RED AND YELLOW COLOURS REPRESENT 100% AND 75-95% RESPECTIVELY.....3
FIGURE 1-2: PKNG ORGANISATION SHOWING THE 750 RESIDUES AND ALL THE DOMAINS WITH DIFFERENT FUNCTIONS.....8
FIGURE 1-3: CHEMICAL STRUCTURE OF THE INHIBITOR AX20017 BOUND TO THE KINASE DOMAIN OF PKNG (RIBBON REPRESENTATION) RESOLVED BY X-RAY CRYSTALLOGRAPHY NICOLE SCHERR ET AL. PNAS 2007;104:12151-12156.....9
FIGURE 1-4: SCHEMATIC DIAGRAM OF AN ANALYTE GOING THROUGH A TRIPLE QUADRUPLE INSTRUMENT. (LANGE ET AL., 2008). IONS ARE SEPARATED BASED ON THEIR POLARITY AND STABILITY AND TRAVEL THROUGH THE QUADS VIA A VOLTAGE. SELECTION OF DIFFERENT RADIO FREQUENCY (RF) VOLTAGES ALLOWS FOR SEPARATION OF IONS WITH M/Z COMPATIBLE TO THAT VOLTAGE TO TRAVEL THROUGH Q1, THAT WAY ONE CAN CHOOSE A VOLTAGE THAT WILL SCAN THE PEPTIDES OF INTEREST IN AN MRM RUN. Q2 ACTS AS A COLLISION CELL BY FRAGMENTING THE PRECURSOR ION WITH A GAS, AND THE RESULTANT FRAGMENT ION IS SELECTED IN Q3 WHERE IS CONVERTED INTO A MASS SPECTRUM.....21
FIGURE 3-1: SAMPLE LOADING VOLUMES OPTIMISED TO YIELD TIC COMPARABLE BETWEEN SAMPLES. ALL SAMPLES WERE PILOTED AND THE VOLUME NEEDED TO ACHIEVE A DESIRED TIC IN EACH SAMPLE WAS CALCULATED FROM THE INITIAL VOLUME THAT OBTAINED THE TIC AND RELOADED ONTO THE LC/MS/MS WITH THE NEW VOLUME USING THE FORMULA: SAMPLE VOLUME = VOLUME LOADED X TIC OBTAINED/TIC DESIRED.....35
FIGURE 3-2: DIGESTION EFFICIENCY MONITORED BY THE NUMBER OF MISSED CLEAVAGES (MC) PER EXPERIMENT.....36
FIGURE 3-3: DATA QUALITY: MASS ERROR ACROSS SAMPLES IN BOTH M.SMEGMATIS AND M.BOVIS BCG PHOSPHO EXPERIMENTS.....36
FIGURE 3-4: MANUAL VALIDATION OF PHOSPHOPEPTIDES WITH MAXQUANT "VIEWER". PHOSPHORYLATION OF M. BOVIS BCG CELL DIVISION FTSQ (THR24) AND PROBABLE CONSERVED PROTEIN MEMBRANE MMPS3 (TYR70. TOP: FRAGMENTATION SPECTRA FOR MODIFIED PEPTIDE BEARING THE PHOSPHORYLATED THR24. BOTTOM: FRAGMENTATION SPECTRA FOR MODIFIED PEPTIDE BEARING THE PHOSPHORYLATED TYR_{70}.....37
FIGURE 3-5: DISTRIBUTION OF IDENTIFIED PHOSPHOSITES AFTER APPLYING FILTERS IN BOTH SPECIES OF MYCOBACTERIA. M. SMEGMATIS

HAS A THIRD OF PHOSPHORYLATED RESIDUES COMPARED TO PATHOGENIC MYCOBACTERIA IN ACTIVELY GROWING CULTURES (A). M. BOVIS BCG'S PHOSPHORYLATION LANDSCAPE (B) IS COMPARABLE TO THAT OF M. TUBERCULOSIS.....38
FIGURE 3-6: SEQ2LOGO ALIGNMENT ANALYSIS DERIVED FROM 60 KDA CHAPERONIN REVEALED AN OVERREPRESENTATION OF TYR358. SEQ2LOGO ANALYSIS INDICATE THAT A CONSERVED TYR358-360 IS FOUND IN ADDITIONAL THREE PATHOGENIC SPECIES, SPECIFICALLY SHIGELLA SPP, KLEBSIELLA SPP AND SALMONELLA SPP.....41
FIGURE 3-7: A HISTOGRAM SHOWING THE GO MOLECULAR FUNCTIONS OF IDENTIFIED PROTEINS AND PHOSPHOPROTEINS AS PREDICTED FROM THEIR RESPECTIVE GENOME ANNOTATIONS.....44
FIGURE 4-1: (A) GROWTH CURVES MEASURED BY OD600 OF THE M.BOVIS BCG STRAINS USED IN THIS STUDY IN NUTRIENT RICH 7H9 MEDIA. BOTH THE WT AND THE PKNG KNOCK-OUT MUTANTS HAD COMPARABLE GROWTH RATES. THIS IS IN LINE WITH WHAT HAS BEEN PREVIOUSLY OBSERVED IN LITERATURE. (B) PKNG PEPTIDE (INSFGYLYG) IDENTIFIED EXCLUSIVELY IN THE WILD TYPE M.BOVIS BCG AND UNAMBIGUOUSLY ABSENT IN THE PKNG KNOCK-OUT MUTANT BY PRM ANALYSIS.....57
FIGURE 4-2: SCHEMATIC PRESENTATION OF EXPERIMENTAL PROCEDURES: EXPONENTIALLY GROWING CELLS OF M. BOVIS BCG REFERENCE STRAIN AND PKNG KNOCK-OUT MUTANTS WERE LYSED AND PROTEINS PRECIPITATED AND DIGESTED WITH TRYPSIN. PHOSPHOPEPTIDES WERE ENRICHED FOR WITH TIO2 AFTER DIGESTION, FOLLOWED BY LIQUID-CHROMATOGRAPHY TANDEM MASS SPECTROMETRY (LC/MS/MS). MS DATA WAS MATCHED TO M.BOVIS BCG USING MAXQUANT SOFTWARE AND DOWNSTREAM STATISTICAL ANALYSIS ON PERSEUS. CANDIDATE SUBSTRATES WERE VALIDATED BY PRM AND ANALYSED IN SKYLINE SOFTWARE.....58
FIGURE 4-3: FRAGMENTATION SPECTRA OF THE PHOSPHOPEPTIDE SHOWING BOTH B- AND Y-IONS OF THE PHOSPHORYLATED PEPTIDE FROM ONE OF THE CANDIDATE SUBSTRATE CHAPERONE PROTEIN CLPB 59
FIGURE 4-4: A PROFILE PLOT OF THE DATA OVERVIEW BEFORE AND AFTER PAIRWISE NORMALIZATION. THE TOP PANEL SHOWS THE HIGH VARIABILITY OF PHOSPHOPEPTIDES BETWEEN SAMPLES AND THE BOTTOM PANEL SHOWS THE DATA AFTER RESCALING USING THE MEDIAN OF THE PHOSPHOPEPTIDES IN AN UNENRICHED SAMPLE UNAFFECTED BY THE ENRICHMENT TECHNIQUE.....60
FIGURE 4-5: VALIDATION OF IDENTIFIED PHOSPHOPEPTIDES BY TARGETED PRM'S. THE TOP FIGURES (A-C) SHOWS PHOSPHOPEPTIDES THAT WERE EXCLUSIVELY IDENTIFIED IN THE WILD TYPE M.BOVIS BCG AND NOT IN THE PKNG KNOCK-OUT MUTANT (A: A0A0H3M7J9 B: A1KML3 C: A1KI28), WHILST FIGURE D-F SHOWS DIFFERENTIAL

PHOSPHORYLATION OF THE SUBSTRATES OF PKNG (D: A0A0H3M0X2 E: A1KMQ3 F: A0A0H3M751).....66
FIGURE 4-6: PHOSPHORYLATION SITE MOTIF ANALYSIS GENERATED USING ICELOGO. SHOWING OVERREPRESENTED AMINO ACIDS AROUND THE PHOSPHORYLATION SITE.....67
FIGURE 4-7: (A) PKNG BINDING WITH (PDB ID: 4Y0X) WITH GARA. PKNG CHAIN IN GRAY COLOUR AND GARA PEPTIDE IN PINK. THE THREONINE RESIDUE NEAR TO THE CATALYTIC RESIDUES SHOWN AS BALL AND STICK MODEL. THE □- HYDROXYL GROUP IS WITHIN HYDROGEN BONDING DISTANCE OF HYDROGEN DISTANCE OF CARBOXYL GROUP OF ASP211. **(B-E)** SHOWS THE INTERACTION OF THE HIGH CONFIDENCE SUBSTRATES WITH THE CATALYTIC CORE OF PKNG.....69
FIGURE 4-8:FUNCTIONAL CATEGORIES OF ALL IDENTIFIED CANDIDATE SUBSTRATES OF M.BOVIS BCG PKNG. THE MOST REPRESENTED FUNCTIONAL CATEGORIES ARE TRANSLATION, ATP BINDING, BIOSYNTHESIS AND ANTITOXIN.....71
FIGURE 5-1 WALBURGER RESULTS OF INTRACELLULAR SURVIVAL DYNAMICS OF M. BOVIS BCG WILD TYPE COMPARED TO THE PKNG KNOCK-OUT MUTANT. ELECTRON MICROSCOPY LOCALIZATION OF MACROPHAGE HARBOURING BOTH STRAINS OF M. BOVIS BCG TWO HOURS POST-INFECTION. **ANNE WALBURGER ET AL. SCIENCE 2004;304:1800-1804** [36]**.**.....81
FIGURE 5-2: DATA QUALITY: SAMPLE LOADING VOLUMES NORMALIZED TO OBTAIN TIC (TOTAL ION CHROMATOGRAMS) FOR EACH REPLICATE ON THE MS.....83
FIGURE 5-3: DISTRIBUTIONS OF LOCALIZATION PROBABILITY AND PEP VALUES OF HIGHLY CONFIDENT PHOSPHOPEPTIDES IDENTIFICATIONS. THE MAJORITY OF PHOSPHOPEPTIDES HAD A LOCALIZATION PROBABILITY OF > 0.75 AND PEP VALUES OF <0.01.....84
FIGURE 5-4: GO-TERM ENRICHMENT ANALYSIS OF CANDIDATE MACROPHAGIC SUBSTRATES OF PKNG USING PANTHER ONLINE BIOINFORMATIC TOOL HIGHLIGHTS PKNG'S ABILITY TO PHOSPHORYLATE KEY CELLULAR FUNCTIONS INCLUDING ORGANELLE MIGRATION AND LOCALIZATION.....89
FIGURE 5-5:NETWORK INTERACTION ANALYSIS FROM STRING DATABASE. THE NODES REPRESENT PHOSPHORYLATED PROTEINS, THE EDGES REPRESENT CONNECTIONS. THE RED AND BLUE COLOUR REPRESENT PROTEINS INVOLVED IN CELLULAR ORGANIZATION GO BIOLOGICAL TERM.....91
FIGURE 5-6: WEBLOGO OF IDENTIFIED PKNG SUBSTRATES.....91
FIGURE 5-7: A SCHEMATIC FIGURE SHOWING SUBSTRATES PHOSPHORYLATED IN THE PRESENCE OF PKNG AND A SUMMARY OF ACTIN POLYMERIZATION SIGNALLING PATHWAYS THAT THE KINASE MAY INTERFERE.....93

LIST OF TABLES:

TABLE 3-1: LIST OF TYROSINE PHOSPHORYLATED PROTEINS/SITES IDENTIFIED IN M. BOVIS BCG AND M.SMEGMATIS.....40
TABLE 3-2: SUMMARY OF THE PHOSPHORYLATED SITES FOUND IN MORE THAN ONE MYCOBACTERIAL SPECIES.....42
TABLE 4-1:DIFFERENTIALLY PHOSPHORYLATED PROTEINS BETWEEN WT M.BOVIS BCC AND PKNG KNOCK-OUT MUTANT.....62
TABLE 4-2: CANDIDATE SUBSTRATES OF PKNG ONLY PHOSPHORYLATED IN WT M.BOVIS BCG. KNOWN PKNG SUBSTRATES GARA AND L13 WERE NOT IDENTIFIED IN THIS CHAPTER, HOWEVER, WERE INCLUDED IN THE ANALYSIS FOR COMPARISON PURPOSES.....64
TABLE 5-1:A SUMMARY OVERVIEW OF DATA QUALITY.....82
TABLE 5-2:LIST OF HOST'S SUBSTRATES PHOSPHORYLATED BY M. BOVIS BCG PKNG AS DETERMINED BY LABEL-FREE PHOSPHOPROTEOMICS. .85

LIST OF ABBREVIATIONS

ABC	Ammonium bicarbonate
ACN	Acetonitrile
ARP	Actin related protein
ATP	Adenosine triphosphate
BCG	Bacille Calmette Guérin
BSA	Bovine serum albumin
cdc42	Cell division control 42
CID	Collision Induced Dissociation
CLIPs	Cytoplasmic Linker Proteins
CRIB	Cdc42/Rac Interactive Binding motif
DDNL	Data Dependent Neutral Loss
DHB	2.5 di-hydroxybenzoic acid
DIA	Data Independent Acquisition
DMEM	Dulbecco's Modified Eagle's medium
DOCK-8	Dedicator of Cytokinesis 8
DTT	Dithiothreitol
ECM	Extracellular matrix
EDTA	Ethylendiamine tetraacetate
ESI	Electrospray ionisation
ETD	Electron Transfer Dissociation
FA	Formic acid
FAK	Focal Adhesion Protein
FCS	Foetal calf serum
FDR	False discovery rate
FHA	Fork Head Associated domains
GEFs	Guanine Nucleotide-exchange Factors
GO	Gene ontology
GRB2	Growth factor receptor-bound protein 2

HCD	High Collision Dissociation energy
HILIC	Hydrophilic Interaction Chromatography
IAA	Iodoacetamide
IMAC	Immobilized Metal Affinity Chromatography
IP	Immunoprecipitation
IRF	IFN regulatory factor
iTRAQ	Isobaric Tags for Relative and Absolute Quantification
LC	Liquid chromatography
LC-MS-MS	Liquid chromatography coupled to tandem mass spectrometry
LFQ	Label-free quantification
M. smegmatis	*Mycobacterium smegmatis*
M. tuberculosiss	*Mycobacterium tuberculosis*
m/z	Mass-to-charge ratio
MALDI	Matrix assisted laser desorption ionisation
MAPK	Mitogen Activated Protein Kinase
MDR	Multi drug-resistant (strains)
MeOH	Methanol
MRM	Multiple Reaction Monitoring
MS	mass spectrometry
MT	Microtubule
MTOC	Microtubule Organizing Centre
NaCl	Sodium chloride
NPF	Nucleation-Promoting Factor
OADC	Oleic acid, albumin, dextrose and catalase supplement
OD	Optical density
PAMP	Pathogen-associated molecular patterns
PBS	Phosphate buffered saline
PEP	Posterior Error Probability
Pi3K	Phosphoinositol-3-kinase
PknG	Protein Kinase G
PRM	Parallel Reaction Monitoring
PSM	Peptide Spectrum Matching

PTM	Post-translational modifications
PTP-PEST	Tyrosine-protein phosphatase non-receptor type 12
Ptps	phosphatases
Rho	RAS Homolog Family Member
RhoA	RAS Homolog Family Member A
RhoGAP	Rho GTPase activating proteins
RhoGDI	Rho GDP dissociation inhibitor
ROS	Reactive Oxygen species
SCX	Strong Cationic Exchange
SDS	Sodium dodecyl sulphate
Sept	Septin
Ser/Thr/Tyr	Serine/Threonine/Tyrosine
SH-P1	Tyrosine-protein phosphatase non-receptor type 6
SILAC	Stable isotope labelling by amino acids in cell culture
SRM	Selected Reaction Monitoring
STAGE tips	Stop and Go Extraction Tips
STPKs	Serine/Threonine Protein Kinases
TB	Tuberculosis
TIC	total ion chromatogram
TiO_2	Titanium Dioxide
TMT	Tandem Mass Tag
TPR	Tetratricopeptide repeat
Tris-HCl	Tris(hydroxymethyl)aminomethane - hydrochloric acid
UHPLC	Ultra-high pressure HPLC
WASP	Wiskott–Aldrich syndrome protein
WT	Wild type

1. MYCOBACTERIAL KINASES: STRUCTURE, FUNCTIONS AND SUBSTRATES

1.1 Signaling biology

Post-translational modifications (PTMs) by protein phosphorylation/dephosphorylation represent a central mechanism for specific signal transduction in various cellular processes, via sensor kinases and phosphatases present on the bacterial membrane and cytosol. These PTMs enable the bacterium to adapt, and therefore survive, in hostile host conditions [1]. The role of kinases in signal transduction is ubiquitous. During the process of infection, phosphorylation of proteins on hydroxyl amino acids occurs at different stages, catalysed in a reversible fashion by specific protein kinases and phosphatases that belong to either the invading bacterial cells or the infected eukaryotic host cells.

Protein kinases are a family of well-characterised enzymes that mediate the intracellular response to extracellular stimuli [2], thereby regulating developmental changes and host-pathogen interactions. All protein kinases characterised so far fall into two broad categories based on similarities and enzymatic specifications, namely: the serine/threonine (Ser/Thr) and tyrosine-specific kinases superfamily [3] and the histidine kinase superfamily (two component system), which auto-phosphorylates conserved histidine residues (Stock et al,. 1989). Both classes of kinases have a short stretch of amino acids that can be used to predict whether the putative kinase will phosphorylate serine/threonine or tyrosine residues [3].

Their catalytic domain (approximately 30 kDa) lies on the carboxyl terminus in most single subunit enzymes, while in those with multiple subunit structure, subunit polypeptides consisting almost entirely of catalytic domain are common.

1.2 Eukaryotic signalling

In eukaryotes, the backbone of signal transduction pathways occurs via serine/threonine protein kinases (STPKs) and phosphatases (Ptps). Phosphorylation by these kinases results in phosphorylated serine, threonine and tyrosine residues. STPKs catalyse the transfer of gamma-phospho ATP, by binding the ATP phosphate donor as a complex with either magnesium or manganese to the receptor hydroxyl group (Hunter et al. 1995). The resulting negative charge from the phosphate group can cause changes in the conformation of the phosphorylated protein, which can lead to significant changes in the protein's function and activity. Recent studies have revealed that some bacteria and archaea also possess these Hanks-type STPKs [5–15]. These are involved in pathogenicity, stress response and regulation of development in bacteria [15–21], generally via signalling within the bacterial cells.

Amino acid alignment of these STPKs has revealed 15 conserved residues within their catalytic domain (between 150 and 200 amino acid residues) (**Figure 1.1**). This catalytic site is where the substrate is bound, in the presence of ATP and a divalent cation like Mg^{2+}, and a phosphate group is attached to the residue on the substrate. ADP is then released, and the phosphorylated protein is unbound from the kinase [3,4]. PknM (Rv3576) was eliminated as a Ser/Thr kinase since its catalytic site didn't possess this fingerprint used to define STPKs [22]. The STPKs may have evolved in different bacteria while they were adapting to different conditions, even though the genes have the same common ancestry [23], or alternatively, these genes may have been acquired through horizontal gene transfer from eukaryotes to prokaryotes [24]. A recent publication by Stancik and colleagues proposed the omission of the term eukaryotic-like kinases[25]. They argued that they did not find any evidence of horizontal gene transfers and all

the bacterial kinases have a common evolutionary origin in the lineage leading to the last universal common ancestor (LUCA).

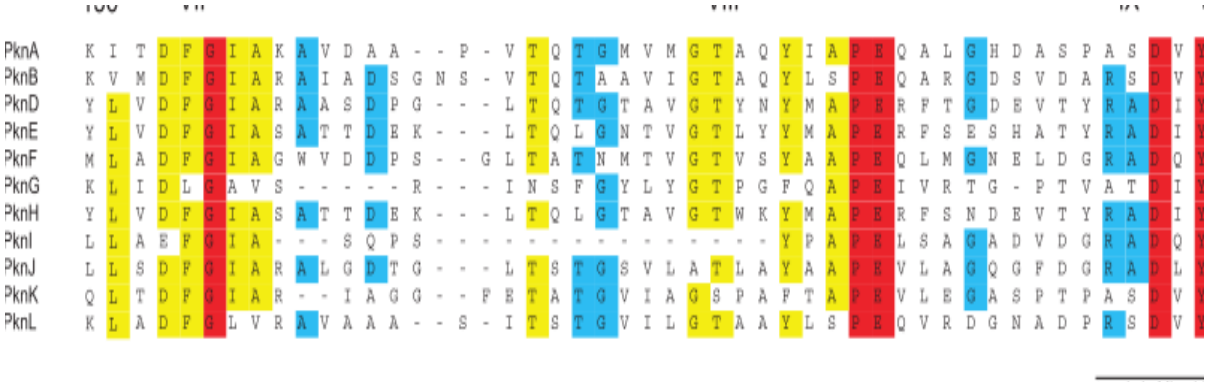

Figure 1-1. Sequence alignment of M. tuberculosis STPKs performed by Av-Gay's team using Clustal W. The figure shows the conserved residues within the catalytic site (between 156 and 202 residues) of these kinases [22] *.The red and yellow colours represent 100% and 75-95% respectively.*

1.3 Mycobacterium tuberculosis' kinases

Signalling in mycobacteria occurs through both the two-component system and STPKs. Early sequencing studies of the genome of *Mycobacterium tuberculosis* (*M. tuberculosis*) revealed a family of 11 Hanks-type STPKs and four phosphatases, and Av-gay and colleagues first showed their functionality in *M. tuberculosis* by identifying six phosphorylated proteins *in vitro* [16,26,27]. The 11 Hanks-type STPKs share about 30% sequence similarity with their human homologs [28]. Most are receptor-like trans-membrane proteins, with the kinase domain located inside the bacterial cell wall, except two (PknG and PknK), which are soluble (Av-Gay et al., 2000). Up until the work published by Chow, it was assumed that tyrosine phosphorylation was not supported by *M. tuberculosis*, however, Chow and several subsequent studies, including work published by our laboratory, support the fact that *M. tuberculosis* does make use of tyrosine phosphorylation [17,29–35]. *M. tuberculosis* has the same number of STPKs as histidine kinases, while other Mycobacteria have a higher number of STPKs (Narayan et al., 2007). *M. tuberculosis* use Hanks-type STPKs to regulate intracellular metabolic pathways, including cell division and molecular transport, but also to interfere with the host's signalling mechanisms [16,18,21,36–40]. The

significance of these *M. tuberculosis* STPKs in pathogenesis and their contribution to survival within macrophages is poorly understood. Understanding the role of these protein kinases and phosphatases would give us an important insight into the regulation of the signalling underpinning host–pathogen interactions. The function of these STPKs depends solely on the substrates they phosphorylate *in vivo*. In this chapter, we summarized the current knowledge of the 11 Hanks-type STPKs of *M. tuberculosis.*

1.4 Classes of STPKs

Sequence alignment of these STPKs revealed that 15 residues are conserved throughout this family, and these kinases were therefore grouped into three groups based on their sequence similarities for discussion below [22].

Group I: PknA, PknB, PknD

These kinases play an important role in viability of mycobacteria. PKnA and PknB are expressed during exponential growth of mycobacteria and are essential for growth and cell division. Gene-knockout studies of PknA and PknB resulted in death of mycobacteria [18], making them attractive targets for drug discovery. Both *pkn*A and *pkn*B genes reside on the same operon, which controls the switch between peptidoglycan elongation and septum formation in other bacteria like *E. coli* [41]. Sequencing studies have shown that the gene *mstp*, encoding mycobacterial Ser/Thr phosphatase (Mstp), a trans-membrane protein, is on the same gene cluster as *pkn*A and *pkn*B, and other genes involved in cell biosynthesis [27]. Chopra *et al.* in 2003 showed that Mstp dephosphorylates phosphorylated PknA and PknB, suggesting that this phosphatase is involved in regulating mycobacterial cell division [38]. PknA is involved in the regulation of morphological changes during cell division by phosphorylating and regulating Wag31, which induces an irregular phenotypic shape and unbalanced septum formation [40,42,43]. The structure of PknB revealed that the catalytic domain displays autophosphoryation properties, while the extracellular domain has 68 amino acid repeats that are characteristic of penicillin binding proteins, further supporting its function in cell wall synthesis [44]. Its known substrate is Rv20020c, an FHA domain contain protein with an unknown function [45]. PknD is essential for growth and cell division. The gene coding for PknD, *pkn*D, lies on the same

operon as *pstS,* which codes for a component of a phosphate-uptake system, suggesting that PknD could also be involved in the regulation of phosphate transport [22].

Group II: PknE, PknF and PknH

The genes coding for PknE and PknF lie on the same operon as an ATP-binding cassette (ABC) transporter gene (Rv1747), which suggests a possible regulatory role of this transport system [46]. ABC transporters are translocators that are responsible for the uptake and export of molecules across the cell membrane, in a process coupled to ATP hydrolysis. The physiological role of PknE is to mediate the survival of *M. tuberculosis* intracellularly by supressing apoptosis during nitrogen stress [47]. In 2014, Parandhaman and co-workers carried out a study to decipher the influence of the gene *pkn*E on intracellular signalling and on the outcome of HIV/TB co-infection. They infected a human macrophage cell line with *M. tuberculosis* wild type strain expressing *pkn*E or a *pkn*E knock-out mutant. Their results indicated that *pkn*E influences the crosstalk between the mitogen activated protein kinase (MAPK) cascades to regulate inflammation and HIV/TB co-infection. In the mutant strains, MAPK was not phosphorylated, while there was increased phosphorylation in the wild-type infected samples [48].

PknF is a 460-amino acid transmembrane kinase that is activated through autophosphorylation of Ser/Thr residues, and this autophosphorylated protein interacts with the ABC transporter. Rv1747 possesses two fork head associated domains (FHAs) and a phosphopeptide recognition domain with a 55- to 75-amino-acid homologous region that mediates specific phosphorylation-dependent protein–protein interactions, which suggests that the function of Rv1747 is regulated through phosphorylation [49–51]. Molle and colleagues

investigated the relationship between PknF and Rv1747 using an *in vitro* kinase assay, since the genes coding for both PknF and Rv1747 are adjacent on the chromosome, and there is a strong suggestion of cross-regulation of the two proteins [52]. Their results demonstrated that recruitment and phosphorylation of Rv1747 depends on the interaction between its two non-redundant FHA domains and the autophosphorylated form of PknF. These results suggest that PknF is autophosphorylated on two different residues that will allow the kinase to phosphorylate the two FHA domains of Rv1747 simultaneously. This study was important in unlocking the role that kinases play in transporting nutrients into the cell.

The physiological role of PknF was investigated by Deol and co-workers using an antisense strategy with *M. tuberculosis* expressing PknF and its kinase mutant in non-pathogenic *M. smegmatis* [53]. Immunoblotting experiments have shown that PknF is absent in *M. smegmatis*. Expression of PknF in *M. smegmatis* resulted in reduced growth rate and in deformed cell morphology. They observed an increase in glucose uptake compared to that of the wild type strain by analysing the uptake of ^{3}H- and ^{14}C-labeled substrates in the anti-sense *M. tuberculosis* strain. The authors concluded that PknF plays a regulatory role in the transport of glucose, as well as cell growth, and septum formation and elongation[21].

PknH controls the expression of a variety of cell wall-related enzymes, and plays a role in virulence [37]. Papavinasasundaram and colleagues infected mice with pknH knockout strains of *M. tuberculosis* and found that the mutant strain was hyper virulent and showed greater resistance to acidified-nitrite treatment, suggesting that PknH might be involved in the control of *M. tuberculosis* growth in the presence of nitric oxide. They treated both the wild-type and the knockout PknH mutants with ethambutol, and found that, in the wild-type strain, PknH induces the expression of a set of genes within the *emb*CAB and *ini*ABC operons [54]. The knock-out mutant failed to produce this response. This suggests that PknH regulates signalling cascade-mediated proteins involved in cell wall biosynthesis. In 2007, the same authors predicted that PknH could phosphorylate several substrates controlling different metabolic and physiological pathways. They identified 40 potential substrates using a bioinformatics approache, and two

substrates were found to be phosphorylated by recombinant PknH *in vitro*: Rv0681, a transcriptional regulatory protein, and DacB1, a penicillin binding-protein [55]. The mycobacterial transcription factor regulator in cell wall biosynthesis, EmbR, is another known substrate of PnkH [56]. Embr is an FHA domain-containing protein, and mutations in the FHA domain results in inhibition of phosphorylation, leading to the conclusion that this domain facilitates PknH phosphorylation of Embr [56].

Group III: PknK, PknL and PknG

PknK is a predicted secreted kinase. It lacks the transmembrane domain but has been found in the culture supernatant of *M. tuberculosis*. Its role in the intracellular survival of the bacteria and localization was first demonstrated by Malhorta and colleagues a few years ago [57]. They found that, in human macrophages obtained from peripheral blood of healthy volunteers infected with *M. tuberculosis*, the expression of PknK was increased 18 hours post infection. Their results implied that PknK expression correlated with driving the bug into a slow growing, non-replicating state which is more resistant to acidic stress and hypoxia during persistent infection in a mouse model. They also showed that PknK modulate host pro-inflammatory cytokines early on in the mouse model infected with *M. tuberculosis* mutant lacking *pkn*K gene. IFN-γ, IL-12 was downregulated whilst TNF-α was significantly upregulated [57]. The same authors later described the mechanism of survival and host modulation mediated by PknK. Through overexpression of the kinase in *M. smegmatis*, it was demonstrated that PknK activation is through autophosphorylation, and the active kinase then regulates the expression of growth factors dependent on the growth phase of the bacteria [58].

PknL is a 43KDa transmembrane kinase with 399 amino acid residues. Most STPK’s have a Lysine on the active site, except for PknL, which has an Asparagine on its active site, but studies have shown that it has kinase activity and other conserved residues characteristic of mycobacterial kinases [22,59]. It is thought to play a role in virulence and pathogenicity due to its homologue present in pathogenic *Mycobacterium leprae*. A recent study that demonstrated the role

that PknL plays in survival of pathogenic mycobacteria under stress was carried out by Refaya and colleagues [60]. Their results showed that the wild type strain had better growth kinetics at lower pH (5.5) than the mutant lacking the kinase. These findings demonstrate that PknL drives the bacteria into a slow, non-replicating state in acidic conditions inside the phagolysosome as a means to adapt and ultimately cause disease.

PknG is a multi-domain 80kDa protein with 750 amino acid residues. It lacks a trans-membrane domain and, therefore, predicted to be a cytosolic protein [53]. It has a Rubredoxin (Rdx) domain 99 residues from its N-terminus containing two characteristic CXXC motifs. This Rdx domain gives rise to the deep substrate binding cleft of the kinase, through its tight association with the small lobe of the kinase domain. The Rdx domain has high affinity to metal binding, making it a possible redox-dependent regulator [61]. PknG also has Tetratricopeptide repeat (TPR) at residue 405 in the C-terminus (**Figure 1.2**). Knock-out studies of the TPR domain did not have any effect on the activity of the kinase [62]. The *PknG* gene lie on the same operon as *glnH* gene encoding a glutamine binding protein. PknG has been shown to play a role in glutamate metabolism under nitrogen deficient conditions through phosphorylation of GarA, this ties in with the hypothesis that both *pknG* and *glnH* transcription is upregulated at the same time in nitrogen limited media [37].

PknG is secreted via secA2 secretion [63], and its role during survival in the vacuole was described by Walburger and colleagues [36]. Macrophages were infected with *M.bovis* BCG Wt, and a mutant lacking the *pkn*G gene s. Using confocal microscopy, Walburger *et al* observed that the mutant lacking the *pkn*G gene was trafficked to the phagolysosome, whilst the wild-type strain was localised in the phagosome. To further validate these findings, they overexpressed *M. tuberculosis* p*kn*G into non-pathogenic soil mycobacteria *M. smegmatis* and repeated the experiment. The results proved the role of PknG in survival when *M. tuberculosis* PknG was localized in the vacuole, while the wild type was localized in the phagolysosome. The task now is to find the exact mechanism of survival mediated by PknG, by identifying host substrates phosphorylated by this kinase, since the function of kinases are dependent on the substrates they phosphorylate. In culture, the known functions of PknG are

biofilm growth regulation through phosphorylation of its substrate ribosomal protein L13 [64], as well as intrinsic resistance to first-line TB drug Rifampicin [65].

Figure 1-2: PknG organisation showing the 750 residues and all the domains with different functions

1.5 Structural studies of PknG

Structural studies of these STPKs, which is the first step in understanding kinase substrate relationships, have advanced rapidly in recent years. A few STPK x-ray crystal structures have been resolved [61,62,66,67]. These structural studies have revealed mechanisms of kinase activation and substrate specificity for these kinases. The conversion of an inactive kinase to an active kinase involves conformational changes in the protein that lead to the correct disposition of substrate binding and catalytic groups and relief of steric blocking to allow access of substrates to the catalytic site[68]. The structures of active kinases display a similar conformation in key regions involved in ATP and protein substrate recognition, but the structures of inactive kinases show considerable differences in their ATP binding sites. The activation segment, a region ranging between 19 to 32 residues at the centre of the kinase domain, plays a crucial role in activation of most kinases, in substrate recognition and in promoting the correct environment for the catalytic residues[69].

Scherr and colleagues first resolved the structure of PknG in complex with a low molecular weight inhibitor, AX20017, by x-ray crystallography (**Figure 1.3**). The crystallized structure of PknG revealed the deep kinase binding cleft that the inhibitor binds to, thereby targeting the active conformation of the kinase domain [61]. Lisa and colleagues' work is interesting because they revealed the mechanisms by which PknG binds to and phosphorylates its substrates [62]. They knocked out specific regions along PknG and did biochemical assays to determine which region of the kinase confers its specificity, using one of the accepted substrates GarA [70]. They knocked out the first 45 amino acids, the TPR region, which is speculated to be the site that the kinase uses to be secreted out of the cytosol since it doesn't have a membrane region [37]. They determined that it is the N-terminal region of the kinase that is required for substrate specificity, and furthermore, that the kinase is more specific to full length protein as a substrate than to short peptide sequences. These studies served as important stepping stones in the quest to try to understand the physiological role this regulatory protein.

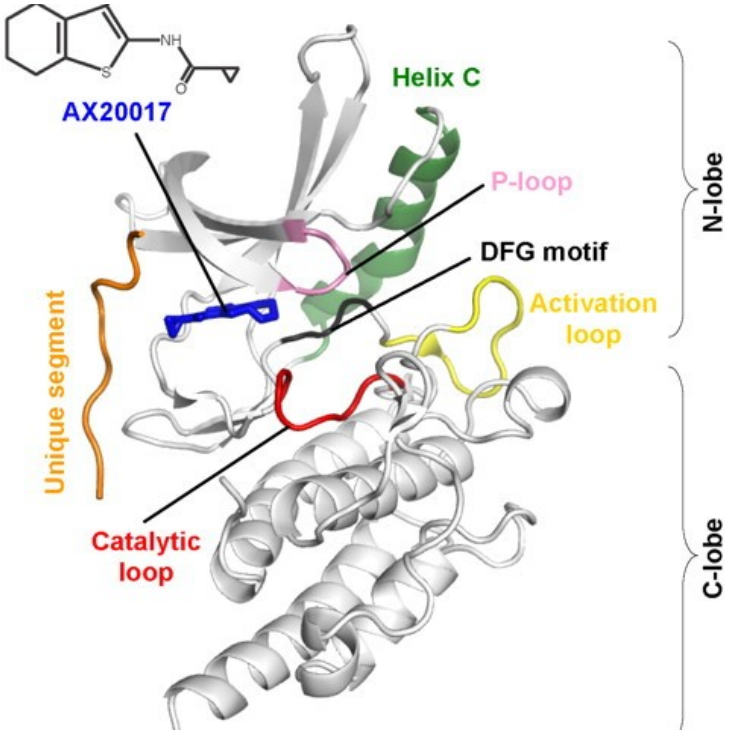

Figure 1-3: chemical structure of the inhibitor AX20017 bound to the kinase domain of PknG (Ribbon representation) resolved by X-ray crystallography Nicole Scherr et al. PNAS 2007;104:12151-12156

1.6 Mass spectrometry as a platform to study phosphorylation and identification of kinase substrates

Protein phosphorylation is a critical step in the flow of information from outside the cell to the cytosol, so the cell can respond appropriately by regulating important proteins, whether the modified protein's functions are influenced positively or negatively depends on the environment the cell is in. The site of phosphorylation on the substrates is very important, the phosphate group on a particular protein has been shown to act as a potential protein-protein interaction recognition site [71]. A single change from one phosphorylation site to the one adjacent to it can change the effect of that phosphorylation on that substrate significantly. The turn-over for phosphorylation is rapid, taking place in a matter of minutes, since the cell must respond to constant stimuli. Thus, efficient platforms available currently have to be able to capture snap-shots of phosphorylation at that moment.

1.6.1 Top-down phosphoproteomics

Before mass spectrometry became the platform of choice to study PTM's, biochemical assays were the only available option. These approaches rely on separation of proteins by two dimensional gels (2D gels) stained with radioactive dyes and in vitro kinase assays [72–74]. However, as mass spectrometry methods became more popular, there was a shift towards this superior technique. Top-down phosphoproteomics is an approach that identifies whole proteins separated by 2D-gel electrophoresis. One assay that is well established and has been used successfully is immunoprecipitation (IP) pull down [75–77]. Antibodies specific to phosphorylated tyrosine residues are immobilized and bind to phosphotyrosines in digested lysates, followed by analysis on the mass spectrometer. Tyr phosphorylation is different from Ser and Thr due to the placement of the phosphate group on the O_4 position on the amino acid residue [78]. There are a few pitfalls with this method, for example, it is essential to have prior knowledge of which phosphosite to target, and to have antibodies against that particular site. That becomes difficult in discovery phosphoproteomics, where the phosphoproteomic landscape at that time point is unknown. Another downfall is

that the method is only specific for phosphorylation that occurs only on tyrosine residues. Our work and that of others in mycobacteria has shown that tyrosine phosphorylation only occurs at low frequency, less than 4% of the total phosphoproteome [29–31]. When it comes to kinase substrates discovery, this method is not suitable since kinase-substrate interaction are transient, due to the nature of the interaction. The negative charge that results from the gain of the phosphate group at the phosphorylated residue, repels and unbinds the kinase from the substrate, therefore, it is difficult to capture and purify the kinase bound to its substrate with this method. As mentioned earlier, the site of phosphorylation is the key to understand the underlying physiological regulation, however, this platform is inadequate in site specific phosphorylation determinations. These methods, however, are still invaluable when it comes to validation of phosphorylation events identified by mass spectrometry techniques [79–81].

1.6.2 Bottom-up phosphoproteomics

Advances in mass spectrometry field have greatly improved in the last 20 years since it was first developed over 100 years ago [82]. Today, with improved resolution and accuracy we can identify and characterize thousands of proteins in a single experiment. Fractionation decreases the complexity of the protein sample for better sensitivity and quantitation [83]. Mass spectrometry is therefore the superior platform to study phosphorylation and other post-translational modifications. The work presented in this thesis was performed on the Q-Exactive Orbitrap mass spectrometer (Thermo Fischer). We made use of a “bottom-up” proteomics approach, whereby peptide information is correlated back to the protein it was digested from. It is an unbiased way to survey deep into the proteome and can identify different isoforms of proteins and modifications those proteins hold. Bottom-up proteomics identifies peptides based on their mass to charge ratio (m/z), which makes it an attractive platform since only one amino acid is modified in most PTMs, so data on a single peptide can have significant biological implications.

High precision mass spectrometry identifies and quantifies peptides in the gas phase created by the ion source, usually electron spray ionization (ESI), which ionises peptides in the liquid phase, or matrix assisted laser desorption ionization (MALDI), which ionizes peptides with a laser. Typically, cells are lysed in appropriate buffers and conditions depending on the cell type, as discussed in detail later. Proteins are then precipitated and digested into peptides, mostly tryptic, that is, using the protease enzymes like Trypsin to cut long chains of amino acid into smaller peptides by cleaving them at carboxyl-terminus of the Lysine and Arginine residues. Trypsin digests proteins into thousands of short length amino acid peptides, generally around 300 to 3000 Daltons (Da). In this work we also use LysC endoptidase, which cleaves denatured proteins only on the carboxyl-terminus of Lysine residues, in combination with Trypisn to aid with the digestion [84]. The combination of these two endopeptidases usually gives us efficient cleavage, with on average 2% missed cleavages, which is imperative in the in the identification of phosphorylated peptides [85,86].This high cleavage efficiency, as good as it is, it gives arise to high numbers of peptides and that have a negative influence on ionization and therefore lead to low identification numbers. The solution to that is to separate peptides by polarity in the liquid chromatography (LC) phase.

MS based phosphoproteomics still has many challenges to get unbiased phosphopeptide identification. These are mostly due to the negatively charged, hydrophilic nature of phosphopeptides. Firstly, they can be lost during loading onto the reverse-phase analytical column, ie. less retention [87], there is also the problem of selective ionization suppression of the phosphopeptides in the presence of unmodified peptides which results higher peak intensity of unmodified peptides, which can be partly circumvented by using new generation MS that ionizes by electrospray dissociation [88]. Separation in the reverse phase LC packed with lunar beads as solid phase, which binds to peptide species based on polarity, takes advantage of the unique chemical properties of the negatively charged phosphopeptides to bind. The mobile phase used to elute peptides is normally varying concentrations of Acetonitrile (ACN) acidified with Formic acid (FA) and the solvents used will elute them directly, at a slow flow rate, into the ion-trap tandem MS. For positively charged peptide species, which is most of the

non-modified peptides, they will elute last. The column length of the LC also affects separation and resolution of peptides, therefore, identification.

The peptide precursor ions then enter the gaseous phase, where high collision dissociation energy (HCD), usually kinetic energy, or collision induced dissociation (CID), where a neutral gas like Nitrogen, fragments the precursor peptide backbone along the amide bonds, which results in b and y fragment ions and neutral losses of ammonia and water, or in the case of phosphopeptides, the loss of phosphoric acid [88,89]. In this work, we employed HCD fragmentation, where both the precursor and the resultant ions are analysed at high resolution and mass accuracy in the Orbitrap. HCD fragmentation is superior to CID in phosphoproteomic studies due to the improved high resolution of fragmentation spectra and easily distinguished charged states, an important feature that improves phosphosite localization score [90]. Although CID has been successfully used in short peptide chains, there are pitfalls in CID fragmentation: it's affinity to the lower charge state of the precursor ion influences its effectiveness and it introduces biases especially in phosphorylated peptides, that are characterized by a higher charge state, leading to the loss of the labile phosphate group during fragmentation [91]. Another fragmentation strategy of new generation MS like the Orbitrap Fusion is via electron transfer dissociation (ETD), a more attractive method for identifying and correctly localizing post-translationally modified peptides since it keeps the modification intact during fragmentation [92]. ETD uses low electron binding energy anion donor to collide with the precursor ion and cleave the disulphide and N-C_α bonds at multiple sites on its peptide backbone to give rise to c and z fragment ions [93]. This allows for multiply charged precursor ions to be fragmented and sequenced [94]. In the past decade, researchers has found that a combination of different fragmentation methods in MS instruments like the Orbitrap resulted in improved identifications of different species of peptides [95,96]. Collins and colleagues presented a strategy which combined both ETD and CID for improved phosphopeptide fragmentation, they coined it the data dependent neutral loss triggered-ETD (DDNL). This method fragments precursor ion by CID first and if the characteristic neutral loss of phosphoric acid is observed, it is then subjected to ETD fragmentation. The authors reasoned that only those peptides that are *bona fide* phosphopeptides will be fragmented by

the time consuming, more sensitive ETD method [97]. They tested this approach and it yielded confident phosphopeptide identification and localization.

The detector coupled to the mass analyser generates the structure information of fragmented ions given as raw files containing the spectral library. Mass spectra are then searched and mapped to a proteome database obtained from a six-frame translation of a genome using a search engine. There are a few wildly used and trusted search engines. [98–105]. All of them uses a False Discovery Rate (FDR), usually by reversing the database used to identify the spectra submitted, to give the confidence levels for false-positives of the acquired data. Posterior error probability (PEP) is the negative probability that the peptide spectra matched to the database is true. It is usually set at <0.01.

Liquid Chromatography (LC) coupled to mass spectrometry-based phosphoproteomics offers the ability to identify novel phosphorylated sites with high confidence site localization. When a residue is phosphorylated, the resultant mass shift of the peptide and the added phosphate group (PO_4) is then used to determine the exact residue that is phosphorylated. Phosphosite localization and specificity is hampered by stoichiometry, since only a fraction of the total proteome is phosphorylated, therefore, improved protocols, from sample handling and preparation to phosphopeptide enrichment increases the rate of isolation and identification of phosphorylated peptides. Another factor influencing a successful phosphoproteomic experiment is the labile nature of the phospho peptide, therefore, careful measures that have to be thought of and implemented in the process. Post-translational modifications of proteins' turn-over time is very rapid, changing the phosphoproteome landscape of the same system within seconds due to external environmental stimuli and signals are transmitted into the cell to respond accordingly. In comparison to the protein turn over, phosphorylation is orders of magnitude more rapid, with a half-life of a few seconds [106]. This is the reason why sample handling and enrichment protocols must be improved all the time.

1.6.3 Phosphopeptide enrichment techniques

As mentioned earlier, the sub-stoichiometry nature of phosphopeptides is a challenging step in phosphoproteomic experiments. Enrichment strategies revolutionized and improved identification and quantification of phosphopeptides. Ideally, one would fractionate the peptide mixture to decrease sample complexity before enriching for phosphopeptides. Strong Cationic Exchange (SCX) is a peptide fractionation method that takes advantage of the polarity of peptides. The principle is that under strong acidic chromatography conditions, the N-terminus of tryptic peptides becomes positively charged through protonation and whilst the C-terminus will become neutrally charged. The difference in the charge state of peptide species will bind to the negatively charged chromatography resins. The bound peptides are then eluted from the SCX column using different salt gradients. This method of fractionation and enrichment has been widely applied in phosphoproteomics studies [107–111], where unenriched peptide mixtures are fractionated and then enriched for phosphopeptides by methods described in the next section. The combination of SCX and other enrichment strategies improved the number of p-sites per experiment [112]. The downside of this method is that it takes a lot of MS time since each fraction has to be enriched and run as an independent sample on the MS. In a resource limited setting, that can sometimes not be the most feasible approach.

Immobilized Metal Affinity Chromatography (IMAC)

IMAC is one of the efficient protocols to enrich for S/T/Y phosphopeptides that was developed by Andersson and colleagues in 1986 [113]. Since then, the protocol has been optimized and improved and it is still one of the popular methods for phosphopeptide enrichment. It has high affinity and selectivity to multiply phosphorylated peptides in most lysis buffers, which is easily overcome by a buffer exchange during peptide clean up just before data acquisition on the LC-MS/MS. The procedure uses tri-valent metals, which has high affinity to phosphates, to bind the negatively charged peptides. These metals, mostly Fe^{3+}, Ga^{3+}, Ti^{4+} or Zr^{4+}, immobilized in a column packed with porous material, forms complex with the phosphate group. The specificity of the metals varies

depending on the chemistry of the organic solvent used in the protocol, for example, Ga3+ has optimal selectivity when iminodiacetate columns were used [114]. Although IMAC has been used to study the phosphoproteome, like most phosphopeptide enrichment strategies, they must be continuously improved as technologies improve. McNulty and colleagues used a multidimensional strategy combing IMAC with hydrophilic Interaction Chromatography (HILIC) [115] separation to decrease complexity of the protein mixture before phosphopeptide enrichment [116]. In this system, there's better retention of hydrophilic peptides introduced by the phosphate group on the HILIC column as compared to the reverse phase column, resulting in better selectivity and fractionation of phosphopeptides and therefore identification. One of the latest development in improving this technique is by the use of nanomaterials to produce Fe^{4+} IMAC, for example: Fe3O4@SiO2@PEG-Ti4+-IMAC nanoparticle has a high phosphopeptide recovery (over 70%) and low limit of detection[117,118]. This is due to the combination of the hydrophilic surface and the high binding capacity of the grafted PEG brushes that have a high chelating capacity of titanium ions[119].

Titanium Dioxide (TiO_2) enrichment for phosphopeptides

Titanium Dioxide-based solid phase material was first proven effective in capturing phosphate group on a peptide by Pinkse and colleagues [120]. They made an on-line two-column system where the TiO_2 column firstly trapped the phosphopeptides and the unmodified peptides flowed through and were captured on a reverse phase column. Phosphopeptides were then eluted from the TiO_2 under strong alkaline conditions before LC-MS/MS. The same year, Sano and colleagues used "column switching" to capture phosphopeptides by HPLC. The pre-column contained TiO_2 and an anion exchange analytical column coupled to a UV detector before MS analysis [121]. The principle of this workflow is that TiO_2 binds to organic phosphate under acidic conditions and its amphoteric chemical stability makes it a suitable metal of choice [122]. The method has been improved over the years, for example: the addition of 2.5 di-hydroxybenzoic acid (DHB) reduces non-specific biding of peptides with acidic residues to the TiO_2 column, while retaining high specificity for phosphopeptides [123]. DHB is a MALDI matrix, it comes with caveats during an MS run because it binds to the column leading to

MS instability and overheating of capillaries. Another improvement to the workflow was coating magnetic nano-particles with TiO_2 which increased the surface area, therefore more binding capacity and deeper phosphoproteome identification. Due to their magnetic properties, the TiO_2 coated nano-particles bound to phosphopeptides could be readily separated using a magnetic field. This method, however is not compatible with ESI MS since bound peptides are not eluted from the nano-particles but are instead used as a matrix and analysed on a MALDI [124]. As discussed earlier, IMAC has proven efficient in phosphopeptide enrichment, however, due to its electivity for multiply phosphorylated peptides [125], a new method was proposed by Thingholm and colleagues where they used IMAC coupled with TiO_2 to capture both singly and multiply phosphorylated peptides. They coined it SIMAC, but it is not a popular choice of phospho-enrichment due to its low recovery that has been attributed to the use of two different chromatography columns [126].

1.6.4 Database search engines and Quantification of phosphopeptides

CID fragmentation results in spectra that is dominated by large peaks of neutral loss of the phosphate group plus water, if the peptide harbours a modification compared to their unmodified counterparts. ETD, on the other hand, preserves the modification on the peptide and its becoming a popular choice for not only phosphorylation, but other PTM studies too. Computational analysis of raw spectra is influenced by the type of fragmentation method used. Additional processing might be required before the spectra is matched to the database of interest, and the downfall is that there is an increased search space that could lead to false identifications. For example, modified peptides are complex by nature, when we consider other variable modifications that can occur on the same peptide, like variable modifications that are purely due to sample processing protocols, eg oxidation of a Methionine and cabarmidation of cysteins, the search space becomes compounded. Another layer of complexity is the increase missed cleavages if the modification occurs after either Lysine or Arginine, the two tryptic cleavage sites. The current peptide spectrum matching

(PSM) softwares take into account these complexities and have been improved over the past few years to be able to process, search and score the database for phosphopeptide identification [100–102,104,105,127,128].

Computational platforms for Phospho-site localization and occupancy

Data processing after LC-MS/MS is the bottle neck of phosphoproteomics. Phosphorylation can occur on a few residues in a peptide. If a peptide has several phosphorylatable residues, it is of great importance to correctly localize the exact site of phosphorylation. The mass shift after neutral loss of phosphoric acid of a peptide is evidence that that peptide was modified, however, if that peptide has more than one Ser/Thr/Tyr residues, the software should be able to correctly determine which residue out of all possible ones was phosphorylated. The site of phosphorylation has very significant impact on the functionality of the protein. That is the reason why the importance of accurate identification of the site of phosphorylation cannot be over-stated for downstream biological interpretation. Current software used for phosphoproteomic analysis estimates the error of falsely localization of phosphorylation based on the presence and intensity of the fragmentation ion and gives a localization probability score [98,129–133]. In this work, in addition, we manually validated the phosphorylation localization by interrogating the fragmentation spectra for each phosphopeptide.

Phosphorylation stoichiometry is the fraction of phosphorylated proteins in any given state. Knowledge of the changes in phosphorylation stoichiometry between different disease and/or biological states is not sufficient, but the actual phosphorylation site stoichiometry is crucial, and to date it is rarely quantified, highlighting the need for data driven site-specific phosphorylation stoichiometry workflows. It has been argued that the functional relevance of a phosphorylation site is dependent on that site's phosphorylation stoichiometry, that is, biologically relevant (functional) phosphorylation have high phosphorylation stoichiometry [134]. However, some counter-argued that non-functional phosphorylation does not exist, it just hasn't been functionally described yet,

using the yeast's ATP Citrate Lysate (S454) as an example, which was thought to be a non-functional phosphorylation until its function was deciphered [135]. These conflicting arguments from researchers only highlights the importance of studying phosphorylation as a major part of systems biology.

When an increase in phosphorylation at a particular site is observed, there is a possibility that the observed upregulation is due to changes in abundance of that phosphoprotein and not due to regulation at the post-translational level. There are a few ways to correct for that. In a typical phosphoproteomic experiment, an unenriched sample is analysed concurrently with the enriched one and used to correct for the uncertainty of the level of regulation. Biochemical approaches as well as chemical labelling have been utilized in literature. Olsen *et al*, 2010, published their work where they quantitated p-site occupancy (stoichiometry) using SILAC labelling approach and found that most phosphorylation events occur at less than 10% occupancy during mammalian cell cycle [112]. Isobaric tagging like tandem mass tag (TMT) and Isobaric Tags for Relative and Absolute Quantification (iTRAQ) that incorporates labelled tags on the peptides before MS analysis are best for relative quantitation and therefore stoichiometry of phosphopeptides, however, they are not an option in resource limited settings [136–140].

Most recently, Sharma and colleagues came up with a strategy for calculating site occupancy from label-free phosphoproteomics data. Their approach uses a "reference sample' that the Maxquant software algorithm selects from each site per sample, based on its probability to give the lowest error. This sample is then use to obtain ratios of modified peptides and their unmodified counterparts, that is, the proportion of identified phosphopeptides in relation to the protein ratio of the experiment, and the resultant values are then used to give a score, anything less than one is considered as a measure of occupancy reliability [80].

1.7 Statistical analysis of phosphoproteomic data

Mass Spectrometry based discovery phosphoproteomics can identify novel p-sites, however, before biological interpretation, statistical analysis on the data must be done first. That brings its own set of challenges. Data analysis is done at the peptide level instead of the proteome level in discovery proteomics. We

discussed earlier the enrichment techniques that improves p-sites identification, these techniques, however invaluable, introduces a lot of noise from non-specific binding and variation between replicates, therefore careful statistical analysis and, in kinase substrate identification, validation steps are imperative.

Missing values in label-free phosphoproteomics occur due to losses during sample preparation and poor MS/MS identification scores for those peptides just above or below the limit of detection of the instrument. As a result, Label free phosphoproteomic data are sparse and with significant data gaps. There have been a few methods proposed to deal with these missing data [141]. The first is to increase the number of both biological and technical replicates to minimise under sampling and give statistical validation. The second way is to not include in the analysis all those peptides that are only identified in one replicate and not the others, which mostly happens if the peptide is present but is below the limit of detection of the mass spectrometer. If two or more replicates have intensity values, then an appropriate, yet controversial way of dealing with those few data gaps is through missing value imputation that was initially developed for microarray data [142,143]. It has been argued that since imputing gives values to unknown peptide information, it can be misleading [141]. The principle of imputing missing values with the lowest value from the normal distribution with means and variance estimated from the observed data is the most widely accepted and easily implemented method of dealing with data gaps.

A proposed method by Wang and colleagues [144] for normalizing proteomics data with missing values is through rescaling the data and using a probability model to investigate the intensity-dependent missing values and provide possible substitution. Rescaling involves using information from peptides with values in both replicates to work out the scale difference of the overall experiment and using that information to estimate intensities of peptides with missing values. The assumptions made by this workflow is that in any MS based experiment, the number of features that change between samples is fewer compared to the overall features and that sample intensities are related by a constant factor, therefore the distribution of the measurements of all features across all experiments should roughly be the same. Proteomic data is usually logarithmical to give a normal distribution before any downstream statistics can be performed

to obtain statistically significant results. A recently published method specific for normalization of phosphoproteomic data is by Kauko and colleagues that we have used in this work. They termed it the “Median pairwise normalization”. The principle is that since the phosphopeptide enrichment introduces variability, to overcome this is to normalize the enriched peptides by adjusting their intensity values with those that are identified in an unenriched sample [145].

The steps discussed above has enabled us and other researchers to interrogate the global phosphoproteome and perform accurate quantitative analysis of protein events at the phosphopeptide level [11,12,17,48,80,109,110,146,147]. In addition, several studies using quantitative phosphoproteomics have identified hundreds of kinase substrates in varying eukaryotic systems [79,108,145,148,149]. More recently, a similar quantitative phosphoproteomic analyses have been successfully applied to identify novel substrates Bacillus subtilis of the Ser/Thr kinase PrkC and phosphatase PrpC [110] and of the MAPK Hog1 in yeast [150] and in human cells [79].

1.8 Targeted mass spectrometry in phosphoproteomics

Label free quantitative discovery proteomics is semi-quantitative, and hypothesis generation requires several assumptions to be made, which mandate validation. Furthermore, the complexity of the protein sample can affect which proteins are observed, thus limiting the suitability of discovery proteomics for low-abundance proteins. Western blots have been the gold standard in validating hypotheses derived from discovery mass spectrometry experiments. In this era of high throughput data science, western-blots may be inadequate to validate data from omics experiments. An interesting, recently developed platform that has the potential to quantify proteotypic phosphopeptides with high precision is targeted mass spectrometry, which is a peptide-centric approach. This platform takes advantage of the information gained from discovery ‘data dependent’ (DDA) untargeted proteomic experiments to generate targeted assays for identification and quantitation of peptides of interest based on their known properties (precursor ion mass to charge ratio (*m/z*) and retention time). By monitoring only specific ions and their fragment ions, peptides of interest can be accurately and sensitively identified and quantified. Targeted proteomics allows for

quantification of low-abundance peptides in complex mixtures, which has exciting applications in the high-throughput validation of phosphosites.

There are several targeted MS approaches, depending on the type of instrument used and/or parameters. The first, and most widely used, is so-called 'multiple reaction monitoring' (MRM), sometimes referred to as selected reaction monitoring (SRM) or parallel reaction monitoring (PRM). In an MRM workflow, protein abundances are calculated from the summed intensity of precursor and fragment ion pairs ('transitions') for each peptide, typically in a triple quadrupole MS instrument. The first quadrupole filters the precursor ions based on their *m/z* values, selecting only the target precursor *m/z*. These precursors are then fragmented in the second quadruple through interaction with a collision gas to produce fragment ions (**Figure 1.4**). In the third quadrupole, the fragment ions are again filtered to select only the target fragment ion *m/z*, and the combination of precursor and fragment ion contributes to the specificity of the peptide identification and quantitation. The monitoring of transitions at a defined retention time, known as 'scheduling', allows for multiplexed identification and quantitation of up to 200 transitions in a single run. In contrast, a PRM workflow is applied in hybrid Orbitrap instruments, such as the QExactive (Thermo). The major difference between MRM and PRM is that all possible fragment ions can be are monitored in PRM, due to the high speed and accuracy of the hybrid Orbitrap mass analyser. A scheduled PRM is capable of monitoring up to 100 peptides in a single run [151]. Recent studies, including the present study, have been able to exploit this platform as a means of validating peptides of interest from discovery experiments [152–154].

The second type of targeted assay is the so called 'data independent acquisition' (DIA), which is rapidly growing in popularity. Popular DIA methods include SWATH, which promises accurate identification of a large number of proteins in even the most complex of samples [155]. While the application of DIA is still being explored in phosphoproteomics, this technology is anticipated to revolutionise the field of quantitative proteomics.

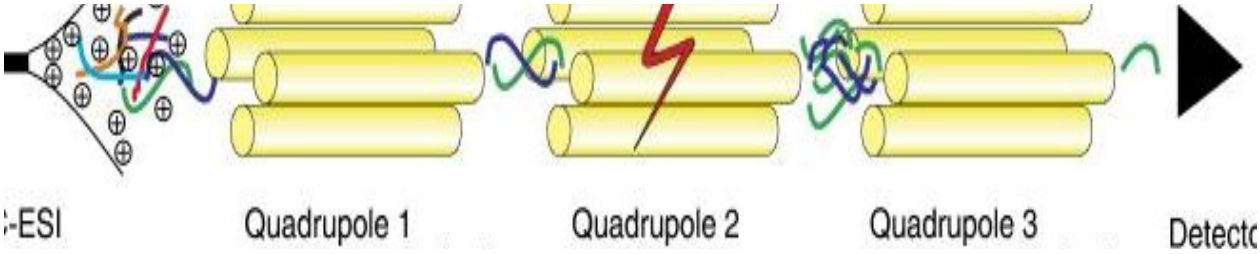

Figure 1-4: Schematic diagram of an analyte going through a triple quadruple instrument. (Lange et al., 2008). Ions are separated based on their polarity and stability and travel through the quads via a voltage. Selection of different radio frequency (RF) voltages allows for separation of ions with m/z *compatible to that voltage to travel through Q1, that way one can choose a voltage that will scan the peptides of interest in an MRM run. Q2 acts as a collision cell by fragmenting the precursor ion with a gas, and the resultant fragment ion is selected in Q3 where is converted into a mass spectrum*

1.9 Objectives of the thesis

Research in signalling pathways involving mycobacterial kinases that can explain the mechanisms this bacterium uses to establish latency and evade the immune system is limited because of the rate limiting steps, ie. knowing the role these signalling proteins play. The functions of these kinases solely depend on the substrates they phosphorylate in changing environments.

Until recently, only a few papers have been published on the phosphoproteomic landscape of mycobacteria in actively growing culture [32,152,156]. The first aim of this work was to identify a network of proteins phosphorylated, and therefore increasing the catalogue of STPK's substrates, in actively growing cultures of two mycobacterium species: the fast-growing *M. smegmatis* and the slow growing *M. bovis* BCG.

The second objective of thesis was to identify new physiological substrates of the *M.bovis* BCG PknG *in vivo*, which is structurally and functionally similar to that of *M. tuberculosis*. We also aimed to validate the identified candidate substrates by downstream *in silico* analysis.

The third objective was to identify the host proteins that are differentially phosphorylated in the presence of PknG and the pathways disrupted that could explain the observed phenotype, ie. blocking of phagosome-lysosome fusion in pathogenic mycobacteria infected macrophages.

Overall, this thesis aims to unpack the way PknG works to be able to play such an important role, and furthering the reasons why this kinase is a potential drug target to finally eradicate tuberculosis.

2. MATERIALS AND METHODS

2.1 Bacterial strains

Bacterial strains used in this thesis were kindly donated by Professor Jean Pieters, University of Basel, Switzerland. The mutants (*M. bovis* BCGΔ*pknG* and *M. smegmatis* mc^{2}155 expressing *M. tuberculosis* pknG) were generated as described in Walburger et. al. 2004 [36].

2.1.1 Culture conditions of bacterial strains

Wild type and mutant strains of *M. smegmatis* mc^{2}155 and *M. bovis* BCG Pasteur strain 1173P2 were grown in 7H9 Middlebrook (BD, Maryland, USA) broth supplemented with 0.05% Tween 80, OADC (Becton Dickinson) and 0.2 % glycerol (v/v). To make bacterial stocks for future use, cultures were plated on 7H10 media containing glycerol and 10% OADC and left to grow at 37°C until colonies formed. They were then scraped and stored in 0.05% glycerol at -80, likewise for liquid cultures, OD was measured and 1mL aliquots of the culture was kept in a cryogenic screw cap and stored at -80°C. Frozen stocks were defrosted and inoculated into 10mL of 7H11 media to make inoculum which was added at 1% to make the main culture for all the experiments. The cells were grown at 37 ^{0}C with continuous agitation (120 rpm). Growth was monitored daily for *M.bovis* BCG and every four hours for *M. smegmatis* by measuring optical Density (OD_{600}) and growth curves plotted.

2.1.2 Harvesting of bacterial strains

Cells were harvested during the exponential phase (OD_{600} ~1.2 and 0.6 for *M. smegmatis* and *M. bovis* BCG, respectively) by centrifugation at 4 000 g for 15

min at 4^{o}C, washed twice with Phosphate Buffered Saline pH 7.5 (PBS). Cells were snap frozen in liquid nitrogen and stored at -80^{o}C until needed.

2.1.3 Bacterial lysis

Frozen pellets were suspended in 800µl lysis buffer (Appendix I). Cells were disrupted by sonication at maximum power for 6 cycles of 30 sec, with 1 min cooling on ice between cycles. Cellular debris was removed by centrifugation at 4 000 g for 10 min and the lysate filtered through 20 µm pore size low-protein binding filters (Merck, New Jersey, USA). Lysates were stored at -20 until needed.

2.2 Eukaryotic cells culture

Murine macrophage cell line RAW 247.6 were used to study the host-pathogen interactions in this study. Murine macrophages have been used as a successful model to study host-pathogen interaction in *M. tuberculosis* studies. Our stocks were kindly donated by one of our collaborators from University of Stellenbosch. To prepare frozen stocks of the cell lines, they we grown (details below) until desired density. Cells when then aliquoted in freezing media (Appendix II) in 1mL aliquots and transferred into “Mr Frosty” (ThermoFischer Scientific), ie. a plastic container with cold isopropanol (4°C), to ensure that cells freeze at a slow rate to minimize cell death before being transferred to -80°C for long term storage.

2.2.1 Culture conditions of RAW 247.6 macrophages

Frozen stocks of the cell lines were defrosted in the water bath set to 37°C. Then cells in suspension were pelleted by centrifugation for 3 min at 800xg. The cell pellets were washed twice with pre-warmed PBS and pelleted. The pellets were re-suspended in five millilitres of Dulbecco’s modified Eagle’s medium (DMEM) (Difco), supplemented with pyruvate and glutamine (Difco) and 10% (v/v) heat-inactivated foetal calf serum (FCS) (Sigma-Aldrich) (D10). And seeded into T25 Tissue culture flasks (Lasec, South Africa) at 30% confluence and grown in a humidified (95%) incubator at 37°C with 5% $C0_2$.

2.2.2 Splitting of macrophages

After three days of incubation, once the cells had reached 90% confluency, with microscopically checking the cells every day, the media used to grow RAW macrophage monolayer was pipetted out. The monolayers were washed twice with warmed PBS. Fresh D10 was added to the monolayer and gently scraped with a plastic cell scraper until they were in suspension and were counted. For cell counting, equal amounts of cells and tryphan blue (0.4% Sigma) were mixed and 20µl was pipetted into a cell counter chamber (Bio-rad) and viable cells were counted microscopically. Tryphan blue is a dye that penetrates dead cell because of the weakened membrane [157], therefore the viable cells will not appear blue under the microscope and those were the only ones counted. Cells were counted on five squares of the cell counter and the cells/mL was calculated as the number of cells per number of squares counter, multiplied by the dilution factor and $x10^4$. The cells were then transferred into new flasks and incubated until needed.

2.2.3 Checking for mycoplasma infection of macrophages

RAW macrophage cell lines are prone to contamination by mycoplasma. To test that our cells were free of infection, the Mycoalert kit (Cambrex) was used as per manufacturer's instructions.

2.2.4 Infection of Macrophages with *M. bovis* BCG

Three days before infection, macrophage cell lines were seeded at the desired number depending on the tissue culture flask used and incubated at 37°C with 5% CO_2. An extra flask was prepared for counting after before infection. On the day of infection, bacterial cells, at the desired OD based on the multiplicity of infection (MOI) were washed twice with PBS and D10 was added to cell pellet. To remove clumps, bacterial cells were sonicated in a water bath sonicator for 10 minutes and passed through a needle 10x and gently centrifuged (1000g for 5 min) to sediment clumps.

Macrophage media was removed and washed twice with pre-warmed PBS and replaced with bacteria in D10 at MOI:4 for *M. bovis* BCG. Cells were incubated for 30 minutes uptake and washed five times with PBS. Fresh D10 was then added and incubated until harvesting.

2.2.5 Harvesting and lysis of eukaryotic cells

At each time point, cells were taken out of the incubator and washed three times with PBS. Modified RIPA buffer (Appendix III) was added to the cells and agitated for 5 minutes on ice. Lysis was confirmed microscopically and 1µl of endonuclease benzonase (Sigma) was added to break down cellular DNA and incubated while shaking for 1 hour at 4°C. Internalized bacteria were pelleted by centrifugation at 14 000xg for 30 min and filtered. The supernatant containing eukaryotic cells was stored at -20°C until needed.

2.3 Biochemical methods

2.3.1 Chloroform-methanol precipitation

Bacterial and eukaryotic lysates were precipitated by the chloroform methanol precipitation method as previously described [158]. Equal amounts chloroform (Sigma) was added to the lysate and two thirds methanol in a glass tube to prevent the strong organic solvents from leeching the plastic. The sample was then inverted a few times to mix the layers and centrifuged at 4000xg to separate the protein from the lipid layer and the nucleic acids. The top layer consisting of mostly lipids was then pipetted out and equal amounts of methanol added to the sample and centrifuged for 2 minutes at 4000g to pellet the precipitated proteins. The pellet was re-suspended in urea buffer (6M urea, 2M thiourea and 10mM Tris-HCl, (pH 8) and kept at -20.

2.3.2 Protein quantification

Modified Bradford method for protein quantification was used to determine protein concentrations of the precipitated samples [159]. The high concentration of Urea in the denaturation buffer used to get proteins in solution interferes with the basic Bradford protocol to give accurate protein yields[160]. The addition of Hydrochloric acid (HCL) (0.012M), normalizes the effects of the interference from the urea buffer. A standard curve was created from known concentrations of Bovine Serum Albumin (BSA) (Sigma) (0, 0.25, 0.5,1,2 and 4 mg/ml) in triplicate (10µL) in a flat bottom 96 well plates (BD). 90µl of the HCl dilution was then added to the wells. The samples with unknown yield were diluted 1 in 10, also in triplicate. The reaction was left on a shaker for 5 min. 150µl of the Bradford reagent (Bio-Rad) was added and incubated in the dark for a further 5 minutes. Absorbance values were then read at 595nm with a path length correction of 250µl using a Bio-Rad iMark™ microplate reader. The concentrations were calculated based on the standard curve.

2.3.3 In-solution digestion

In-solution digestion was carried out on varying amounts of total protein depending on the experiment. For discovery proteomics, 50µg of proteins were digested whilst for the TiO_2 phospho enrichment protocol required 2.5mg or 500 µg of proteins, for prokaryotic and eukaryotic cells respectively, to be digested per experiment. Proteins re-suspended in Urea buffer were denatured with 1 mM dithiothreitol (DTT) for 1 hour at room temperature while slightly shaking. This step removes the thiols on the secondary structure of proteins leaving the cysteines free of the hydrogen bonds that forms the disulphide bridge. The reduced samples were then alkylated for 1 hour in the dark with 5.5 mM iodoacetamide (IAA) which binds to the cysteines (carboamidomethylation) after the disulphide bonds are broken to prevent the now available cysteines to reform the disulphide bonds which will interfere with proteolysis. Proteins were pre-digested with Lys-C endopeptidase (Wako) for 3 hours before being diluted four times with HPLC grade water to a final concentration of 2 M Urea. The diluted sample was then digested overnight with trypsin (NIB) (1:100 ratio) and digestion quenched with Triflouroacetic acid (TFA) (Sigma Aldrich) and pH checked, ideally 2-3.

2.3.4 Peptide clean-up

Digested peptides (10µg) were desalted and cleaned up of the contaminating solvents used in the protolysis step, using in-house reverse-phase C18 chromatography (Millipore) in preparation for MS analysis. Firstly, C18 column were equilibrated with Solvent B, consisting of 80% acetonitrile (ACN) (Sigma) and 0.1% formic acid (FA), added at 100µl and centrifuged at 3000xg for 30 secs, twice, making sure that the membrane doesn't dry up. A wash step twice with Solvent A (2% ACN and 0.1%FA) then followed before the sample was added was added to the column. After washing twice with Solvent A, peptides were eluted with Solvent C (60% ACN and 0.1% FA) and dried down at room temperature in a SpeedyVac (Savant). Before samples were loaded onto the mass spec they were resuspended in Solvent A to make a final concentration of 200ng/µl.

2.3.5 Phosphopeptide enrichment

A total of 2.5 mg digested prokaryotic peptides were subjected to three rounds of phosphopeptide enrichment by titanium (TiO_2) chromatography as we have previously described [30]. Briefly, Acetonitrile (ACN) (Sigma Aldrich, St Louis, USA) was added to the peptide mixture at a final concentration of 30%. Titasphere TiO_2 beads (MZ Analysentechnik, Mainz, Germany) in loading buffer (30 mg/ml 2,5-dihydrobenzoic acid (Sigma Aldrich, St Louis, USA), 80% ACN) were added to the sample and incubated at room temperature with rotation for one hour. The beads were pelleted and the decanted supernatant was further incubated with a fresh batch of 5 mg of beads for 30 minutes, and repeated once more. TiO_2 beads were washed sequentially with 1 mL of wash buffer 1 (30% acetonitrile, 3% trifluoroacetic acid) followed by buffer 2 (80% acetonitrile, 0.1% trifluoroacetic acid). TiO2 bound phosphopeptides were transferred onto the in-house C8 tips and subsequently eluted three times with 50µl Elution buffer (40% Mass-spec grade NH_4OH [aq, 25% NH_3; Sigma Aldrich, St Louis, USA], 60% acetonitrile) and dried in a speed drying vacuum at room temperature. Phosphopeptides were resuspended in 20 µl Solvent A (2% ACN, 0.1% formic acid) before desalting.

For eukaryotic cells, TiO2 phosphopeptide enrichment kit (ThermoFischer Scientific) was used as per manufacturer's instructions. Firstly, the TiO_2 column was prepared by the addition of 20µl of wash buffer and 20µl

equilibration/binding buffer, with a 2 min centrifuge step in between the buffer exchange. The dried, cleaned-up sample was resuspended in 150µl of Binding/Equilibration buffer and transferred onto the prepared TiO_2 spin column and centrifuged for 5 min at x1000g. The flow through was collected and reapplied onto the spin tip and centrifuged for a further 5min at x1000g. The column with bound phosphopeptides was washed twice, alternating between 20µl wash buffer and equilibration/binding buffers, with a final wash step using 20µl HPLC grade water. Phosphopeptides were eluted from the spin tip with 50µl elution buffer into a glass insert to minimize polymer contamination and dried immediately in a speed vacuum concentrator. Dried phosphopeptides were resuspended in 20µl of Solvent A before LC-MS/MS.

2.3.6 LC-MS/MS

Cleaned-up phosphopeptides were resuspended in 15 µl of solvent A, of which 5µl were loaded on to the LC-MS/MS system, ie. HPLC chromatograpy (Dionex Ultimate 3500 RSLC Nano System (Thermo Fisher Scientific)) coupled to a Q Exactive mass spectrometer (Thermo Fisher Scientific). The LC delivered a flow rate of 0.4µl/min to an in-house built 40 cm column (75 µm internal diameter, packed with 3.6 µm particle Aeris C18 beads; Phenomenex) and maintained at 40°C. Solvent A was 0.1% Formic Acid in HPLC grade water and solvent B was 0.1% Formic Acid in Acetonitrile. Gradient consisted of 1% solvent B for 10 minutes, then increasing to 6% B over 2 minutes, and followed by increasing to 35% B over 118 minutes; washing with 80% B followed.

For both proteome and phosphopeptide data acquisition, the mass spectrometer acquired spectra in top 10 data-dependent acquisition mode, with precursor ions fragmented by higher-energy collision-induced dissociation (HCD) with a normalized collision energy of 27 and at a resolution of 70 000 with a target value (ACG) of 3e6 ions and a maximum integration time of 250 ms. MS2 scans were acquired at a resolution on 17 500, an isolation window of two hours and scan range of 200 to 2000 m/z. ACG value was set at 1e5 ions and maximum fill time was 80 ms.

2.3.7 Targeted Mass Spectrometry (PRM)

Identified PknG substrates were validated by targeted mass spectrometry. The discovery phosphoproteomic data was used to identify peptides with confidently localised phosphosites (phospho probability of >0.75) that were present in the *M.bovis* BCG Wt and absent in the PknG knock-out mutant. A spectral library was generated using the discovery phosphoproteomic data in Skyline (version 3.6.0.10162), with the best representative spectrum for each identified peptide and phosphopeptide. Retention times were calculated based on the average retention time observed in the discovery phosphoproteomic analysis. An isolation list was generated with a 10-minute retention time window around each peptide's calculated retention time. This isolation list was used to carry out a 2-plex scheduled PRM analysis with 100 ms injection time and a total cycle time of 2 seconds on a Q-Exactive hybrid Orbitrap MS. The AGC target was set to maximum, and a 2 m/z mass error window was allowed. Targeted MS2 data was acquired at a resolution of 35000. The chromatography setup was identical to that of the discovery phosphoproteomic analysis. The resulting PRM data was analysed in Skyline with the background *M. bovis* BCG or *Mus musculus* database obtained from Uniprot (www.uniprot.com) for each experiment requirement. The spectral library was used to confirm the identity of the targeted peptides

2.3.8 Kinase-substrate interactions

To understand the kinase–substrate interaction of the target peptides, a structure-based modelling study was undertaken. The target peptides were modelled and docked into an existing ADP-bound PknG structure (PDB id 4Y0X) using CABS-dock web server (http://biocomp.chem.uw.edu.pl/CABSdock) to identify each peptide's binding site. The server performed a simulation search (using a set of 10,000 models) for the binding site, allowing for full flexibility of the peptide. A small fluctuation of the receptor backbone during binding was allowed. A final model was selected using a two-step procedure of (i) initial filtering of lowest binding energy model and (ii) k-medoids clustering. The best peptide binding was chosen from the lowest binding energy which is the sum of Lenard-Jones and Coulombic potential functions from popularly used force fields [161,162]. Figures were generated using PyMol (www.pymol.org).

3. COMPARATIVE SER/THR/TYR PHOSPHOPROTEOMICS BETWEEN TWO MYCOBACTERIAL SPECIES: THE FAST-GROWING *MYCOBACTERIUM SMEGMATIS* AND THE SLOW GROWING *MYCOBACTERIUM BOVIS* BCG.

(Based on Nakedi et. al, 2015)

Summary

Ser/Thr/Tyr protein phosphorylation plays a critical role in regulating mycobacterial growth and development. Understanding the mechanistic link between protein phosphorylation signaling network and mycobacterial growth rate requires a global view of the phosphorylation events taking place at a given time under defined conditions. In the past, the use of mycobacterial strains such as *M. smegmatis* and *M. bovis* BCG as model organisms have significantly contributed to our current understanding of *M. tuberculosis* biology and environmental adaptation. In this chapter, we qualitatively compared the phosphoproteomic landscape of actively growing two mycobacterial model organisms: the fast-growing *Mycobacterium smegmatis* and the slow growing *Mycobacterium bovis* BCG. Our workflow included three rounds of TiO_2 chromatography to enrich phosphorylated peptides, followed by subsequent analysis of phosphorylation-events using liquid chromatography coupled with state-of-the-art high resolution tandem mass spectrometry (LC/MS/MS), in order to compare the phosphoproteomes of these two model mycobacterium species during exponential growth. We detected a total of 185 phospho-sites in *M. smegmatis*, of which 106 were confidently localized (localization probability (LP) ≥0.75; PEP≤0.01). In *M. bovis* BCG, however, the phosphoproteome comprised 442 identified phospho-sites, of which 289 were confidently localized. The percentage distribution of Ser/Thr/Tyr phosphorylation was 39.47, 57.02 and 3.51

% for *M. smegmatis* and 35, 61.6 and 3.1% for *M. bovis* BCG. The results of this study revealed a number of conserved Ser/Thr phosphorylated sites and conserved Tyr phosphorylated sites across different mycobacterial species. Overall a qualitative comparison of the fast and slow growing mycobacteria suggests that the phosphoproteome of *M. smegmatis* is a simpler version of that of *M. bovis* BCG. In particular, *M. bovis* BCG exponential cells exhibited a much more complex and sophisticated protein phosphorylation network regulating important cellular cycle events such as cell wall biosynthesis, elongation, cell division including immediately response to stress. The differences in the two phosphoproteomes are discussed in light of different mycobacterial growth rates.

3.1 **Introduction**

The ability of mycobacteria to adapt to, and overcome, hostile environmental conditions in order to survive within host cells depends on a fine-tuned and orchestrated series of events (*e.g.* response to stress; metabolic remodeling; changes in growth rate) that will ultimately define the success of establishing and maintaining long term infection [163,164]. *M. tuberculosis* infection is often described by two distinct phases: an active phase, in which the microorganism is thought to be growing at or close to its maximum rate; and latent infection, in which the bacilli are thought to persist in a viable but perhaps more dormant-like state with lower or non-existent growth rate.

Alongside the increasing number of new TB infections there is the emergence and spread of multi- and extensively drug resistant *M. tuberculosis* strains. Here, unique growth related mechanisms of *mycobacteria* which facilitate adaptation to different adverse micro-environments are thought to play an important role in the mechanisms of drug tolerance and acquired resistance that are observed during infection [165,166]. For instance, a recent study showed that diverse growth-limiting stresses trigger a common signal transduction pathway in *M. tuberculosis* that induces triglyceride synthesis, which is associated with slowing down of growth and reduced antibiotic efficacy [167]. Therefore, further investigation of the signaling pathways which regulate mycobacterial growth rate might reveal important information regarding the capacity of *M. tuberculosis* to adapt to its environment and in particular how this relates to drug tolerance and to the ability to establish infection.

In *M. tuberculosis*, Ser/Thr phosphorylation is essential for growth and environmental adaptation (as reviewed by [168]. For instance, the Ser/Thr protein kinases (STPKs) PknA and PknB are essential for growth of *M. tuberculosis* in culture, indicating that phosphorylation plays a pivotal role in the survival of this bacterium [16,31,40,169,170] These STPKs are encoded by an operon which regulates genes involved in cell shape determination, cell wall synthesis and cell division [21,31,40]. In addition to PknA and PknB, another group of STPKs comprised of PknG, PknL and PknF appear to be involved in different aspects of *M. tuberculosis* growth regulation [10,21,37]. In support of the likely important role played by STPKs in *M. tuberculosis*, a mass spectrometry-based phosphoproteomic study identified more than 500 Ser/Thr phosphorylation sites on 300 proteins in *M. tuberculosis* [29] and, more recently, a complementary study detected a number of Tyr phosphorylated proteins in *M. tuberculosis* [31]. Notably though, the physiological significance of these findings remains largely unexplored. STPKs are not evenly distributed among different mycobacteria and closely related actinomycetes, their distribution is also uneven in other bacteria phyla [156]. The pathogenic *M. smegmatis* encodes for all the Mtb STPKs except for PknI (www.uniprot.com), whilst the genome of *M. bovis* BCG encodes for all 11 STPKs. The deleted region of *M. bovis* BCG does not encode for any of these kinases[171].

In the past years, the use of mycobacterial models such as *M. smegmatis* and *M. bovis* BCG have significantly contributed to our current understanding of *M. tuberculosis* biology and environmental adaptation (as reviewed by Shilooh 2010). *M. bovis* BCG is an attenuated bovine tuberculosis bacillus by a serial passage in the laboratory [172] . This mycobacterium is a particular convenient model in part due to it slow growth rate similar to that observed in *M. tuberculosis*. On the other hand, *M smegmatis* is a fast growing mycobacterial species (with a doubling time of approximately four hours) that has been widely used to investigate different aspects of mycobacterial physiology [173–175]. As part of a concerted program to associate protein phosphorylation in mycobacteria with subsequent macromolecular events which determine growth rate and eventual environmental adaption, we have carried out a phosphopeptide enrichment and high throughput mass spectrometry-based study to investigate and compare the phosphoproteome of two actively growing model mycobacterial organisms - the fast-growing *M. smegmatis* and the slow growing *M. bovis* BCG.

3.2 **Aims:**

To elucidate the phosphorylation events and subsequent signal transduction pathways coordinating differential mycobacterial growth rates, which may in due course lead to important insights into *M. tuberculosis* physiology during active and latent infection - including aspects of slow growth associated drug resistance.

3.3 **Results:**

3.3.1 Data quality

Three biological replicates were used per experiment in both mycobacterial strains to ensure statistically significant results. MS1 and MS2 spectra was acquired using parameters detailed in Chapter 2. To be able to confidently infer that the observed differences at the phosphopeptide level are due to biological differences instead of sample loading variability, we optimised the amount peptides loaded onto the LS/MS/MS by ensuring that all the samples had Total Ion Chromatogram (TIC) in the same range as illustrated in **figure 3.1**. Data quality was assessed by running an in-house R-script to generate a PDF showing data summary. Firstly, protease digestion efficiency was determined by the number of missed cleavages in an experiment as shown in **figure 3.2** and absolute mass error across all samples was low as indicated in **figure 3.3**. We considered all phosphorylation-events that were detected in all the biological replicates, and only confidently localized phospho-sites (p-sites), with a localization probability of >0.75 and manually validated by observing the fragmentation spectra using

the Maxquant “Viewer “option as demonstrated in **figure 3.4** were considered for qualitative comparative analysis and further discussion.

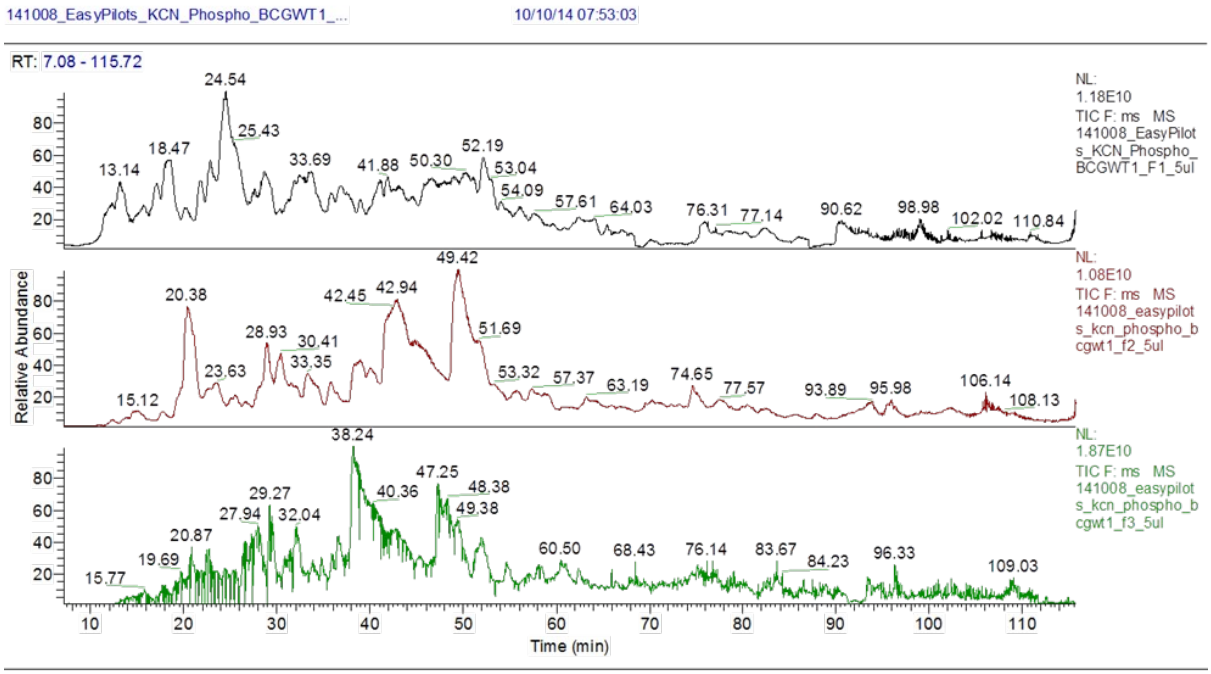

Figure 3-5: Sample loading volumes optimised to yield TIC comparable between samples. All samples were piloted and the volume needed to achieve a desired TIC in each sample was calculated from the initial volume that obtained the TIC and reloaded onto the LC/MS/MS with the new volume using the formula: sample volume = volume loaded x TIC obtained/TIC desired.

Figure 3-6: Digestion efficiency monitored by the number of missed cleavages (mc) per experiment.

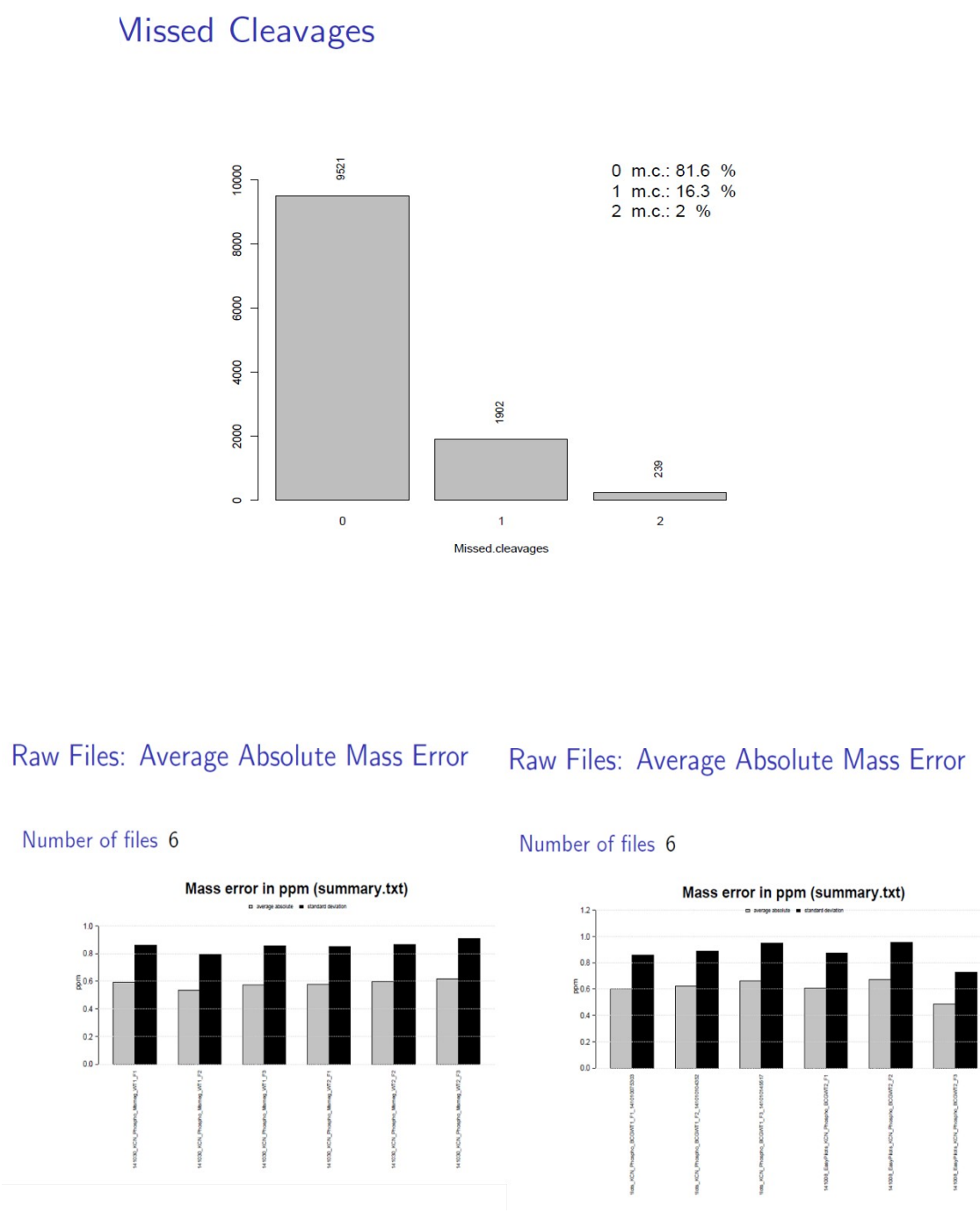

Figure 3-7: Data quality: Mass error across samples in both M.smegmatis and M.bovis BCG phospho experiments

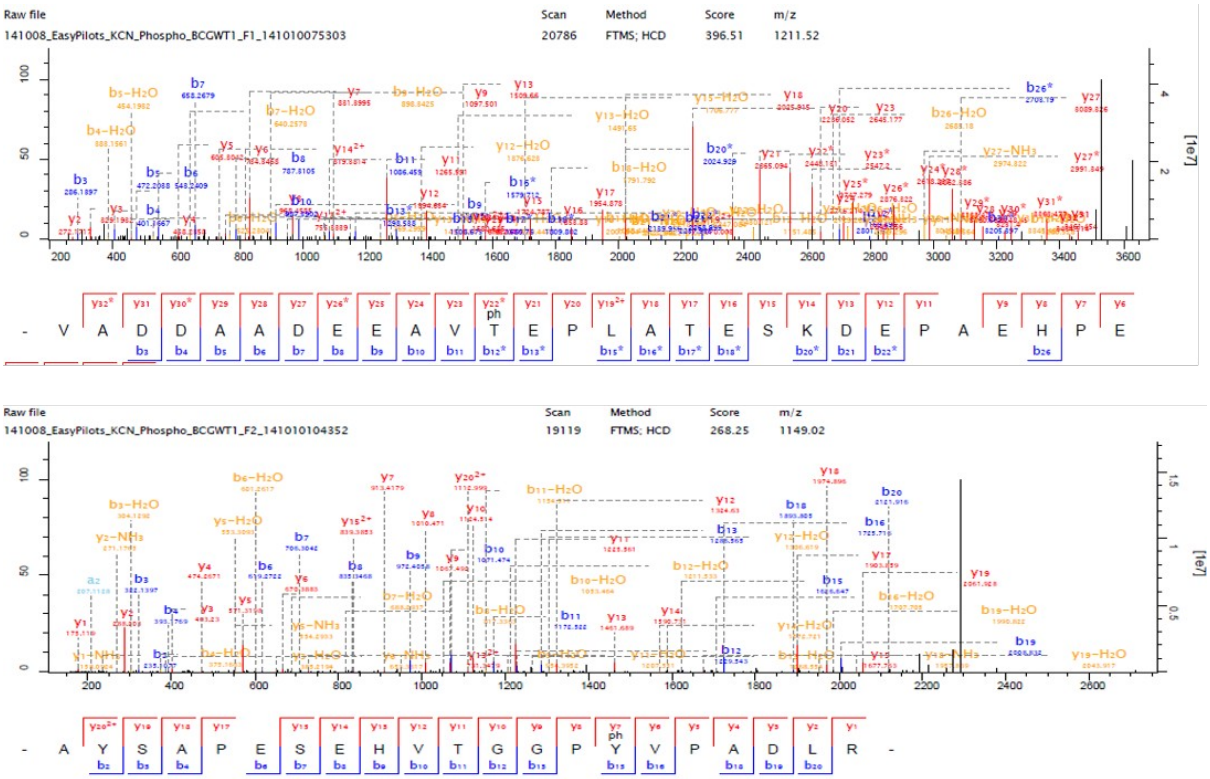

Figure 3-8: Manual validation of phosphopeptides with Maxquant "Viewer". Phosphorylation of M. bovis BCG Cell division FtsQ (Thr24) and probable conserved protein membrane mmpS3 (Tyr70. Top: Fragmentation spectra for modified peptide bearing the phosphorylated Thr24. Bottom: Fragmentation spectra for modified peptide bearing the phosphorylated Tyr_{70}.

In the three *M. bovis* BCG replicates, we detected a total of 442 p-sites of which 289 were confidently localized (Localization probability (LP) ≥0.75; PEP≤0.01) and 169 of the 289 had a LP ≥ 0.99. We identified 88,822 MS/MS spectra corresponding to 7,784 non-redundant peptide sequences and 1,765 protein groups (402 were identified by a single peptide). The estimated false discovery rate (FDR) was 0.32 at the peptide level, 0.30 at the modification level and 1.03 at the protein level. Our initial analysis of two biological replicates of *M. smegmatis* revealed considerable differences in the number of identified p-sites between the two Mycobacterial species, 77 p-sites for *M. smegmatis* compared to 289 for *M. bovis* BCG. To verify that these differences observed were biological, we further analysed three additional biological replicates for *M. smegmatis*. Phosphoproteomic analysis of five biological replicates of *M. smegmatis* protein extracts resulted in identification of 180, 396 MS/MS spectra, corresponding to 16, 185 non-redundant peptide sequences and 2, 462 protein groups (464 were identified by a single peptide). The estimated false discovery

rate (FDR) was 0.22 at the peptide level, 0.21 at the modification level and 0.98 at the protein group level. We detected a total of 185 phospho-sites in *M. smegmatis*, of which 106 were confidently localized (LP ≥0.75; PEP≤0.01) and 64/106 had a LP≥0.99.

3.3.2 Phosphorylation frequency between two mycobacterial species

In detail, for *M. bovis* BCG, we detected 289 p-sites on 203 phoshoproteins: 35.3% on serine (pSer), 61.6% on threonine (pThr) and 3.1% tyrosine (pTyr). For *M. smegmatis* we detected 106 p-sites on 76 phosphoproteins: 39.47% on serine (pSer), 57.02% on threonine (pThr) and 3.51% on tyrosine (pTyr) **(Figure 3.5 A and B).** Both phosphoproteomes were biased toward Thr compared with Ser (57-61%; 41-35%), which agrees with previous reports on *M. tuberculosis* H37Rv [29].

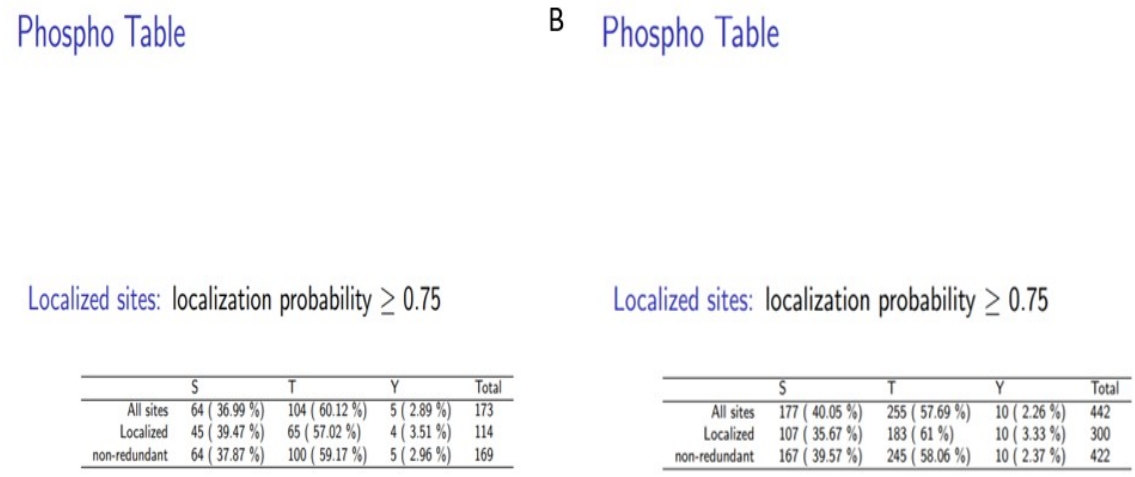

Figure 3-9: Distribution of identified phosphosites after applying filters in both species of mycobacteria. M. smegmatis has a third of phosphorylated residues compared to pathogenic mycobacteria in actively growing cultures (A). M. bovis BCG's phosphorylation landscape (B) is comparable to that of M. tuberculosis.

3.3.3 Tyrosine phosphorylation in mycobacteria

Although it had previously been suggested that Tyr phosphorylation was non-existent within mycobacterial species, it was recently confirmed that Tyr phosphorylation does in fact occur on a number of diverse *M. tuberculosis* proteins [31]. Here, we have confidently identified nine Tyr p-sites in eight proteins in *M. bovis* BCG and four in *M. smegmatis* **(Table 3.1),** of which four were also found to be phosphorylated in *M. tuberculosis* [31]: FHA-domain-containing protein (Tyr_{215} and Tyr_{232}), 60 kDa chaperonin 1 (Tyr_{358}) and conserved membrane protein mmpS3 (Tyr_{70}). These results supports earlier suggestions that phosphorylation on Tyr residues occur in different mycobacterial species [31]. The number of phosphorylated peptides varied significantly between the two species. Importantly, the percentage of Tyr phosphorylation in *M. bovis* BCG was closer to that reported in *M. tuberculosis* [31].

Our data included tyrosine phosphorylated FHA-domain-containing protein, which is a substrate of numerous STPKs, including PknB. Phosphorylation of FHA by PnkB has implication in cell wall synthesis with a possible involvement in mycobacterial virulence [176]. Likewise both 60 kDa Chaperonin and conserved membrane protein mmpS3 have been implicated in mycobacterial virulence [177]**.** Based on our data, we searched for possible conservation of these peptides across other bacterial species. For identification of tyrosine-phosphorylation site motifs , we used the Motif-X algorithm [178]. We defined a sequence window of +/- 10 amino acids on each side of the tyrosine site and generated the sequence logo by Phosphosite logo generator using the algorithm PSP production (Cell signalling Technology). A sequence motif derived from 60 kDa Chaperonin Tyr_{358} (RQEIEN**SDSDYDREKL**QERLA) using Seq2Logo revealed an overrepresentation of Tyr_{358} (**Figure 3.6**). A conserved Tyr_{360} residue on apparently conserved peptide (**SDSDYDREKL**) was found in three Gram negative pathogenic species, specifically Shigella spp, Klebsiella spp and Salmonella spp, suggesting that this

conserved Tyr phosphorylation site warrants further investigation for possible roles in bacterial pathogenesis.

Table 3-1: List of Tyrosine phosphorylated proteins/sites identified in M. bovis BCG and M.smegmatis

ACc.number [a)]	**Protein description**	**Phosphorylated peptide sequence and phosphorylated site**	**Position of the phosphorylated Tyr**
A1KEI8	Uncharacterized protein FHA domain-containing protein	HPGQGDYPEQIG**Y(1)**[b)]PDQGGYPEQR	215*
		GGYPPETGGYPPQPG**Y(1)**PRPR	232*
A1KFR2	60kDa chaperonin 1	VAQIRQEIENSDSD**Y(0.919)**DREK	358*
A1KFP3	Uncharacterized protein Hydrolase domain-containing protein	GLAEGPLIAGGHS**Y(1)**GGR	99
A1KI63	Uncharacterized protein	SA**Y(0.913)**PDGIADHDRPLAPR	8
A1KKP0	Probable isocitrate lyase aceA	MGIEAI**Y(0.998)**LGGWATSAK	104
A1KKP0	Probable conserved membrane protein mmpS3	AYSAPESEHVTGGP**Y(1)**VPADLR	70*
A1KKR9	Uncharacterized protein CYTH-like domain containing protein	**Y(0.847)**TAATGADNVSQEAK	428
A1KPH7	Conserved hypothetical mce associated protein	RDCASVMV**Y(0.973)**LNRTVTDK	122
^A0QWX0	Carbohydrate kinase FGGY	**Y(1)**NYDTLAGR	1
^A0QQ14	Carbohydrate kinase FGG	ISAW**Y(0.968)**VER	5
^ A0QSS3	10 kDa chaperonin	**Y(1)**GGTEIK	1

^A0QQU5	60 kDa chaperonin 1	AEIENSDSDY(0.915)DREK	10

(*) Tyr phosphorylated sites that were previously identified in *M. tuberculosis* H37Rv (Kusebauch 2013)

(^) Tyr phosphorylated sites in *M.smegmatis*

a) Uniprot protein accession number

b) Phosphorylated Tyr (Y) and respective Localization probability

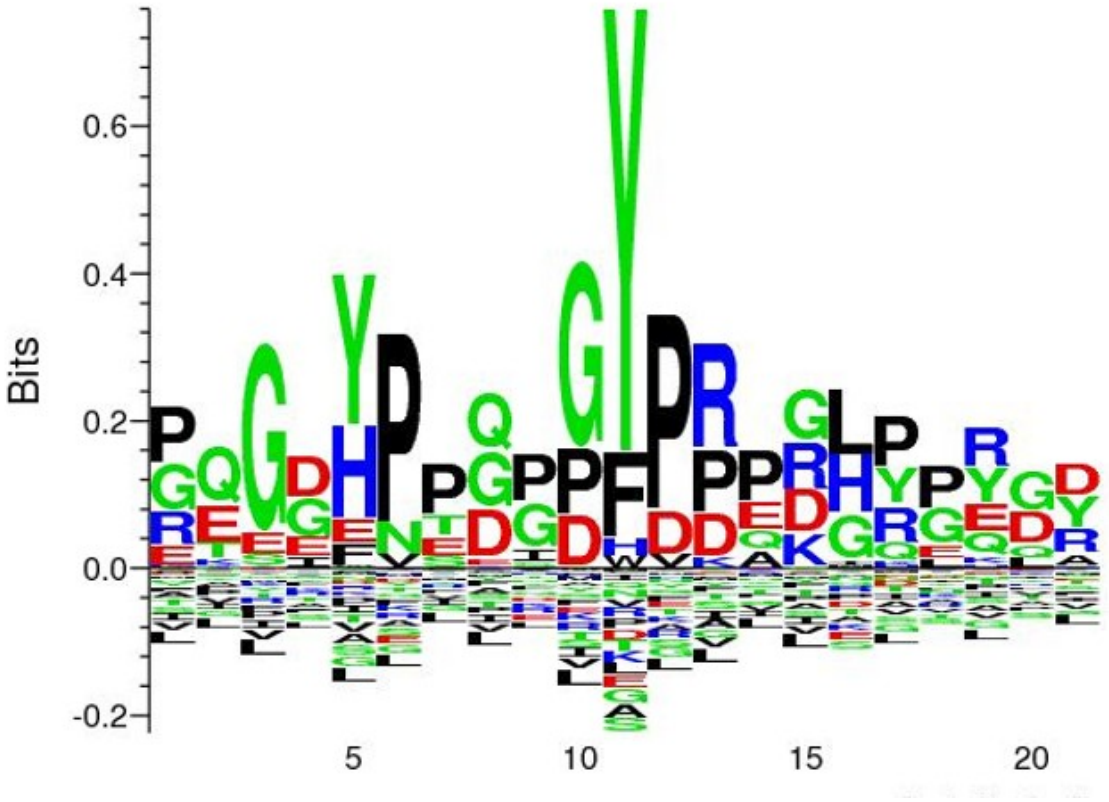

Figure 3-10: Seq2Logo alignment analysis derived from 60 kDa chaperonin revealed an overrepresentation of Tyr358. Seq2Logo analysis indicate that a conserved Tyr358-360 is found in additional three pathogenic species, specifically Shigella spp, Klebsiella spp and Salmonella spp

3.3.4 Functional characterization and localization of phosphoproteins

To understand how mycobacterial phosphoproteins are organized within a cell - which provides physiological context to their function - we predicted the subcellular localization of all the phosphorylated proteins corresponding to the identified phosphopeptides (**Table 3.2**) using the TBpred webserver that predicts

mycobacterial proteins based on their subcellular localization (available at http://www.imtech.res.in/raghava/tbpred/). Predicted Gene Ontology (GO) cellular functions of identified phosphoproteins with high confidence from two mycobacterium strains were obtained from DAVID (The Database for Annotation, Visualization and Integrated Discovery (DAVID) v6.7*)* and were grouped into functional categories. To compare the identified phosphoproteomes of these two mycobacterial species, we identified homologues of the *M. smegmatis* phosphorylated proteins in *M. bovis* BCG using the University of Cape Town's Computational Biology online bioinformatics tool found at http://galaxy-fen.uct.ac.za/root. Gene ontology (GO) terms revealed that in both *M. bovis* BCG and *M. smegmatis*, the phosphoproteins/phosphosites were functionally enriched in nine distinct groups, (e.g. ATP binding, translation, kinase activity, cell division). Of interest, a great deal of phosphorylated proteins in *M. bovis* BCG was clustered into the Transmembrane group (**Figure 3.7**). This included a considerable number of multiple phosphorylated proteins and some phosphorylated in internal as well as external regions, like BCG_3967, it is a probable trans-membrane protein and we found it to be phosphorylated four times, at position 10, which like on the flagellin domain and position 801 and 801, the kinase domain. This suggests that there are transmembrane proteins with a potential role in signal transduction. Additionally, it was visible that *M bovis* BCG phosphoproteome comprised a notable group of phosphoproteins involved in cell division, possible implications of this is discussed later.

Table 3-2: Summary of the phosphorylated sites found in more than one Mycobacterial species

ACc.number [a)]	**Protein description**	***M. bovis* BCG**	***M. smegmatis***	**Mtb H37Rv***
P65727	Ser/Thr-protein kinase PknA	Ser_{309} [b)]	Ser_{310}	Ser_{309}
		Ser_{316}	Thr_{316}	-
		Ser_{299}; Thr_{301};Thr_{302}	-	Ambiguous Residues $_{299-302}$
		Thr_{224}		Thr_{224}

P0A5S5	Ser/Thr-protein kinase PknB	Thr_{173}	Thr_{173}	Thr_{173}
		Thr_{171}	Thr_{171}	-
Q02251	Mycocerosic acid synthase	Ser_{2111}	-	Ser_{2111}
Q7TVL9	Possible acyltransferase	Ser_{230}	-	Ser_{230}
P64169	Cell division protein FtsQ	Thr_{24}	-	Thr_{24}
Q7TY31	Conserved alanine and glycine and valine rich	Thr_{232}	-	Thr_{232}
Q7U2K5	Possible conserved transmembrane transport protein MMPL3	Thr_{910}	-	Thr_{910}
		Thr_{893}	-	Thr_{893}
Q7U2N3	Probable conserved MCE associated membrane protein	Thr_{16}	-	Thr_{16}
Q7VEQ4	L-aspargine permease 1	Thr_{474}	-	Thr_{474}
Q7U280	Isoniazid inductible gene protein	Ser_{62}	-	Ser_{62}
		Ser_{58}	-	Ambiguous residues $_{58-66}$
P65379	Putative membrane protein mmpS3	Thr_{66}	-	Thr_{66}
		Thr_{47}	-	Thr_{47}
		Thr_{50}	-	Thr_{50}
P0A515	Guanylate Kinase	Thr_{9}	-	Thr_{9}
Q7TXB8	Phosphoglucomutase PGMA	Ser_{147}	Ser_{147}	Ser_{147}
		-	Ser_{142}	Ambiguous residues $_{135-152}$
P0A521	60 kDa chaperonin 2	Thr_{146}	-	Thr_{146}
P45811	30S ribosomal protein S4	Thr_{147}	-	Thr_{147}
Q7U046	Probable lipase LIPH	Ser_{165}	-	Ser_{165}
Q7TXZ1	Cell division transmembrane protein FTSK	Thr_{642}	-	Thr_{642}
P66947	Probable acetolactate synthase	Thr_{5}	-	Thr_{5}
P66843	Signal recognition particle receptor FtsY	Thr_{72}	-	Thr_{72}
P66890	Sec-independent protein translocase TatA	Thr_{60}	-	Thr_{60}
		Thr_{78}	-	Thr_{78}
P0A549	Chaperone protein DnaJ1	Thr_{120}	-	Thr_{120}
Q7TVL6	Possible phosphotransferase	Ser_{250}	-	Ser_{250}
P6387	Chaperone protein ClpB	Thr_{79}	-	Thr_{79}
P63857	Cytochrome c oxidase	Thr_{7}	-	Ambiguous

				residues $_{2-14}$
	subunit 3	Thr_{13}	Thr_{13}	Ambiguous residues $_{2-14}$
Q7TYA1	Export membrane protein SecF	Ser_{396}	-	Ambiguous residues $_{372-407}$
Q7U241	Probale Phosphoribosylglycinamide	Thr_{206}	-	Thr_{206}
Q7TVC7	Probable peptidoglycan hydrolase	Thr_{43}	-	Thr_{43}
Q7TTR2	Long-chain-fatty-acid-AMP FadD32	Thr_{552}	-	Thr_{552}

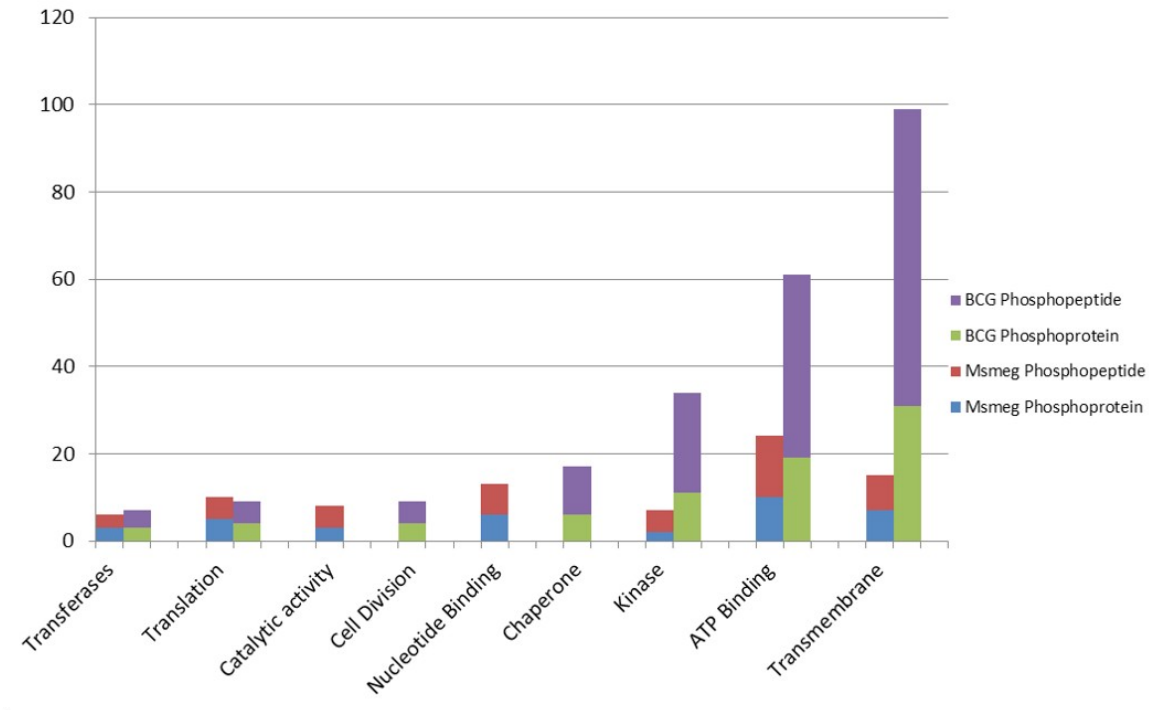

Figure 3-11: A histogram showing the GO molecular functions of identified proteins and phosphoproteins as predicted from their respective genome annotations

.

3.3.5 Sequence alignment of all identified phosphopeptides

The differences between the compared phosphoproteomes compelled us to investigate whether some of these dissimilarities could be explained by genomic events rather than post-translational control. We aligned genomic sequences of both strains using the online tool, obtained from http://www.ebi.ac.uk/Tools/msa/clustalw2/ and respective fasta files were obtained from Uniprot. The multiple sequence alignment of 130 selected *M. bovis* BCG phosphoproteins with their respective *M. smegmatis* orthologues (**Data available as supplementary Figure S3A, Nakedi et, al 2015**) revealed that from 197 *M. bovis* BCG Ser/Thr/Tyr phosphorylated sites: 12 are conserved across the two mycobacterial species and were found to be phosphorylated in both species, while 94 conserved Ser/Thr/Tyr residues were found to be phosphorylated in *M. bovis* BCG only. Furthermore, whereas 91 *M. bovis* BCG phosphorylated residues were aligned with a different non-phosphorylated *M. smegmatis* residue, 72 of these were aligned with a non-phosphorylated amino acid and 19 were aligned with different non-phosphorylated Ser/Thr/Tyr residue. Conversely, the multiple sequence alignment of 64 *M. smegmatis* phosphoproteins with their respective *M. bovis* BCG orthologues showed that besides the 12 conserved Ser/Thr/Tyr residues phosphorylated in both species, 31 conserved residues were found to be

phosphorylated in *M. smegmatis* only. In this case, while 43 *M. smegmatis* phosphorylated residues were aligned with a different non-phosphorylated *M. bovis* BCG amino-acid, 36 of these were aligned with a non- phosphorylated amino acid residue and 7 were aligned with different non- phosphorylated Ser/Thr/Tyr residue.

3.4 Discussion

Phosphoproteomic Analysis Reveals Conserved Ser/Thr/Tyr Phosphorylated Sites Across Mycobacterial Species.

Macek et al. 2008 reported evidence of a possible high degree of conservation within potential bacterial phospho-sites although, as noted by those authors, the conservation of residues does not mean that they are phosphorylated in all species. In fact, as the number of bacterial phosphoproteomic studies increases, it is becoming clearer that the degree of conserved phospho-sites among bacterial species is rather limited and certainly lower than reported within eukaryotic phosphoproteomes (e.g. [179]). Here, a comparison between the *M. smegmatis, M. bovis* BCG and *M. tuberculosis* H37Rv [29,31] phosphoproteomes

revealed that these three mycobacterial species share a number of conserved phosphorylated sites (**Table 3.2**). Interestingly, we found that *M. bovis* BCG and *M. tuberculosis* H37Rv phosphoproteomes share at least 32 Ser/Thr conserved phospho-sites on 27 proteins, of which three were conserved in all three species (**Table 3.2**). As pointed out by Freschi and colleagues [179], phosphorylation sites that are phosphorylated in different species are more likely to be functional and this conservation criterion could be used to prioritize phosphorylation events for additional characterization.

In the present study we have focused in particular on the STPKs PknB and PknA that have known or predicted functions in cell wall generation and growth in *M. smegmatis, M. bovis* BCG and *M. tuberculosis* [31,180]. We found PknB to be phosphorylated in Thr_{173} in all three species and in Thr_{171} in *M. smegmatis* and *M. bovis* BCG (**Table 3.2**). Previous *in vitro* assays demonstrated that both Thr_{173} and Thr_{171} are conserved auto-phosphorylated residues that lie in the activation loop of PknB [181]. Additionally, a *M. tuberculosis* double mutant Thr_{171}/Thr_{173} was 300-fold less active than respective wild-type PnkB, suggesting a combined effect of both Thr_{171} & Thr_{173} residues on kinase activity. Subsequent studies confirmed that the mutation of these residues had a strong effect not only on PknB kinase activity but also in the process of activation loop-mediated recruitment of its substrates [182]. Here we have provided evidence that Thr_{173} and Thr_{171} phosphorylation both occur *in vivo* during the exponential phase, at which PknB is most abundant and is thought be at its maximum activity. Thus, our data reinforces a previous hypothesis suggesting that *in vivo* this enzyme is regulated through an auto-phosphorylation mechanism involving the phosphorylation state of *both* Thr_{173} and Thr_{171}.

Another proposed mechanism of PknB regulation relates to the maintenance of an inactive state *via* the interaction of the juxtamembrane region with the kinase domain. In this model, the auto-phosphorylation of specific residues in the juxtamembrane sequences releases the inhibition by making the sequence available for further interactions with domains of target proteins [183]. However, previously it was not clear whether Thr_{294} and/or Thr_{309} were the target residues involved so it is notable that our data clearly demonstrate that PknB of *M. bovis* BCG is in fact phosphorylated on Thr_{309}.

Our analyses indicate that PknA is phosphorylated in at least one conserved residue, Ser_{309}/Ser_{310} (**Table 3.2**). Intriguingly, in this study *M. bovis* BCG PknA was found to be phosphorylated on seven different residues (three Ser and four Thr respectively), all located in the juxtamembrane region. Unlike PknB, in PknA the juxtamembrane region, encompassing residue 269-338 is indispensable not only for auto-phosphorylation of PknA but also for its substrate phosphorylation ability [184]. STPks exhibit a wide variety of mechanisms for their regulation. Taking into account the degree of phosphorylation verified here in the juxtamembrane region of *M. bovis* BCG PknA compared to that observed in *M. smegmatis* PknA, it is tempting to speculate that this level of phosphorylation of the juxtamembrane region could be in fact limiting the access of PknA to its substrates and this way controlling the action of the enzyme. Importantly, whilst the structure and mode of activation of PknB and PknA have been well established *in vitro*, the structure-function relationships of the various domains have yet to be investigated in the context of mycobacterial growth [185]. Here through a MS based phosphoproteomic approach we have established (at the phospho-site level) the phosphorylation state of different domains for both PknA and PknB *in vivo* during growth at exponential phase.

Sequence alignment of phosphorylated residues

The differences observed between the two phosphoproteomes can be explained by the absence of the corresponding amino acid residue, indicating that during exponential growth phase these two mycobacterial species present an inherently

different sub-set of Ser/Thr/Tyr kinase substrates. Additionally, there are some interesting examples in which orthologous proteins were phosphorylated at different p-sites. This suggests that kinase specificities for a substrate could be intimately related with the actual site of phosphorylation. Finally, it is notable that on those occasions that the STY residue was aligned with different Ser/Thr/Tyr residue (in most cases S for T and vice versa) in some punctual situation the respective residue was phosphorylated (eg PknB) but for most of the cases these were aligned with non-phosphorylated Ser/Thr/Tyr residue. This intriguing observation leaves open the possibility that Ser/Thr exchange could be a result of an evolutionary processes/environmental adaptation, in which the replacement for the respective residue would probably favour site phosphorylation and therefore the gain of an additional mechanism of protein functional regulation. Although speculative, it would be interesting to explore further in which conditions these subsets of Ser/Thr/Tyr sites are phosphorylated.

Finally, the number of phosphoproteins/sites identified in *M. smegmatis* is comparable to those reported in other soil bacteria, e.g. *E. coli* [12,186], *Bacillus subtilis* [147] and *Pseudomonas putida* [19], as well as in some pathogenic bacteria such as *Pseudomonas aeruginosa* [19], *Streptococcus pneumonia* [187], *Helicobacter pylori* [7] and *Klebsiella pneumonia* [20]. Whereas, the number of phosphorylated Ser/Thr/Tyr detected in *M. bovis* BCG phosphoproteome is comparable to that described in *M. tuberculosis* H37Rv [29]. It is of particular interest that the *M. bovis* BCG phosphoproteome shows a number of phosphoproteins/sites that are orthologous to those reported in *M. tuberculosis* H37Rv [29] but also a number that are not conserved. Recently a comparison between the Ser/Thr/Tyr phosphoproteomes of *Acinetobacter baumannii* reference strain (ATCC17978) and a highly invasive, multidrug resistant clone (AbH12O-A2) demonstrated that, during stationary phase, the multidrug isolate showed twice as many phosphorylation-events as the reference strain [11]. In contrast to reports on *Pseudomonas* species [19], our current study supports the notion that bacteria within the same genus/species may utilize differing numbers of phosphoproteins

Phosphorylation Events Observed in Proteins that Regulate Mechanisms of Growth and Cell Division.

Both PknA and PknB are encoded by genes (*pkn*A and *pkn*B respectively) located on the same operon as protein phosphatase PstP, RodA (implicated in cell shape control) and PbpA (implicated in peptidoglycan synthesis) [27]. This locus includes also two FHA (forkhead-associated) domain-containing proteins and in mycobacteria is found near the origin of replication. In *M. bovis* BCG, all proteins referred to above (except PbpA) were found phosphorylated at a total of 15 p-sites: PknA [38]; PknB [181]; RodA [167]; PstP [167] and FHA domain containing protein [181]**.** In *M. smegmatis*, however, only a few proteins were found phosphorylated at a total of 5 p-sites: PknA; PknB and FHA domain containing protein. These observations suggest that the slow growth of *M. bovis* BCG preserves this central set of cell division proteins under a tight regulatory network in which key elements are intimately inter-related by an important series of functional (de)phosphorylation events. For example, PknA and PknB are regulated by PstP-mediated phosphorylation [38,181]; additionally, recently it has been shown that both PknA and PknB phosphorylate PstP [188].

As discussed above, our results showed that both *M. smegmatis* and *M. bovis* BCG PknB has conserved phosphorylation on Thr_{171} and Thr_{173} – both of which sites are known to be substrates for PstP – thus suggesting that in both cases PstP is at least partially inactive. This would make sense considering that during exponential phase PknA and PknB are likely to be at their peak of activity. PstP has been reported to be phosphorylated by PknB on Thr_{173}, Thr_{141}, Thr_{290} and Thr_{137} in its cytosolic domain and on Thr_{174} by PknA [188]. Curiously phosphorylated PstP has been reported to be more active than its unphosphorylated form [188]. Here, our results indicate that PstP of *M. bovis* BCG is phosphorylated *in vivo* on the high confidence p-site, Ser_{155}. Interestingly, PstP contains three metal-binding centres in its structure [189], sharing the fold and two-metal centre of human PP2Cα whilst having a third Mn^{2+} in a site created by a large shift in a flap domain next to the active site; this Mn^{2+} occurs at the position of Ser_{160} so it is plausible that phosphorylation of Ser_{155} may directly interfere with PstP activity, thus accounting for our deduction here of reduced PstP activity during exponential phase growth.

Overall, *M. bovis* BCG has 3 times more STPks and nearly 4 times respective p-sites compared to *M. smegmatis*. Apart from PknA and PknB, the *M. bovis* BCG phosphoproteome is comprised of PknG (Thr_{95}), PknH (Thr_{174}), PknE (Ser_{304} and Ser_{326}) PknF (Thr_{287}). Some of these enzymes have previously been directly implicated in mycobacterial growth (e.g. PknG [9], PknH [55], PknE and PknF [190]) and it is therefore conceivable that some of the proteins comprising the *M. bovis* BCG phosphoproteome are in fact substrate of some of these phosphorylated protein kinases (*vide infra*). It is worth noting that our study has also identified several Two Component sensory signal transduction proteins as phosphoproteins (e.g. Two component sensory transduction protein regX3 (Thr_{151} & Thr_{153}), Two component sensor histidine kinase ppr (Ser_{446}), Two component transcriptional regulatory pprA (Ser_{20}). These results are reminiscient of those previously described in *B. subtilis* [191] and suggest that in *M bovis* BCG there may be cross talk between Ser/Thr/Tyr phosphorylation and Two component systems, which would add extra complexity to the overall protein phosphorylation signal transduction pathways regulating exponential growth of *M. bovis* BCG cells.

Phosphorylation Events Observed in Proteins that Regulates Mechanisms of Cell division and elongation

In mycobacteria, cell elongation is regulated by a macro complex that regulates peptidoglycan remodeling during growth by means of hydrolytic and synthetic roles (as reviewed by [168]). Our data indicate that in *M. bovis* BCG, three important proteins of the macromolecular elongation complex are phosphorylated during exponential growth, namely Wag31 (Ser_{245}), CwsA (Thr_{77}) and a putative hydrolase (BCG_0021 involved in peptidoglycan catabolic process) (Thr_{43}). In mycobacteria, Wag31 is phosphorylated by PknA and is essential for correct polar localization and biosynthesis [42,192]; in addition, Wag31 is stabilized by the cell wall protein CwsA. Wag31 is thought to be phosphorylated during exponential phase and remains non- or lowly-phosphorylated during stationary phase [39,40]. Interestingly, Wag31, CwsA and the putative peptidoglycan hydrolase

were not found amongst the *M. smegmatis* phosphorylated proteins in the present study. Whilst we cannot rule out that our assay did not isolate phosphorylated *M. smegmatis* Wag31, it is perhaps more likely that in the fast-growing *M. smegmatis* the elongation complex is regulated by alternative non-phosphorylated mechanism.

Another macromolecular complex, named divisome, is responsible for mycobacterial cell division. Assembly and disassembly of this complex is regulated by protein phosphorylation [168]. According to our data, in *M. bovis* BCG there are five divisome proteins which are phosphorylated, including cell division FtsQ (Thr_{24}), FtsW-like protein (Thr_{29}), CwsA (Thr_{77}) as well as other additional phosphorylated cell division proteins such as RodA (Thr_{463}), cell division transmembrane protein FtsK (Thr_{325}; Thr_{642}) and FtsY (Thr_{72}), strongly suggesting that divisome assembly and indeed cell division in *M. bovis* BCG is subject to a high level of phosphorylation.

Of interest, in our analysis we have detected Hup, a conserved histidine-like protein, phosphorylated on three different p-sites (Thr45, Thr65 and Ser90). In Mycobacterium sp., the homologue of Hup (Mhpl) is implicated in bacterial adaptation to stress response conditions, possible inhibition of cellular metabolism and reduction of bacterial growth rate through nucleoid reorganization [193–195]. Apparently, hup is expressed in exponentially growing cells of *M. tuberculosis* H37Ra and it is shown to be maximally expressed during stationary phase, while Hup kinases (PknE, PknF and PknB) were found to be constitutively expressed during exponential phase [190]. It has been suggested that the phosphorylation of HupB during the exponential phase by the referred kinases would limit the interaction with DNA [190]. In our *M. bovis* BCG data we have identified all the intervenient proteins involved in the described posttranslational regulation mechanism, including the phosphorylation of phosphosite Hup Thr65. It is therefore appropriate assume that the same mechanism takes place in *M. bovis* BCG exponential growing cells and although under limited action it remains possible that the rate of unphosphorylated HupB would have an impact on the overall growth rate. In contrast, we did not find any evidences indicating that similar mechanism operates in *M. smegmatis* exponential growing cell.

Stress Related Proteins

In rich broth during exponential phase, bacteria experience nearly optimal conditions of growth where there is excess nutrients and little accumulation of by products, in addition to scarce competition between bacterial cells. Surprisingly, under these conditions we observed an unexpected number of chaperones and stress related proteins in the *M. bovis* BCG phosphoproteome: For instance, hyperosmotic and heat shock related proteins such as the chaperon protein DnaJ (Thr_{120}) chaperon protein DnaK (Ser_{558}) and GrpE (Ser_{12} and Thr_{2}), multiply phosphorylated 60 kDa chaperonin, ,10 kDa chaperonin, and Copper-sensing transcriptional repressor CsoR (Thr_{93}). On the other hand, none of these stress related proteins were found in the *M. smegmatis* phosphoproteome, which suggests that even under optimal environmental conditions, slow growing mycobacteria such as *M. bovis* BCG maintain a preventive basal level of stress-related proteins that may act as frontline defence barrier to ensure adequate and prompt response to any sudden change in local environmental conditions. In this scenario protein phosphorylation would keep most of these proteins in an inactive state, whereby dephosphorylation could then immediately recruit these proteins when environmental conditions become unfavourable. A convenient and versatile regulatory mechanism such as this could in fact be a determinant for the survival and persistence of some bacteria.

3.5 Conclusion and perspectives

This work demonstrated that there are major differences between a fast growing and a slow growing mycobacterial phosphoproteome. The *M. smegmatis* phosphoproteome observed here is in many aspects similar to those reported in other soil-dwelling bacterial models and can be viewed as a minimalist phosphoproteome compared to that of *M. bovis* BCG. This latter organism presents a much more complex and sophisticated protein phosphorylation network, regulating important cellular cycle events such as cell wall biosynthesis,

elongation, and cell division, as well as apparently being involved in regulating response to stress, which over all would allow a quick cellular response to abrupt environmental changes. However, this regulatory advantage might be associated with a cost, reflected by reduced metabolic fitness and slower growth rate.

The results of this section of the thesis demonstrates *M. bovis* BCG is a good model to study aspects of mycobacterial phospho-dependent signal transduction pathways, including those involved in persistence and slow growth, including that associated with drug resistance. By contrast, the substantial differences reported here in the phosphoproteomes of *M. smegmatis* and *M. bovis* BCG suggest that exponentially growing *M. smegmatis* cells *in vitro* are of limited relevance when modelling phosphorylation networks and phospho-regulation events likely to occur in *M. tuberculosis* at the site of disease during an infection.

4. IDENTIFICATION OF PHYSIOLOGICAL SUBSTRATES OF *M. BOVIS* BCG PROTEIN KINASE G (PKNG) IN ACTIVELY GROWING CULTURE BY LABEL-FREE MASS-SPECTROMETRY BASED PHOSPHOPROTEOMICS

(Based on Nakedi et.al. 2018)

Abstract

Mycobacterial Ser/Thr kinases play a critical role in bacterial physiology and pathogenesis. Linking kinases to the substrates they phosphorylate *in vivo*, thereby elucidating their exact functions, is still a challenge. The aim of this work was to associate protein phosphorylation in mycobacteria with important subsequent macro cellular events by identifying the physiological substrates of PknG in *Mycobacterium bovis* BCG. The study compared the phosphoproteome dynamics during the batch growth of *M. bovis* BGC versus the respective PknG

knock-out mutant (ΔPknG-BCG) strains. We employed TiO_2 phosphopeptide enrichment techniques combined with label-free quantitative phosphoproteomics workflow on LC/MS/MS. The comprehensive analysis of label-free data identified 603 phosphopeptides on 307 phosphoproteins with high confidence. 55 phosphopeptides were identified, 28 were differentially phosphorylated between the two strains, whilst 23 phosphopeptides were phosphorylated in *M. bovis* BCG wild-type only and not in the mutant. These were further validated through targeted mass spectrometry assays (PRMs). Kinase-peptide docking studies based on a published crystal structure of PknG in complex with GarA revealed that the majority of identified phosphosites presented docking scores close to that seen in previously described PknG substrates, GarA, and ribosomal protein L13. Six out of the 23 phosphoproteins had higher docking scores than GarA, consistent with the proteins identified here being true PknG substrates. Based on protein functional analysis of the PknG substrates identified, this chapter confirms that PknG plays an important regulatory role in mycobacterial metabolism, through phosphorylation of ATP binding proteins and enzymes in the TCA cycle. This work also reinforces PknG's regulation of protein translation and folding machinery. This chapter reveals a new set of protein targets that may help to elucidate the exact physiological role of PknG and its associated phosphorylation networks during adaptive strategies in mycobacteria to changing environments.

4.1 Introduction

In bacteria, protein phosphorylation is a central mechanism for signal transduction of important cellular events, as reviewed previously [2,6,196,197]. There is increasing supportive evidence indicating that in mycobacteria, Ser/Thr phosphorylation plays a critical role both in the physiology as well as the virulence of this intracellular pathogen [18,36,53,67,170,198–200]. Interestingly, mycobacteria have an unusually large repertoire of kinases for a bacterium, including 11 two-component system and 11 Serine/Threonine protein kinases (STPKs) (PknA-PknL) [3,22,26,27]. Inference of the possible biological role of these STPKs is critically dependent on knowledge of the substrates they phosphorylate *in vivo*. Therefore, a detailed characterization of physiological STPK substrates is essential to gain a better understanding of the mechanisms by which protein phosphorylation regulates important biological responses in mycobacteria [28].

Of all mycobacterial kinases, Protein Kinase G (PknG) is perhaps the best studied, yet, remains the most intriguing. Unlike the majority of other STPKs, PknG exists as a dimer and since it has no membrane-bound domain, is found in the cytosol of mycobacteria [61,67,156]. This protein kinase is ubiquitously present in the Mycobacterium genus and it plays different roles in mycobacterial physiology as well as in pathogenicity. For instance, PknG is known to phosphorylate *in vivo* the mycobacterium fork-head associated protein (FHA) GarA [182], which is important in glutamate metabolism [18,37,70]. Additionally, PknG has been also implicated in the regulation of other important physiological roles such as biofilm formation and redox homeostasis [64] and intrinsic resistance to antibiotics [65]. Importantly, experimental evidence shows that, upon macrophage infection, inactivation of PknG, either by gene disruption or chemical inhibition, results in the intracellular trafficking and localization of PknG-deficient *Mycobacterium bovis* Bacille Calmette-Guérin (*M. bovis* BCG) into the phagolysosome and ultimately to mycobacterial cell death [36,67]. A recent study also demonstrated its role in the survival of mycobacteria following *in vitro* induction of a non-replicating state [201]. Despite this suggested essential role of PknG in ensuring bacterial environmental adaptation and survival, GarA has until recently been the only known and validated substrate for PknG [18,70,202] although a recent study reported that PknG also phosphorylates the 50S ribosomal protein L13 *in vivo* which is important in

biofilm formation and maintaining redox homeostasis [64]. However, these two substrates alone seem insufficient to account for the phenotype of PknG knock-out strain of *M. tuberculosis*. In addition, our previous work in this area strongly suggests that each Ser/Thr kinases in *M. bovis BCG* phosphorylates multiple substrates[203]. Thus, to gain new insights into the protein phosphorylation networks by which PknG mediates important physiological functions, it is crucial that we identify a more comprehensive list of its verified substrates.

Recent advances in mass spectrometry-based methods have revolutionized the research field of phosphoproteomics by allowing global and accurate quantitative analysis of protein events at the phosphopeptide level [11,12,17,30,32,48,80,109,110,146,147]. In addition, several studies using quantitative phosphoproteomics have identified hundreds of kinase substrates in varying eukaryotic systems [79,108,145,148,149]. More recently, similar quantitative phosphoproteomic analyses have been successfully applied to identify novel substrates of *Bacillus subtilis* Ser/Thr kinase PrkC and phosphatase PrpC [110] as well as of the MAPK Hog1 in yeast [150] and in human cells [79].

4.2 **Aims:**

Despite the increasing utility of large-scale proteomics for the *in vivo* identification of novel kinase substrates, to our knowledge, such an approach has yet to be employed in the search for mycobacterial STKPs substrates. As a proof of principle, we therefore aimed to present the first systematic application of large-scale phosphoproteomic analysis to screen for and verify *in vivo* novel physiological substrates of mycobacterial STPKs.

4.3 Results

4.3.1 Growth monitoring of bacterial strains

M. bovis BCG Pasteur 1172 reference strain and *M. bovis* BCG ΔPknG knock-out mutant were grown in nutrient rich 7H9 broth media and growth rates compared. **Figure 4.1(a)** shows growth curves monitored by measuring optical density (OD_{600}) of the culture over time. The PknG knock-out mutant grew at the same rate as the wild-type strain, in line with previous studies [67,200]. We then validated that the knock-out mutant was indeed lacking PknG by targeted mass spectrometry (PRM). PknG peptides identified by discovery mass spectrometry were quantified by PRM in both strains as illustrated in **Figure 4.1(b)**. PknG peptides were unambiguously identified in the wild type reference strain but not in the ΔPknG knock-out mutant

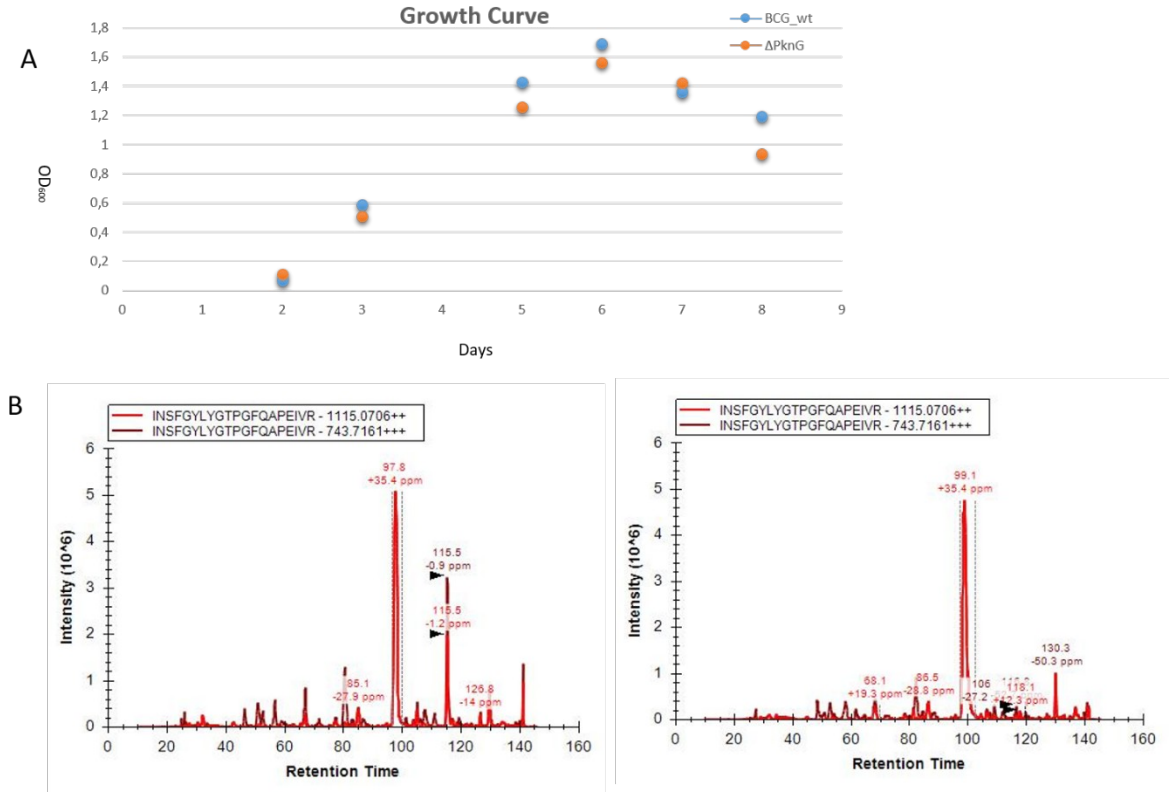

Figure 4-12: (A) Growth curves measured by OD600 of the M.bovis BCG strains used in this study in nutrient rich 7H9 media. Both the Wt and the PknG knock-out mutants had comparable growth rates. This is in line with what has been previously observed in literature. (B) PknG peptide (INSFGYLYG) identified exclusively in the wild type M.bovis BCG and unambiguously absent in the PknG knock-out mutant by PRM analysis

4.3.2 Identification of physiological substrates for PknG

We employed large-scale label-free quantitative phosphoproteomics to study global phosphorylation dynamics associated with *M. bovis* BCG PknG and to identify *in vivo* physiological substrates for this kinase in actively growing bacterial cells in rich media, to try to understand the regulatory role it plays whilst in the cytosol. We compared the phosphoproteome of wild-type and PknG knock-out strains of *M.bovis* BCG, in biological triplicate. The experimental workflow is shown in **Figure 4.2**. The rationale is that peptides phosphorylated in the presence of PknG and not in the mutant strain would be considered as possible substrates of PknG. Peak height intensities for each phosphopeptide were used to assess phosphorylation. Phosphopeptides with intensity values in all three replicates in the wild type *M.bovis* BCG and not in the mutant lacking PknG were considered as candidate physiological substrates of mycobacterial PknG.

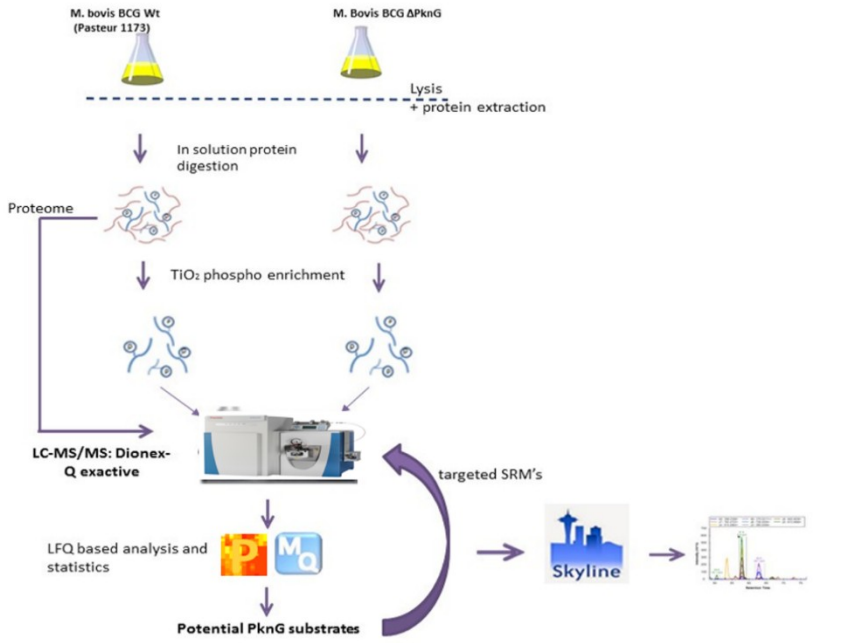

Figure 4-13: Schematic presentation of experimental procedures: Exponentially growing cells of M. bovis BCG reference strain and PknG knock-out mutants were lysed and proteins precipitated and digested with trypsin. Phosphopeptides were enriched for with TiO2 after digestion, followed by liquid-chromatography tandem mass spectrometry (LC/MS/MS). MS data was matched to M.bovis BCG using Maxquant software and downstream statistical analysis on Perseus. Candidate substrates were validated by PRM and analysed in Skyline software

A total of 829 phosphosites (p-sites) were identified. After removing known contaminants and applying filters [80] (localization probability ≥0.75, PEP <0.01, FDR <0.05, Score >40, Delta Score >8), 603 highly confident phosphopeptides were identified on 307 phosphoproteins and were further analysed. Phosphorylated residues were also manually validated by looking at the fragmentation spectra using the Maxquant feature "Viewer" as shown in **figure 4.3**. Approximately 93% of phosphopeptides were singly phosphorylated, while 7% were multiply phosphorylated. The majority of these phosphopeptides were phosphorylated on Thr (64.5%) and Ser (32.84 %) and only a small percentage on Tyr (2.65%). These distributions of p-sites are in line with what we had previously published for the phosphoproteome of *M. bovis* BCG [30], even though we have increased the phosphoproteome coverage by 100% from 442 to 829 p-sites.

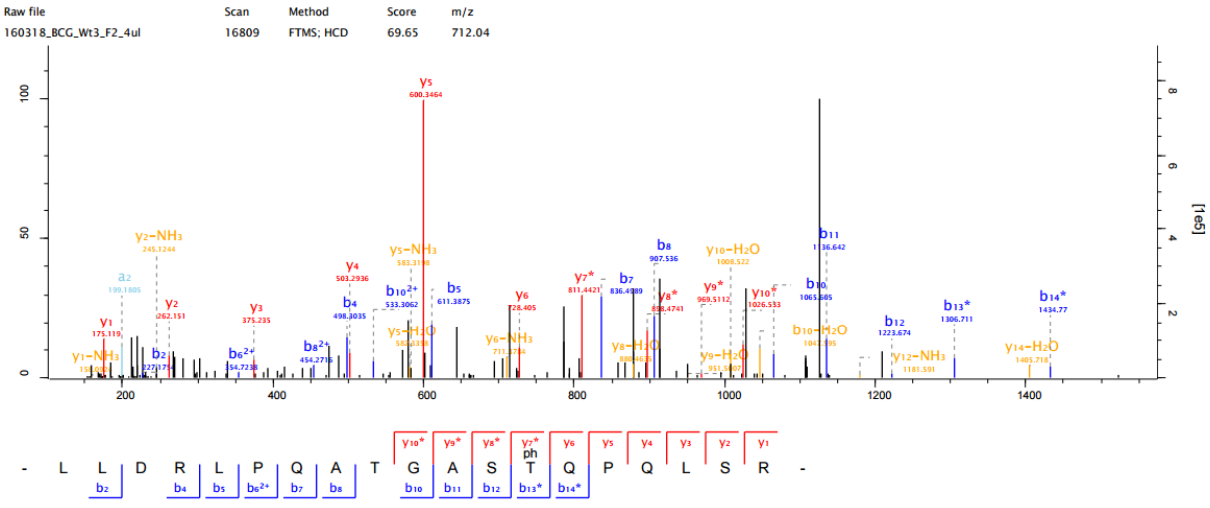

Figure 4-14: Fragmentation spectra of the phosphopeptide showing both b- and y-ions of the phosphorylated peptide from one of the candidate substrate Chaperone protein ClpB

4.3.3 Global phosphorylation changes resulting from PknG gene knock-out

To correlate the global changes at the phosphorylation level as a consequence of PknG gene knock-out, we performed label-free quantitative phosphoproteomic analysis, where we only considered phosphopeptides that were identified in at least two replicates per experiment. Due to the variability introduced by the TiO_2 enrichment step, we normalized the phosphopeptides from the enriched samples by those that could be detected in the unenriched samples according to a previously published workflow named pairwise normalization [145]. The pairwise normalization takes median of the abundance ratios (Normalization factor) of all the phosphopeptides identified in an unenriched sample. After median centering the enriched phosphopeptides, they are then adjusted by the normalization factor of the unenriched phosphopeptides. The principle is that all the phosphopeptides in the unenriched sample are not influenced by the enrichment step which introduces bias, therefore it argues that they can be used to normalize the abundance of phosphopeptides after enrichment. **Figure 4.4** shows our data before and after normalization.

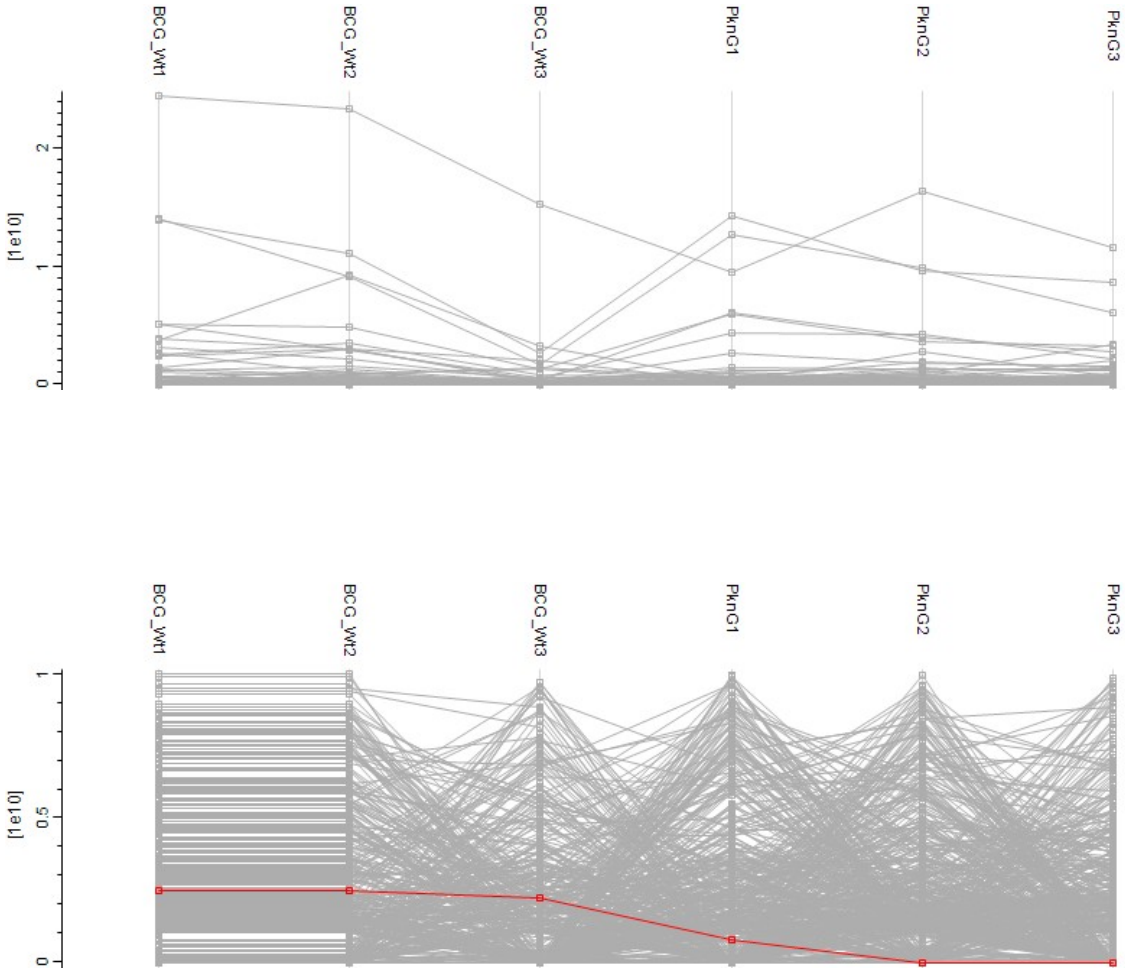

Figure 4-15: A profile plot of the data overview before and after pairwise normalization. The top panel shows the high variability of phosphopeptides between samples and the bottom panel shows the data after rescaling using the median of the phosphopeptides in an unenriched sample unaffected by the enrichment technique.

After normalization and filtering, the differential phosphorylation was determined by a two-sample student's t-test with a significance cut-off *p*-value of 0.05. A total of 31 phosphopeptides were significantly differentially regulated between the wild-type and ΔPknG *M. bovis* BCG strains **(Table 1).** Functional analyses of these differentially phosphorylated proteins showed that they were associated with the biosynthesis of macromolecules, two component system proteins and protein kinase A. For candidate substrates of PknG, we considered those phosphopeptides that were detected in all replicates of the wild-type *M. bovis* BCG but that were not detected in all the replicates of *M. bovis* BCG PknG knock-

out mutant. The 23 p-sites on 22 proteins identified as *bona-fide* candidate substrates of *M. bovis* BCG PknG are summarised in **Table 2**.

Quantification of phosphorylated proteins is important to our understanding of the resultant biological effects. Phosphorylated peptides have an unpredictable ionization when compared to their unmodified pairs, therefore, to ensure that these significantly dysregulated phosphopeptides were not as a result of changes at the proteome level, we performed a quantitative proteome analysis parallel to the phosphoproteomic workflow. All proteomic analyses were done on Perseus version 2.3. We considered all the proteins with intensity values on all three replicates in each experimental group. Logarithmic means (base 2) of the wild type and knock-out mutants were compared using a student's t-test with a cut-off value of p=0.05, and with Benjamini-Hochberg multiple testing correction. Of all the differentially regulated proteins, candidate substrates did not change at the proteomic level, except two (MetE and ClpB, more abundant in the wild-type strain). The lack of change at the protein level is a strong indicator that regulation is at the phosphorylation level and not due to expression levels of the phosphorylated proteins.

Table 4-3:Differentially phosphorylated proteins between Wt M.bovis BCC and PknG knock-out mutant

Gene name	Protein	P-site	Localization probability	-Log Student's T-test p-value
mtrA	Two component sensory transduction transcriptional regulatory protein	T213	1	1.97384
cfp29	29 kDa antigen	T47	0.991988	2.08032
psk13	Polyketide synthase pks13	T569	1	1.85385
ctaE	Probable cytochrome C oxidase (Subunit III) ctaE	T7	0.993445	3.94207
PknA	Transmembrane serine/threonine-protein kinase A	T224	1	2.04384
BCG_1592	Pseudouridine synthase	S56	1	1.41308
35kd_ag	Conserved 35 kDa alanine rich protein	S168	0.971359	1.92842
ansP1	Probable L-asparagine permease ansP1	T474	1	2.59646
rpsQ	30S ribosomal protein S17	T123	0.998357	1.60323
atpFH	ATP synthase subunit b-delta	T78	1	1.59266
BCG_0735	Probable membrane protein	S74	1	1.99181
groL1	60 kDa chaperonin 1	T435	1	1.52333
BCG_134	Uncharacterized protein	S107	0.999885	1.30694
moeW	Possible molybdopterin biosynthesis protein moeW	S107	1	1.48633
infC	Translation initiation factor IF-3	T5	0.932525	1.69633
rpsD	30S ribosomal protein S4	T147	0.999988	1.49155
BCG_0330	Probable conserved transmembrane protein	T4	0.887233	1.64658
BCG_1746	Probable conserved transmembrane protein	T394	0.967662	1.67599
BCG_1664	Probable two-component system transcriptional regulator	S146	0.983817	1.92198
tatA	Sec-independent protein translocase protein TatA	T60	0.999904	1.69263
BCG_1812C	Hypothetical integral membrane protein	T481	0.854165	1.68682
tatA	Sec-independent protein translocase protein TatA	T58	0.999999	1.70645

BCG_2246	Uncharacterized protein	T153	0.984392	1.72215
BCG_0215	Probable conserved MCE associated membrane protein	T62	0.997238	1.4332
BCG_0421c	Possible conserved secreted protein	T210	1	1.31913
PknA	Transmembrane serine/threonine-protein kinase A pknA	S299	1	1.59262
BCG_0194	Probable transcriptional regulatory protein (Possibly tetR-family)	T5	0.983476	1.55204
leuA	2-isopropylmalate synthase	T595	0.999649	1.37648
BCG_0875c	Uncharacterized protein	S82	1	1.94697
metE	5-methyltetrahydropteroyltriglutamate--homocysteine methyltransferase	S95	0.999759	1.3025
mas	Probable multifunctional mycocerosic acid synthase membrane-associated mas	S2111	1	2.70602

Table 4-4: Candidate substrates of PknG only phosphorylated in Wt M.bovis BCG. Known PknG substrates GarA and L13 were not identified in this chapter, however, were included in the analysis for comparison purposes.

Protein Name	Uniprot ID	P-site		Localization Probability	Subcellular Localization	Free Energy	Binding
50S ribosomal protein L2	A1KGI5	S32	1		Cytoplasmic	-2915.29	
Chaperone protein ClpB	A0A0H3M7W9	T79	0.89		Cytoplasmic	-2708.49	
Probable conserved membrane protein	A0A0H3M0X2	S19	0.99		Cytoplasmic	-2704.67	
Uncharacterized protein	A0A0H3M8P9	T12	0.93		Cytoplasmic	-2448.17	
Antitoxin	A0A0H3M1S6	T152	1		Cytoplasmic	-2401.27	
GarA						-2321.83	
Uncharacterized protein	A0A0H3M6A1	S2	0.99		Cytoplasmic	-2250.28	
L13						-2226.24	
Uncharacterized protein	A0A0H3M4P0	S11	0.99		Integral membrane	-2209.59	
metE	A1KHS4	S713	0.99		Cytoplasmic	-2022.95	
ATP synthase subunit beta	A1KI98	S16	0.79		Cytoplasmic	-1856.33	
Uncharacterized protein	A0A0H3M751	Y382	0.99		Cytoplasmic	-1829.71	
ispG	A1KML3	S387	0.97		Cytoplasmic	-1795.16	
Uncharacterized protein	A0A0H3MC79	S277	0.78		Cytoplasmic	-1767.57	
30S ribosomal protein S16	A1KMQ3	S162	0.99		Cytoplasmic	-1735.73	
proline and threonine rich	A0A0H3MAA7	S40	0.98		Integral membrane	-1674.22	

protein		3			
Uncharacterized protein	A0A0H3M751	T371	0.99	Cytoplasmic	-1577.51
DNA gyrase subunit A	A0A0G2Q9F8	S263	1	Cytoplasmic	-1425.1
Uncharacterized protein	A0A0H3M7J9	T7	0.99	Cytoplasmic	-1359.11
Antitoxin	A0A0H3MAL0	T109	0.95	Attached to membrane	-1350.54
Uncharacterized protein	A1KI28	S117	0.83	Integral membrane protein	-1301.16
Uncharacterized protein	A0A0H3M2H1	T25	0.77	Cytoplasmic	-1247.69
RNA polymerase-binding protein RbpA	A0A0H3M6B6	T18	0.95	Cytoplasmic	-1170.72
Malate dehydrogenase	A1KI28	S238	0.92	Integral membrane Protein	-1064.63
Chaperone protein DnaK	A1KFH2	T391	0.99	Integral membrane Protein	-725.77

4.3.4 Validation of candidate substrates by Targeted Mass Spectrometry

To further validate the candidate substrates identified by this phosphoproteomic workflow, we employed targeted mass spectrometry (PRMs). An isolation list for all the peptides that were detected in the wild-type but not in the mutant was created. We selected six of the candidate substrates to be validated by PRMs (Uniprot IDs: A0A0H3M7J9, A1KML3, A1KI28, A0A0H3M0X2 , A1KMQ3, A0A0H3M751), and **Figure 4.5** shows that these phosphopeptides were unambiguously verified to be absent in the PknG mutant but present in the wild-type **(Figure 4.5 (A-C)**. In the remaining cases, we observed a decrease in the amount of the phosphorylated peptide in the PknG knock-out mutant compared to the wild type **(Figure 4.5 (D-F)**. We designed PRM assays to detect both modified (phospho Ser/Thr/Tyr) and unmodified versions of each peptide in the isolation list. We observed a substantial shift in retention during these experiments, which in itself is a technical issue and resulted in the truncation of some extracted PRM chromatograms, so some candidate substrates could not be confidently and unambiguously validated by this targeted approach.

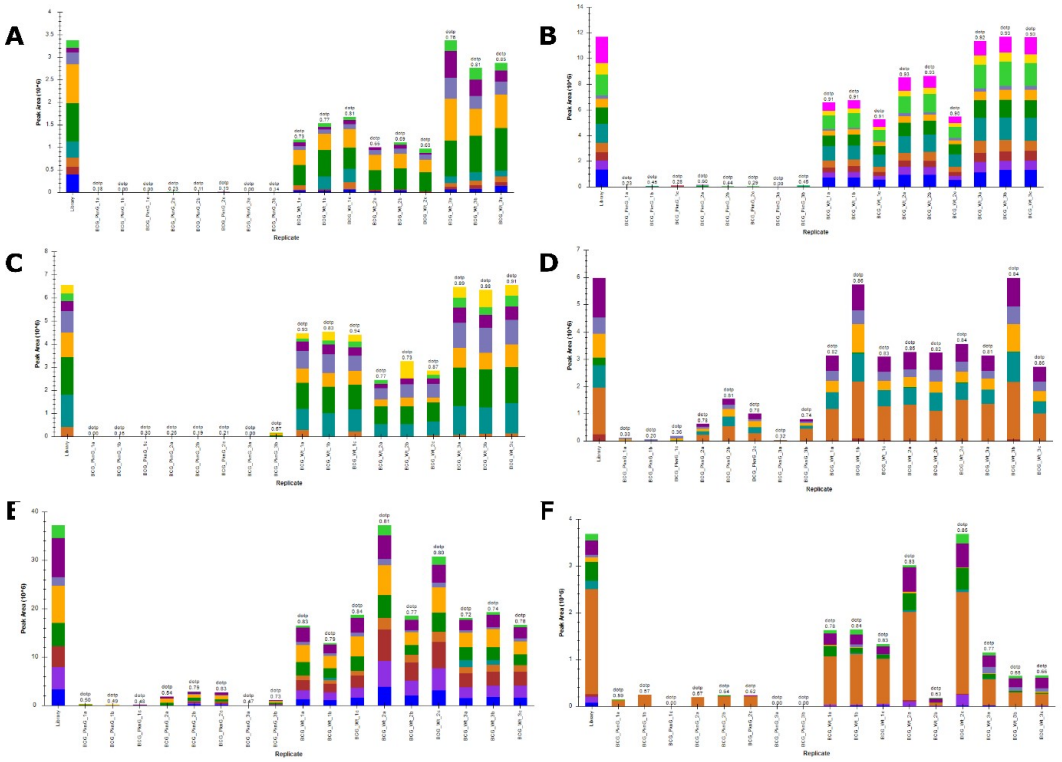

Figure 4-16: Validation of identified phosphopeptides by targeted PRM's. The Top figures (A-C) shows phosphopeptides that were exclusively identified in the Wild type M.bovis BCG and not in the PknG knock-out mutant (A: A0A0H3M7J9 B: A1KML3 C: A1KI28), whilst figure D-F shows differential phosphorylation of the substrates of PknG (D: A0A0H3M0X2 E: A1KMQ3 F: A0A0H3M751).

4.3.5 Kinase-substrate Interactions

To determine if there are any preferential motifs for PknG substrate specificity, we used iceLogo (www.weblogo.berkely.edu) to visualise overrepresented amino acids flanking the phosphorylation sites of candidate substrates that indicate interaction with this kinase **(Figure 4.6)**. This sequence alignment shows a major feature around the (Ser/Thr) phosphorylation site, specifically an over-representation of glycine (G) at position +1 and alanine (A) or proline (P) at position +2. There is also a strong selection of hydrophobic amino acids at these positions adjacent the phosphorylation site. Enrichment for glutamic acid (E), occurred at positions -3 and -5.

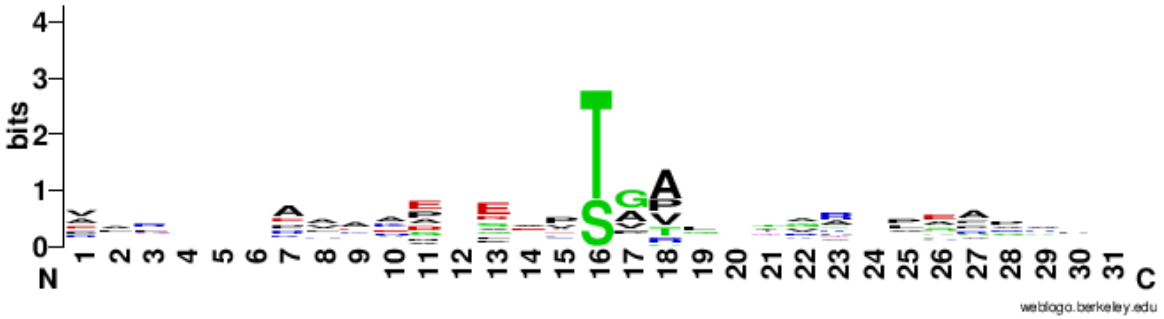

Figure 4-17: Phosphorylation site motif analysis generated using IceLogo. Showing overrepresented amino acids around the phosphorylation site.

The lack of specific motif characteristic of eukaryotic kinases prompted us to investigate the structural basis for the kinase-substrate interaction, using the CABS dock software to simulate interactions of candidate peptides into the catalytic groove of the protein kinase, and with an energy-based optimization that allows for flexibility. Visual analysis was carried out using PyMol version 1.3 software. The crystal structure of PknG in complex with ADP [62] was used as a reference to model the kinase-substrate interactions (PDB ID: 4Y0X). **Figure 4.7(A)** shows the modelling simulation of the validated substrate of PknG GarA kinase-substrates complexes; the highly confident candidate substrates identified in this study interacting with PknG are shown in **Figure 4.7 (B-F)**. Visualization of the interactions shows a unique hydrogen bond between the carboxyl group of Asp211 of the catalytic side of PknG and the γ- hydroxyl group of phosphorylated residues in the candidate substrates. The distance between the hydrogen bonds was within the acceptable distance for protein-peptide interactions, ranging from 2.9 Å for 50S Ribosomal Protein L2, 4.3 Å for Chaperon Protein ClpB, and 3.9 Å for a probable conserved membrane protein

(**A0A0H3M0X2**). These results suggest a similar substrate/kinase interaction to that observed for the GarA interaction with PknG, as well as for the recently proposed substrate of PknG [64], ribosomal L13. The Gibbs free binding energies were predicted and compared to GarA, a previously identified and validated substrate of PknG, as a measure of confidence for binding specificity **(Table 4.2)**. From the 23 candidate substrates, five had lower (better) free binding energy than GarA (-2.3Kcal.mol^{-1}), ranging between -2.4Kcal.mol^{-1} for Antitoxin protein and -2.9Kcal.mol^{-1} for 50S Ribosomal Protein L2, suggesting that these peptides are true interactors of PknG.

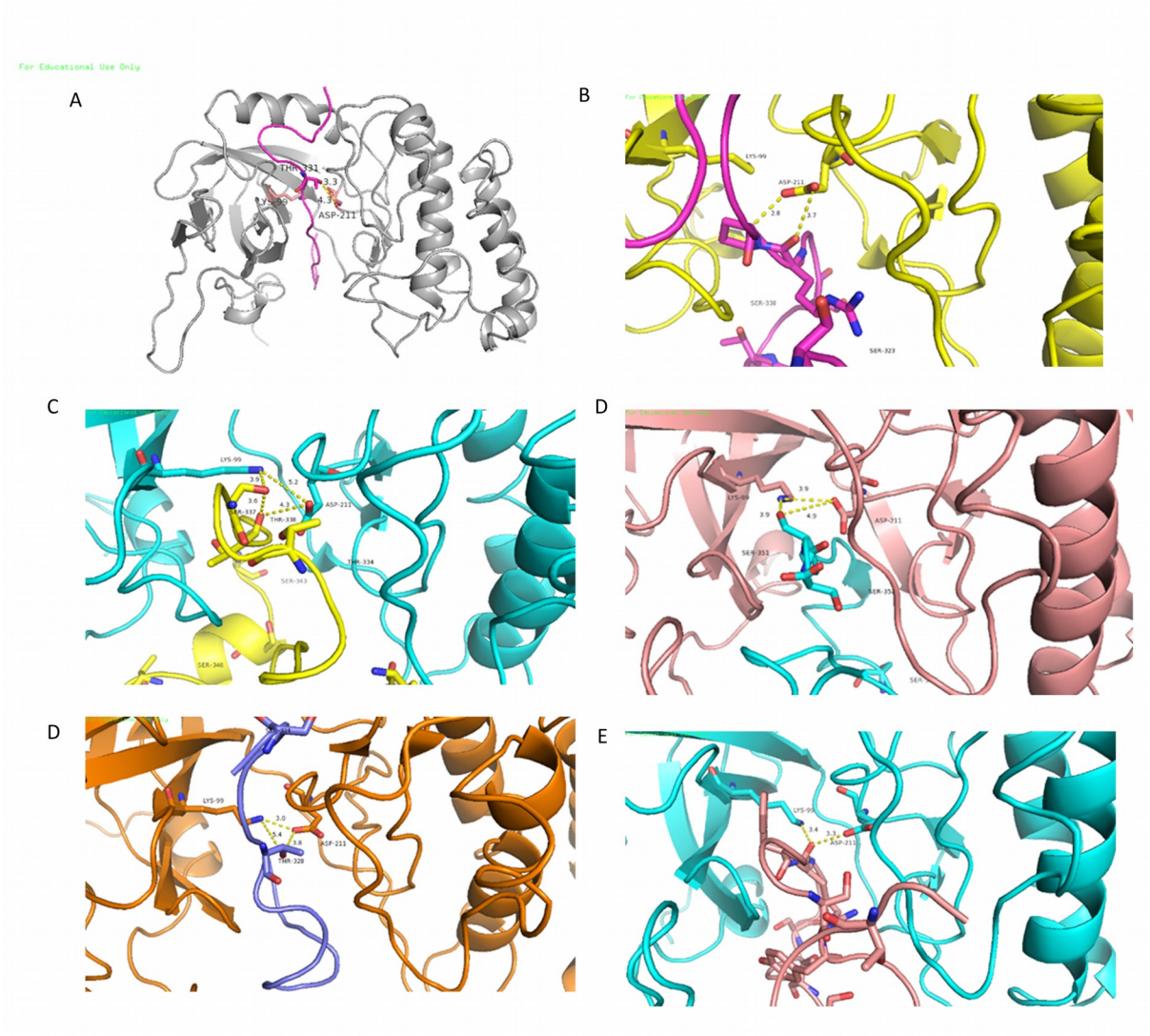

Figure 4-18: (A) PknG binding with (PDB ID: 4Y0X) with GarA. PknG chain in gray colour and GarA peptide in pink. The threonine residue near to the catalytic residues shown as ball and stick model. The - hydroxyl group is within hydrogen bonding distance of hydrogen distance of carboxyl group

of Asp211. ***(B-E)*** *shows the interaction of the high confidence substrates with the catalytic core of PknG.*

4.3.6 Functional and spatial relationships of candidate substrates

Identified candidate substrates of PknG were involved in diverse cellular functions. We used the Uniprot online database to classify the functional categories for each substrate. **Figure 4.8** shows a plot of all the major functional groups represented in the discovery MS analysis. PknG thus appear to regulate a wide variety of biological processes including transcription regulation, metal binding and DNA binding. The most overrepresented categories were ATP binding and ATP synthesis, strongly suggesting that PknG plays an important role in ATP regulation. *M. bovis* BCG has a significant number of proteins that are uncharacterized, and in our data, 8 of the PknG substrates were of unknown function, although a sequence alignment showed that one of these proteins (UniProt ID: A0A0H3M751) is an FHA domain containing protein which has been shown to bind phosphopeptides [204]. As GarA also contains the FHA domain, PknG, like other kinases, has an affinity for FHA domain containing proteins. Another domain enriched among these uncharacterized proteins was the ATPase domain (UniProt ID: A0A0H3MC79). PknG is a cytosolic kinase and it has been experimentally shown that these kinases phosphorylate substrates in the same subcellular sites they are found *in vivo* [205]. With this in mind, we used the TB-pred online tool (www.tbpred.com) to identify the subcellular locations of the candidate substrates, as shown in **Table 4.2**. These co-localization data show

that the majority of the candidate substrates are cytosolic, which adds another layer of confidence that these are indeed *bona fide* substrates of PknG in actively growing cultures.

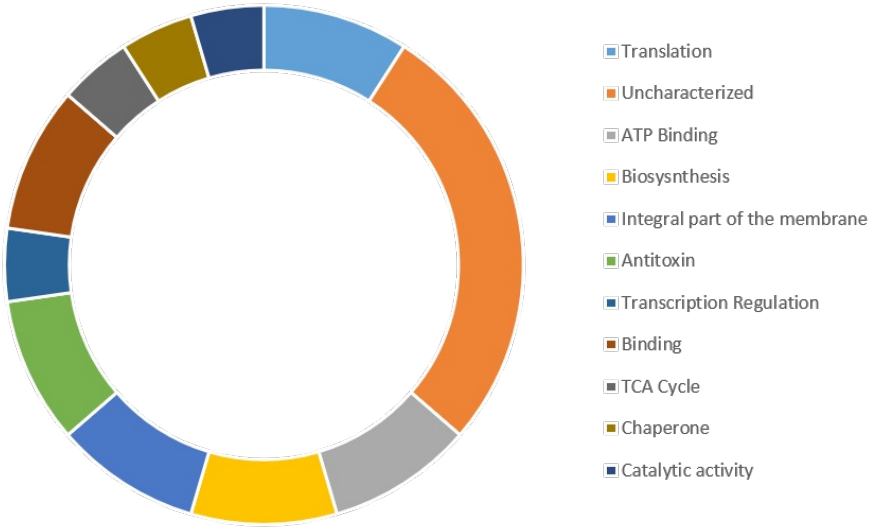

Figure 4-19:Functional categories of all identified candidate substrates of M.bovis BCG PknG. The most represented functional categories are Translation, ATP Binding, Biosynthesis and Antitoxin.

4.4 Discussion

Large scale LC-MS/MS is applicable to search for STPK in vivo substrates

A number of previous studies have examined phosphorylation by mycobacterial STPKs *in vitro* and have identified a considerable number of putative substrates based on these assays [10,40,55,182,188,206–208]. However, a recognized limitation of *in vitro* assays is the high enzyme: substrate ratios (up to 1:1) required to detect phosphorylation [18,202]. This means that, in many cases, the kinase biological selectivity is most probably lost in *in vitro* assays. Thus, the principal conundrum lies in reconstructing accurate *in vivo* phosphorylation networks, linking the kinases to their physiological substrates.

There has been some controversy around the role of PknG during growth in liquid culture. The essential role of PknG in culture is evident based on the growth defects of the *M. tuberculosis* ΔPknG knock-out mutant when compared to the wild-type in nutrient-rich media [37,209]. These studies found that the *M. tuberculosis* mutant lacking the PknG gene had significant growth defect when cultured in different growth media. It is still unclear why these growth defects are evident in *M. tuberculosis* but not in *M. bovis* BCG [36,67,200] as confirmed in the present work. The lack of obvious growth phenotypic differences in *M. bovis* BCG encouraged us to investigate the underlying phosphoproteomic changes regulated by PknG to determine if the kinase plays a redundant role or would still target a specific group of proteins. As proof of principle, the current study presents the first systematic application of large-scale phosphoproteomic analysis to screen for *in vivo* novel mycobacterial STPK physiological substrates.

Previous mass spectrometry-based phosphoproteomics studies have identified several hundred phosphopeptides/proteins in different mycobacterial species including *M. bovis* BCG ([17,29,30,32]. Nevertheless, the physiological significance of these findings remains unclear, especially given the suspected promiscuity of STPKs towards different substrates [210]. In the present analysis, more than 600 phosphorylation events were quantified and of these, <15% showed a differential phosphorylation between wild type *M. bovis* BCG vs ΔPknG. This indicates that under the studied conditions there is a reduced subset of proteins that are potentially regulated by PknG, pointing towards kinase/substrate selectivity, rather than kinase promiscuity. Furthermore, our results clearly identified two categories of differentially regulated phosphopeptides: those that appeared with higher phosphorylation levels in wild type *M. bovis* BCG than in ΔPknG strain and those phosphopeptides that were detected exclusively in wild type (both through discovery and PRM analysis) but not in the ΔPknG strain with high reproducibility. In the first category, it could be argued that those proteins may not be directly phosphorylated by PknG, but instead by other protein kinase(s) whose activity was itself affected by the absence of PknG (for example PknA that appeared among those being differentially phosphorylated). However, the second category of differential phosphorylation events seems more likely to depend entirely on the presence of PknG, although even here, the possibility that these proteins are phosphorylated by other STPKs cannot be completely ruled out. This second category of phosphoproteins can thus be initially considered as potential direct PknG substrates for further validation.

The utilization of targeted MS to follow up phosphorylation events in this study increases the precision and accuracy of the identification of site-specific phosphorylation and proves that targeted mass spectrometry is valuable in phosphoproteomic studies especially where antibodies are not a viable option to validate individual phosphorylation events. We have previously applied PRM to validate phosphopeptides identified by DDA [152] and we used the same methodology in this work validate the identity and localization of candidate substrates. SRMs and MRMs have been previously used to validate phosphosites in mass-spectrometry-based phosphoproteomic datasets [211–215]. By selecting the Ser/Thr/Tyr residue(s) for monitoring it is possible to directly assess the localization of the phosphorylation event. Usefully, PRM differs from SRM in that

all generated fragment ions are monitored simultaneously and so a more confident assignment is possible in label-free PRM p-site validation than in SRM

Importantly, the quantitative mass spectrometry-based phosphoproteomic strategy utilized here allows for confident identification and localization of the phosphorylated sites. This information then allows further analysis to predict/assess the probability of the identified phosphoproteins being phosphorylated by protein kinase in question. As discussed below, here employed *in silico* analysis to further narrow down the initial list of phosphoproteins to a confident list of potential PknG substrates.

PknG protein-peptide docking interactions suggest the basis of specificity

Identification of targeted proteins and the precise phosphorylated peptides provides a unique opportunity to extend our understanding of molecular interactions between kinases and their substrates. Both known PknG substrates GarA and ribosomal L13 have a non-polar amino acid two position before phosphorylatable Thr (Val19 and Gly10 respectively). Similarly, in this study, PknG *in vitro* phosphorylated sites that have non-polar amino acids two positions before the phosphorylatable Thr. This common feature at the -2 peptide residue is suggested to be stabilized by van der Waals interactions within a small pocket comprising hydrophobic groups [62]. Interestingly, the sequence alignment of the candidate substrates presented a predominant presence of non-polar amino acids at +1 and +2 residues from the phosphorylation site. This configuration resembles the mode of the binding of substrates to eukaryotic protein kinases, in which the position of phosphorylation is secured by + a 1 loop that accommodates the neighbouring (P+1) residue. Lee and colleagues found, through sequence alignment and site-specific mutagenesis, that the tyrosine phosphatase Src kinase (CSK) has a high affinity for binding substrates with non-polar residues immediately following the binding site [216]. Our results are thereby

in line with the reported extensive non-polar and polar interactions between the AX20017 inhibitor and PknG, where the inhibitor is bound deep within a hydrophobic PknG binding pocket [61,67]. Finally, the alignment indicated a selection for glutamic acid (E) at positions -3 and -5. Prisic and co-workers demonstrated that acidic residues from -2 to -5 increased the susceptibility for phosphorylation of proteins by most of the *M. tuberculosis* STPKs and that there is an apparent preference for Glu or Asp at this position among the STPKs [29]. In agreement with Prisic's work, our results clearly indicate that PknG shows selectivity for Glu at those positions, however, the molecular role of this residue in phosphorylation by PknG requires further study.

The patterns observed in the peptide sequences are possibly indicative of the low specificity yet high affinity of PknG to its substrates. This supports earlier suggestions that STPKs substrates could be better identified as interacting partners rather than a consensus sequencing surrounding the phosphorylation site [62]. Furthermore, our docking analysis showed that from the 23 candidate substrates, five had lower (better) free binding energy than GarA (-2.3 Kcal.mol^{-1}), ranging between -2.4Kcal mol^{-1} for Antitoxin protein and -2.9 Kcal.mol^{-1} for 50S Ribosomal Protein L2, supporting the notion that these peptides interact with PknG. Visualization of the interactions shows a unique hydrogen bond between the carboxyl group of Asp211 of the catalytic side of PknG and the γ- hydroxyl group of phosphorylated residues in the candidate substrates. The distance between the hydrogen bonds were in the acceptable distance for protein-peptide interactions, ranging from 2.9 Å for 50S Ribosomal Protein L2, 4.3 Å for Chaperon Protein ClpB, and 3.9 Å for a probable conserved membrane protein (**A0A0H3M0X2**). These results suggest a similar substrate/kinase interaction as the GarA interaction with PknG, as well as the recently proposed substrate of PknG [64], ribosomal L13. Of note the five more stable phosphopeptides contain a Pro in position +2 or +3 from the phosphorylation site, suggesting that these positions could be stabilized by van der Waals interactions within a hydrophobic PknG binding pocket. This would imply that in such cases the substrate interaction with the PknG catalytic site occurs in an opposite orientation from that observed in GarA in which -2 or -3 positions are the suggested stabilizing positions.

This chapter has demonstrated the utility of mass-spectrometry-based phosphoproteomics in the screening for STPK substrates by comparing the global phosphoproteome of an *in vivo* system with and without PknG. The consistent detection of specific phosphopeptides in all three biological replicates of the wild type and their respective absence from ΔPknG samples argues that at least these peptides are likely to be specifically targeted by PknG with a biological purpose. It can, therefore, be reasoned that the list of potential PknG substrates identified here are preferentially phosphorylated by PknG and the extent of substrate phosphorylation would then drive a resultant cellular response.

Our protein-functional analysis revealed a number of potential PknG substrates related to protein translation (**Figure 4.7**). Noteworthy amongst these is the presence of two ribosomal proteins, including 50S ribosomal protein L2, that presented maximum localization probability value (1.0) and which had the lowest free binding energy in docking models. This indicates 50S ribosomal protein L2 as a strong candidate substrate of PknG and it is in line with earlier reports that identified ribosomal proteins as substrates of PknG [64]. Interesting proteins that are involved in protein translation included two antitoxin proteins: RelB-like antitoxin protein and VapB. Toxin-antitoxin (TA) modules have been described as potential regulators of growth in *M. tuberculosis* and other bacteria, as reviewed by Page and Peti [217]. RelB-like and VapB are part of type II toxin-antitoxin family in which the toxin normally inhibits cell growth, whereas the antitoxin neutralizes the activity of toxin by forming a tight TA complex [218]. Toxin-antitoxin systems are often described as stress response mechanisms and during batch cell culture might be expected to act later in the growth curve when cells transition into a stationery phase of growth. However, our observation indicates that antitoxins are actually present in exponentially growing mycobacteria cells. It is therefore tempting to picture a scenario where phosphorylation of antitoxins by PknG is part of surveillance mechanism that regulates binding of these antitoxins to their cognate toxins. This suggests in turn that PknG kinase activity may play a role in coordinating mycobacterial adaptation to changing environmental conditions, including dormancy [201].

Finally, GarA and ribosomal protein L13 previously identified as substrates of PknG were not detected in our assay. This apparent contradictory result can be easily explained by the fact that here the cells were harvested during exponential phase, whereas previously both GarA and ribosomal proteins were seen to be phosphorylated by PknG in cells under stressed and/or nutrient limiting conditions, as well as high kinase: substrate ratios in *in-vitro* assays. [64,70,202]. It would therefore be interesting to extend our search for PknG substrates to include conditions that limit cell division and growth.

4.5 **Conclusions**

We have carried out a high throughput mass spectrometry-based phosphoproteomics analysis to characterize substrates of mycobacterial PknG in actively growing *M.bovis* BCG cells. Our results were further validated by in silico docking experiments as well as by targeted mass spectrometry. This described here workflow is robust and should represent a valuable resource to further characterize STPK's substrates in different growth conditions in order to enhance to our understanding of these important regulatory proteins. Future studies would include biochemical kinase-substrate experiments to verify that these identified candidate substrates are phosphorylated by PknG.

5. IDENTIFICATION OF THE HOST MACROPHAGE SUBSTRATES PHOSPHORYLATED BY *M. BOVIS* BCG PROTEIN KINASE G (PKNG): REPROGRAMMING NORMAL MACROPHAGE FUNCTIONS.

Summary

Macrophages and other immune cells control pathogenic infection by their protein expression levels, PTM's, as well as proteins' intracellular localization and secretion. Pathogenic bacteria like *Mycobacterium tuberculosis* modulate the host immune system to evade killing and ultimately survive long-term, resulting in Latent TB Infection. Understanding the mechanisms pathogenic bacteria uses to evade the killing by the host's immune system is critical to better understand the molecular mechanisms of mycobacterial infection. Protein kinase G (PknG) in pathogenic mycobacteria has been shown to play a critical role in avoiding clearance of mycobacteria by the host's macrophages through blocking phagosome-lysosome fusion, however, the exact mechanism is not understood. Here, RAW 246.72 macrophage cell lines were infected with *M. bovis* BCG wild-type and PknG knock-out mutants and lysed. After proteolysis, phosphopeptides were enriched with TiO_2 and subjected to LC-MS/MS to identify peptides phosphorylated in the wild-type infected macrophages and not in the PknG mutant. A total of 3600 phosphopeptides were identified per experiment. After applying filters and data cleaning, 1600 highly confident peptides with a localization probability of ≥0.75 were then used for downstream statistical analysis. A total of 67 phosphopeptides were identified exclusively in the wild-type infected RAW264.7 macrophages and not in the PknG knock-out mutant. These phosphopeptides are considered preliminary candidate substrates of PknG. Functional analysis of our data revealed that PknG reprograms normal macrophage function through interfering with the actin cytoskeleton. Proteins phosphorylated were involved in signalling pathways that were integral to actin polymerization and actin cytoskeleton rearrangement. Our results indicate the possible mechanisms that PknG uses to block phagosome-lysosome fusion.

5.1 **Introduction**

Initial events following phagocytosis of the pathogen by immune cells like dendritic cells, macrophages and natural killer cells are critical in determining whether the pathogen will be eliminated or survive. Macrophages play an important role in phagocytosis and clearance of microbes. They have pathogen recognition receptors on the cell surface, which recognises a variety of mycobacterial ligands, ie. Pathogen-associated molecular patterns (PAMP). These surface receptors, reviewed by Stamm and colleagues [219], are the ones that interact with the bacillus initially. These family of receptors, eg, Toll-like receptors (TLR), recognises microbial PAMP and triggers an intracellular signalling cascade that ends up with the microbe being engulfed into an organelle called the phagosome. This engulfment induces the classical M1 activation of the macrophage, the protective immunity against intracellular pathogens. The M1 activation is an innate immune response and stimulates the release of pro-inflammatory cytokines like Interferon Gamma (IFN-γ) and Tumour Necrosis Factor (TNF) by neighbouring T-cells and NK cells thereby activating macrophages [220].

The macrophages' first defence against the bacteria is the multistep process termed phagosome maturation whereby phagosomes first acidify and then fuse with proteolytic lysosomes to form a highly potent organelle called the phagolysosome in a process regulated by Rab 5 protein [221,222]. The potency of the phagolysosome is mostly due to the production of toxic reactive oxygen and nitrogen species (ROS & NOS), microbicidal peptides and lysosomal hydrolases [223]. The phagolysosome also has limited carbon and nitrogen sources that are central to the survival of bacterial pathogens[224,225]. These strategies work at clearing infection with other bacteria, however, *M. tuberculosis* has evolved strategies to circumvent that. It has dedicated a substantial portion of its genome for the purposes of survival within host cells. After phagocytosis, the bacilli sense the macrophagic environment and has a well-orchestrated sequence

of events to overcome the host induced stresses in order to survive. This highlights the need to continuously improve our knowledge of the interplay between host and pathogen during this crucial time that can determine whether the microbe will be cleared by the macrophage or survives and ultimately cause active disease.

Adaptation and survival of *M. tuberculosis* within the host is critical and the bacillus has strategies it employs to overcome the host macrophages, including secretion of proteins that modulate the host's proteins. These proteins play a pivotal role in the process of pathogenesis and ultimately, escape to neighbouring cells and disease progression. Taking a closer look at the biology of the intracellular *M. tuberculosis* inside the host vacuole has the potential to unlock the mechanisms that this pathogen employs in order to survive and replicate [226] during latent TB infection until it escapes and disseminate to cause active disease. Intracellular life of a pathogen inside a vacuole is an interesting field of study, the more we know the exact mechanisms pathogens use to survive, the better strategies of eradication can be devised. Secreted proteins with varying functions are the key to unlock how pathogens fight for survival.

PknG is a secreted kinase, via the secA2 secretory system [63], and its role in survival in the vacuole was eloquently described by Walburger and colleagues [36]. They infected macrophages with *M.bovis* BCG wild-type and a mutant lacking the *pkn*G gene strains. They found, using confocal microscopy, that the mutant lacking the *pkn*G gene was trafficked to the phagolysosome, whilst the wild-type strain was localised in the phagosome. To further validate these findings, they overexpressed *M. tuberculosis* p*kn*G into non-pathogenic soil mycobacteria *M. smegmatis* and repeated the experiment. The results proved the role of PknG in survival when the *M.smegmatis* mutant harbouring the *M. tuberculosis* PknG was localized in the vacuole and the Wt in the phagolysosome. The task now is to find the exact mechanism of survival mediated by PknG by mass spectrometry based phosphoproteomics to identify host substrates phosphorylated by this kinase, since the function of kinases are dependent on the substrates they phosphorylate.

Hypothesis:

Upon phagocytosis of pathogenic mycobacteria by macrophages, PknG is secreted into the macrophagic cytosol and phosphorylates host's proteins, thereby modulating signalling and ultimately reprogramming normal macrophage function to mediate mycobacterial survival in macrophages.

5.2 Aims:

The aims of this chapter were to identify host's substrates that are phosphorylated by PknG to reprogram normal macrophage function in order to block phagosome-lysosome fusion, an important defence mechanism that mycobacteria utilize to escape killing within the macrophage.

5.3 Results:

5.3.1 Experimental design

Initial events during infection of host cells by pathogens can guide the overall course of infection and determine its eventual outcome. To understand host-pathogen interactions during that crucial time in the course of infection between the host and pathogenic mycobacteria at the post-translational level, we analysed changes in the global phosphoproteome of RAW264.7 macrophage cells after infection with *M. bovis* BCG wild-type compared to those infected with *M.bovis* PknG knock-out mutant. This workflow enabled us to shed new light on the mechanisms by which the kinase reprograms normal macrophage functions to inhibit phagosome-lysosome fusion. We employed label-free quantitative phosphoproteomics to study the dynamics between host macrophages and the mycobacteria. RAW264.7 cell lines were infected with *M. bovis* BCG wild-type and PknG knock-out mutant. Uptake was allowed for 30 min followed by another 30 min chase, the logic being that PknG will be secreted into the macrophagic cytosol earlier on during infection and phosphorylate the host's substrates thereby regulating them for eventual reprogramming. We designed our sample

preparation to ensure that the internalized bacilli remained intact, through 'gentle lysis' of eukaryotic cells as described in chapter two and harvesting of mycobacteria through high speed centrifugation. After cell lysis and proteolysis, phosphopeptides were enriched by TiO_2 and subjected to LC-MS/MS. We included both murine and *M. bovis* BCG databases in the Maxquant search, expecting to identify only murine proteins. Our search identified a few mycobacterial proteins that were membrane proteins (data not shown), adding a layer of confidence that the internalized mycobacteria were not lysed during sample preparation.

Statistical considerations

Four biological replicates per experiment were analysed to increase the phosphoproteome coverage and to give statistically significant results. We considered proteins phosphorylated in at least two of the four macrophage replicates infected with the wild-type strain and not phosphorylated in any of those infected with the knock-out mutant as host proteins phosphorylated by PknG. After filtering low-quality data points, we had a subset of high confidently localized phosphopeptides that were taken for downstream bioinformatics and systems analysis.

Justification of time-point to study phosphorylation dynamics between host and microbe

We based our study design on the reference paper, Walburger et al 2004 [36]. In their work, they monitored survival dynamics of *M. bovis* BCG wild type compared to the PknG mutant, judged by measuring CFUs at five-hour interval post infection (Figure 5.1). They also observed through microscopy that *M. bovis* BCG wild type was localized in the phagosome two hours post-infection whilst the PknG knock-out mutant was localized in the phagolysosome at that time point (**Figure 5.1**). With that in mind, we rationalized that the ideal time point to study the phosphorylation events that lead to their observed phenotype would be 30 min post infection, the earliest time-point where mycobacteria would be localized in the phagosome. We infected RAW264.7 cells in a T75 tissue culture flask. Cells were seeded 7e5 and after three days of incubation, cells were at

about 80% confluency with counts of 2e6 total cells. We infected at an MOI of 4, ie. 8e6 bacterial cells were added to the eukaryotic cells and incubated as described in detail in chapter 2.

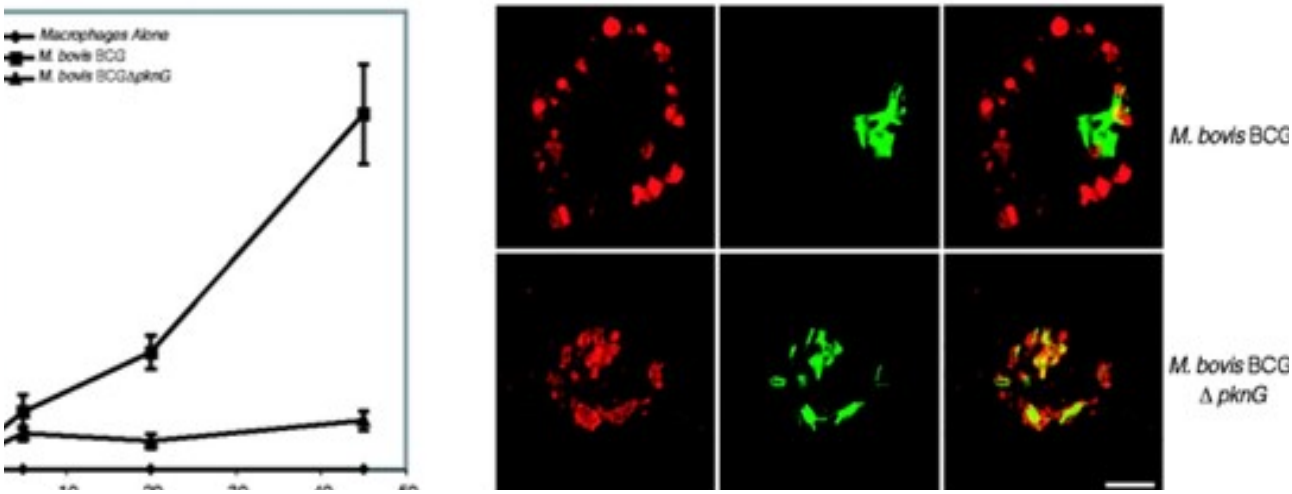

Figure 5-20 Walburger results of intracellular survival dynamics of M. bovis BCG wild type compared to the PknG knock-out mutant. Electron microscopy localization of macrophage harbouring both strains of M. bovis BCG two hours post-infection. ***Anne Walburger et al. Science 2004;304:1800-1804*** [36]***.***

5.3.2 Phosphoproteomic changes in the host's macrophages mediated by PknG

Four independent biological replicates of RAW264.7 cells infected with *M. bovis* BCG wild-type and PknG knock out were lysed and phosphopeptides enriched for using TiO2 after proteolysis and peptide clean-up. The LC-MS/MS parameters are explained in detail in chapter 2. We normalized the sample loading volumes by max TIC as shown in **Figure 5.2 (A-B)**. Raw data were processed, and identifications matched to the Murine database downloaded from UniprotKB (www.uniprot.com), using Maxquant software version 1.5.3.12. Of the spectra submitted, 8 % of those were identified with 15% missed cleavages. This is a relatively lower identification rate. The experiment identified 3 164

phosphopeptides of which, after filtering low-quality data as per Sharma et al 2014, 1 630 were high confident identifications with a localization probability of ≥0.75. PEP < 0.01 (**Table 5.1**) (**Figure 5.3 (A-B)**. Missing values is characteristic of label-free phosphoproteomics data. To this effect, we only analysed those phosphopeptides identified in at least two of the four biological replicates per experiment. We selected all phosphorylated peptides present in the wild-type strain and not the PknG knock out mutant. This present/absent analysis isolated 69 candidate substrates of PknG in the host and these were then taken further for an in-depth systems analysis (**Table 5.2**). Interesting substrates that stand out from **Table 5.2** that possibly explain the consequences of these phosphorylations that result in the observed phenotype, ie. phagosome maturation arrest of macrophages harbouring pathogenic mycobacteria, are involved in actin polymerization signalling pathways. Our data also shows phosphorylation of regulators of integrins adhesion to the cytoskeleton, which is invaluable in organelle fusion and supports the proposed mechanism that PknG blocks phagosome-lysosome fusion as discussed in detail later.

Table 5-5:A summary overview of data quality

DATA QUALITY SUMARY	
Spectra Submitted	330687
Spectra Identified	23551
Protein Groups	1 540
Missed Cleavages (1)	15.2%
Phosphosites Identified	3 164
Localized Phosphosites	1 630

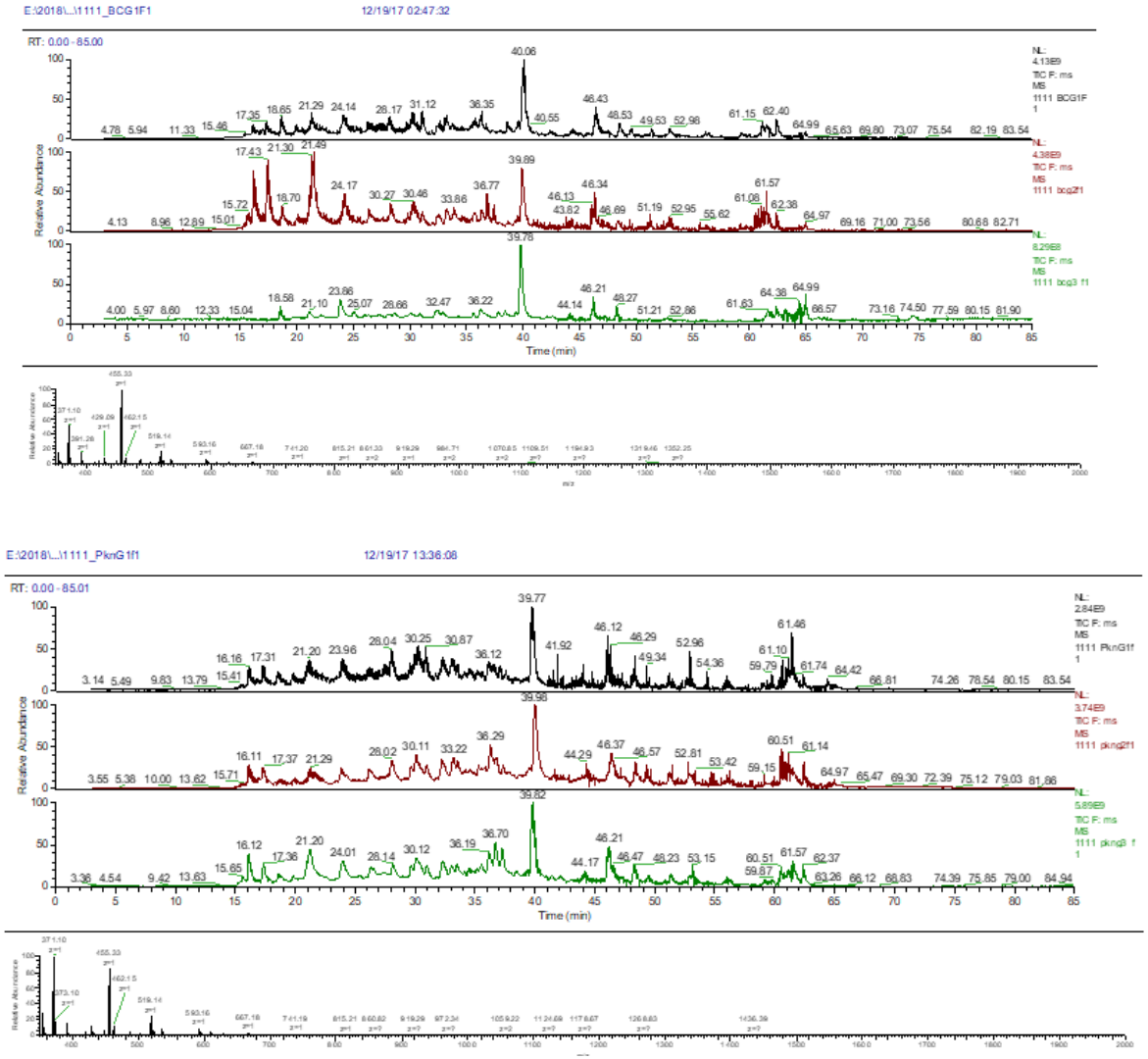

Figure 5-21: Data quality: Sample loading volumes normalized to obtain TIC (Total Ion Chromatograms) for each replicate on the MS.

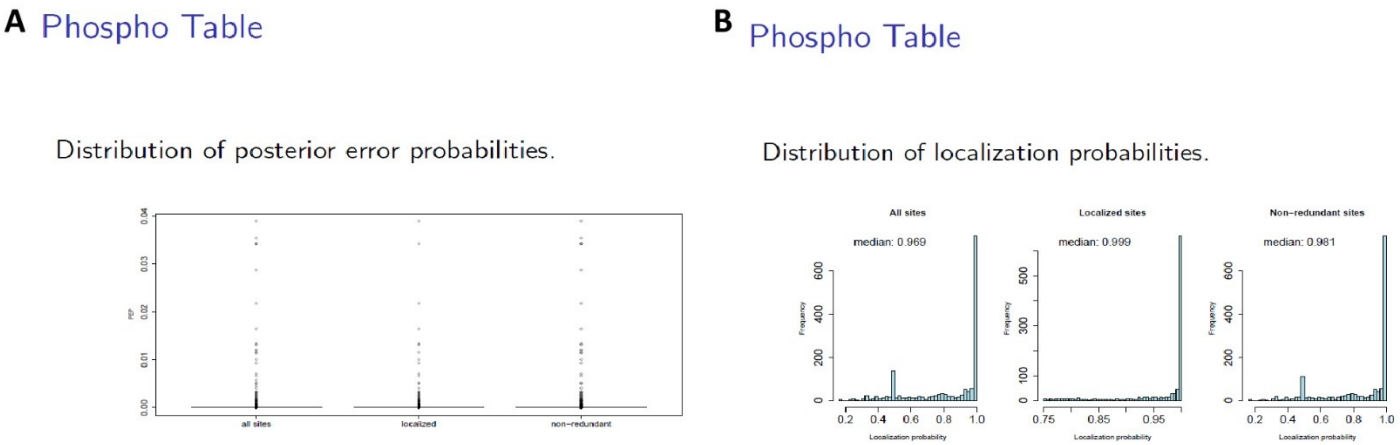

Figure 5-22: Distributions of localization probability and PEP values of highly confident phosphopeptides identifications. The majority of phosphopeptides had a localization probability of > 0.75 and PEP values of <0.01

Table 5-6:List of host's substrates phosphorylated by M. bovis BCG PknG as determined by label-free phosphoproteomics

Gene Name	***UniProt ID***	***Descriptive protein name***	***Localization Probability***	***P-site***
Sept7	Q5DTS3_MOUSE	MKIAA4020 protein	1	S_1
Rps27	A0A0G2JDW7_MOUSE	40S Ribosomal Protein S27	1	S_6
Spag7	SPAG7_MOUSE	Sperm-associated Antigen	1	S_1
Srrm2	SRRM2_MOUSE	Serine/arginine Repetitive Matrix Protein2	1	S_{12}
Golm1	Q4KMM5_MOUSE	Golgi Membrane Protein	1	S_7
Eif2s2	Q3ULL5_MOUSE	Eif2s2 Protein	1	S_3
Arhgdia	GDIR1_MOUSE	RhoGDP-dissociation inhibitor1	1	S_1
Nsfl1c	Q3KQQ1_MOUSE	Nsfl1cprotein	1	S_1
Nsfl1c	Q3KQQ1_MOUSE	Nsfl1cprotein	1	S_3
Eaf1	EAF1_MOUSE	ELL-associated Factor1	1	S_4
Akap8	Q059U9_ MOUSE	A kinase (PRKA) Anchor Protein8	1	S_1
Ppp1r12a	MYPT1_MOUSE	Protein Phosphatase1 Regulatory Subunit 12A	1	S_3
Acss2	D6RHA7_MOUSE	Acetyl-coenzyme A Synthetase, Cytoplasmic	1	S_3
Ncaph	CND2_MOUSE	Condensin Complex Subunit2	1	T_1
Tjap1	TJAP1_MOUSE	Tight-junction-associated Protein1	0.753644	S_3
Clip1	D3Z3M7_MOUSE	CAP-Glydomain-containing linker Protein1	0.773912	S_3

Ptpn12	PTN12_MOUSE	Tyrosine-protein Phosphatase non-receptor type12	0.788012	S_{14}
Efhd2	Q8C845_MOUSE	EF-hand-domain-containing Protein D2	0.800535	S_{10}
Mindy1	B7ZMR0_MOUSE	Fam63a Protein	0.803674	S_{16}
Ppp1r12a	MYPT1_MOUSE	Proteinphosphatase1 Regulatory subunit 12A	0.806299	S_{3}
Wiz	G5E8J8_MOUSE	MOUSEMCG 14253, isoform CRA_a	0.826384	S_{7}
Srrm2	SRRM2_MOUSE	Serine/arginine Repetitive Matrix Protein2	0.84041	S_{3}
Cdc25b	Q9DBN8_MOUSE	Cdc25b Protein	0.852478	S_{1}
A0A068F126	A0A068F126_MOUSE	Glyco-gag Polyprotein	0.85941	S_{9}
Creb1	Q62347_MOUSE	CyclicAMP-responsive element-binding Protein1	0.862448	S_{6}
Ptpn6	Q3UB72_MOUSE	Tyrosine-protein Phosphatase non-receptor-type	0.868047	Y_{6}
Srrm2	Q8BTI8|SRRM2_MOUSE	Serine/arginine Repetitive M matrix Protein2	0.882714	S_{5}
Chchd3	S4R238_MOUSE	MICOS Complex Subunit	0.88571	S_{3}
Ncaph	CND2_MOUSE	Condensin Complex Subunit2	0.897706	S_{8}
Snw1	Q3TM37_MOUSE	Uncharacterized Protein(Fragment)	0.904588	S_{12}
Ndrg1	Q545R3_MOUSE	N-myc downstream Regulated gene1	0.905592	S_{6}
Fam53b	Q3U0R8_MOUSE	Protein FAM53B	0.9343	S_{3}

Nmd3	NMD3_MOUSE	60S Ribosomal Export Protein NMD3	0.96726	S_8
Vim	Q5FWJ3_MOUSE	Vimentin	0.969501	S_1
Snap23	B0R030_MOUSE	Synaptosomal-associated Protein	0.970374	S_{10}
Bin2	S4R2J8_MOUSE	Bridging Integrator2	0.973343	S_4
Nop14	Q8C539_MOUSE	Uncharacterized Protein	0.9759	S_9
p16	Q62019_MOUSE	16kDa Protein	0.977789	S_6
Irf3	A0A140LHE6_MOUSE	Interferon Regulatory factor3	0.980915	S_8
Rbm8a	RBM8A_MOUSE	RNA-binding Protein8A	0.981752	S_7
Arhgap18	RHG18_MOUSE	RhoGTPase-activating Protein18	0.984893	S_9
Pnpla7	PLPL7_MOUSE	Patatin-like phospholipase domain-containing protein7	0.988611	S_3
Scaf11	Q9CSS1_MOUSE	Uncharacterized Protein(Fragment)	0.990928	S_3
Snx17	SNX17_MOUSE	Sorting nexin-17	0.993464	S_7
Ccdc6	F7B4D5_MOUSE	Coiled-coil domain-containing Protein6(Fragment)	0.995051	S_3
Arhgap6	RHG06_MOUSE	Rho GTPase-activating Protein6	0.995535	S_4
Tns3	TENS3_MOUSE	Tensin-3	0.997022	S_{11}
Ncor2	E9PY55_MOUSE	Nuclear Receptor Corepressor2	0.997284	S_1
Ccdc88b	B2RXR1_MOUSE	Coiled-coil domain containing88BOS	0.997664	S_1
Lmna	LMNA_MOUSE	Prelamin-A/COS	0.997727	S_6
Nelfe	G3UY39_MOUSE	Negative Elongation Factor E (Fragment)	0.998301	S_3

Bnip3	A0A1B0GT26_MOUSE	BCL2/adenovirusE1B 19kDaprotein-interacting protein3	0.99841	S_5
Spen	Q3UV27_MOUSE	Uncharacterized Protein(Fragment)	0.99842	T_1
Gpatch2	Q9D3E7_MOUSE	Uncharacterized Protein	0.998451	S_7
Pdha1	Q3UFJ3_MOUSE	PyruvatedehydrogenaseE1 Component subunit alpha	0.99886	S_{12}
Rps3a1	Q9D1S3_MOUSE	40S ribosomal Protein S3a	0.999641	S_{11}
Rrp9	U3IP2_MOUSE	U3 small nucleolar RNA-interacting Protein2	0.999803	S_5
Srsf10	tr|Q3TFP0|Q3TFP0_MOUSE	Serine/arginine-rich-splicing Factor10	0.999819	S_3
Zfp655	A0A0G2JE56_MOUSE	Zinc Finger Protein 655	0.999832	S_{12}
Raly	Q3U3F6_MOUSE	HnRNP-associated with lethal yellow, isoform CRA_f	0.999879	T_8
Dlgap5	Q3UGF9_MOUSE	Uncharacterized Protein	0.999907	S_{13}
Mdn1	A2ANY6_MOUSE	Midasin	0.999936	S_9
Flna	B9EKP5_MOUSE	Filamin, alpha	0.99996	S_7
Srsf10	Q3TFP0_MOUSE	Serine/arginine-rich-splicingfactor10OS	0.999976	S_1
Ripk1	F7D1J2_MOUSE	Receptor-interacting serine/threonine-protein kinase1	0.999994	S_6
Cdc42ep4	BORG4_MOUSE	Cdc42effectorprotein4	0.999998	S_5
Eif2b5	EI2BE_MOUSE	Translation Initiation FactoreIF-2B subunit epsilon	1	S_3
Tpx2	Q9CT36_MOUSE	Uncharacterized Protein	1	S_1

Snw1	Q3TM37_MOUSE	Uncharacterized Protein	1	S4

5.3.3 Functional annotation of host's proteins under the regulation of PknG

To gain insights and to infer biological significance of our data, an online PANTHER online Bioinformatics Resources (http://www.pantherdb.org) was utilized to analyse Gene Ontology (GO) biological terms that are over-represented associated with candidate substrates phosphorylated by PknG. The tool compares the statistically significant frequency of candidate substrates to the reference list, which the PANTHER tool set as the mouse proteome. GO terms with at least four phosphopeptides per term with a cut-off of Bonferonni adjusted *p*-value of 0.1 were included in the analysis. GO Biological Process annotation (redundant terms grouped) of candidate substrates of PknG are shown in **Figure 5.4**. The most interesting terms that were enriched were cellular component organization or biogenesis (GO:0071840) and cellular process (GO:0009987). These GO processes result in reassembly, rearrangement of cellular components and organelles.

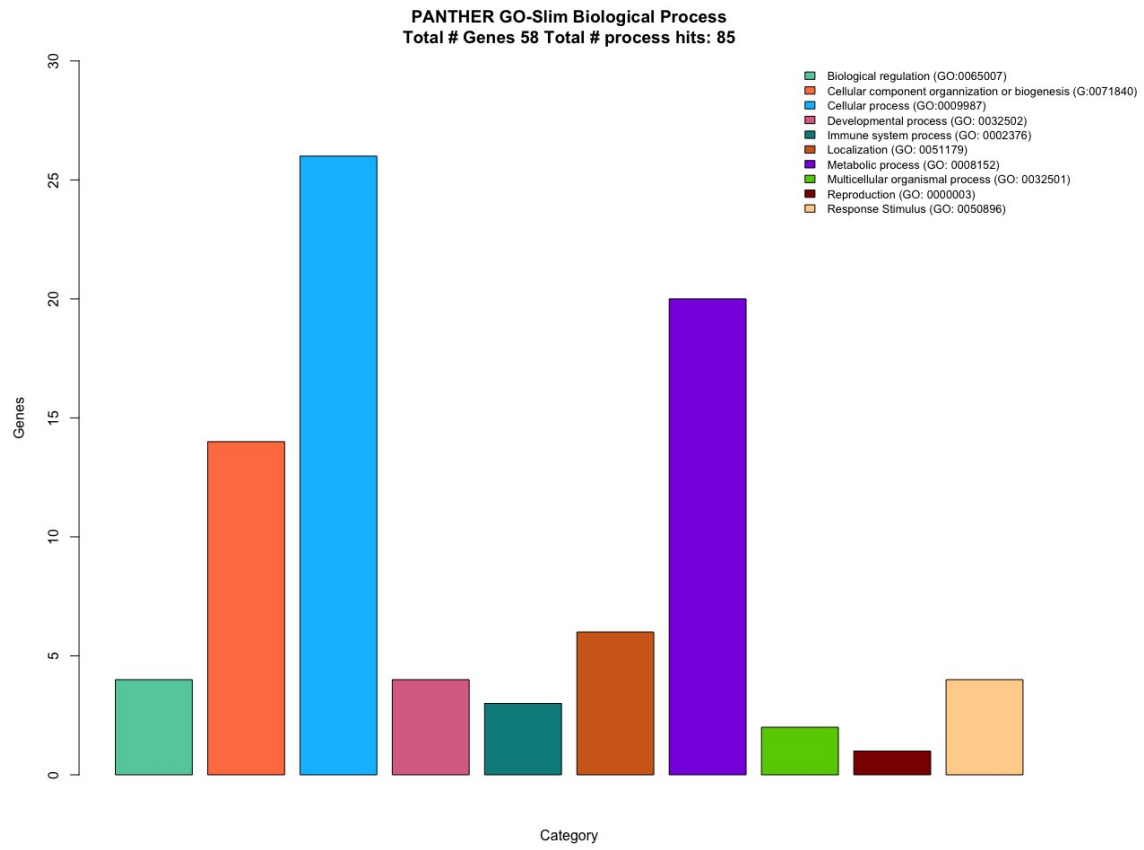

Figure 5-23: GO-term enrichment analysis of candidate macrophagic substrates of PknG using PANTHER online bioinformatic tool highlights PknG's ability to phosphorylate key cellular functions including organelle migration and localization

5.3.4 Network analysis and visualization of candidate substrates of PknG

Protein-protein interaction network of our candidate substrates were analysed and visualized using the STRING database (https://string-db.org) [227]. These data (**Figure 5.5**) show that PknG regulate a network of substrates that are involved in interlinked multiple and diverse cellular processes. There is a clear network of 13 nodes interconnected of phosphoproteins phosphorylated by PknG. Of the 67 host substrates phosphorylated by PknG. 25 where annotated to the cellular organization term. The two major regulators of Rho GTPases were also identified. Proteins involved in integrin recycling and activation were also amongst the substrates that are under the regulation of PknG in the host's macrophages. These host substrates of PknG strongly suggests that disruption of key cytoskeletal regulators is the mechanism that pathogenic mycobacteria employs to block phagosome-lysosome fusion as discussed in detail in the next section.

5.3.5 Consensus sequences (Motifs) of candidate substrates

To determine if there are any preferential motifs for PknG host substrate, we used iceLogo (www.weblogo.berkely.edu) to visualise overrepresented amino acids flanking the phosphorylation sites of candidate substrates that indicate interaction with this kinase **(Figure 5.6)**. This sequence alignment shows a preference for Proline at position +1 after Ser phosphorylation. These data are consistent with what we have already demonstrated with PknG physiological substrates in the previous chapter, where there were no significant preferential motifs. It is interesting to note that the lack of specific motifs characteristic of eukaryotic kinases doesn't affect the specificity of the substrates phosphorylated by PknG. This is supported by the enriched GO terms explained above, where these substrates are not phosphorylated at random but are inter-connected biologically.

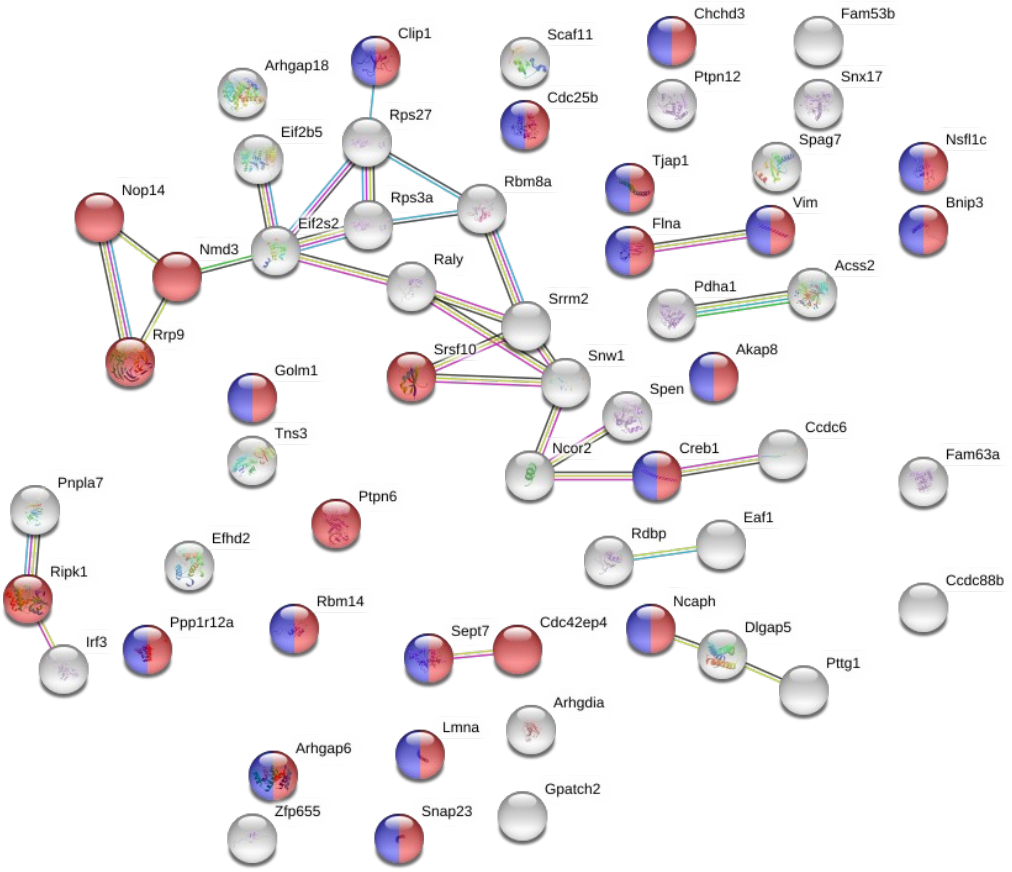

Figure 5-24:Network interaction analysis from STRING database. The nodes represent phosphorylated proteins, the edges represent connections. The red and blue colour represent proteins involved in cellular organization GO biological term.

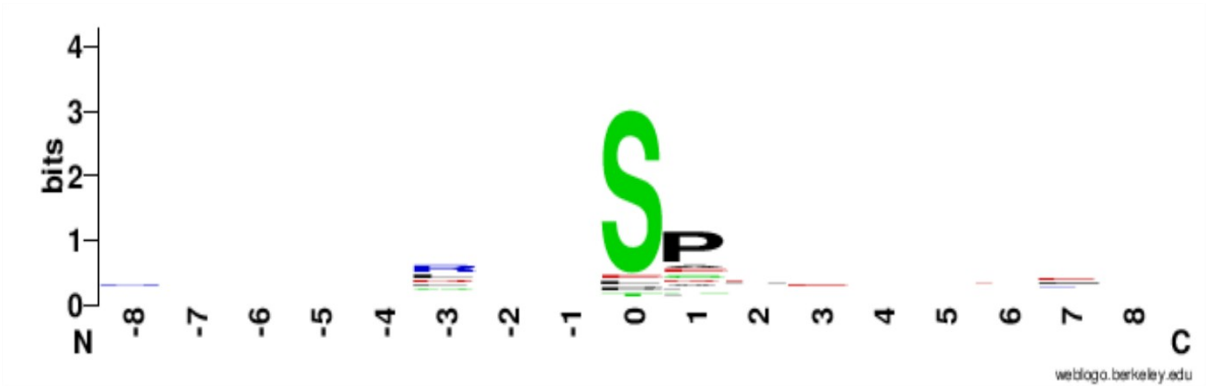

Figure 5-25: Weblogo of identified PknG substrates.

5.4 Discussion

Macrophages are able to change their phenotype and physiology in response to stimuli in order to clear the invading pathogen. Pathogenic mycobacteria have evolved strategies that enable them to evade the hostility of the host's immune response and therefore survive inside macrophages sometimes for a lifetime. Protein Kinase G plays an important role in reprogramming macrophage function to aid in the survival of the pathogen. It has been shown that macrophages harbouring *M. bovis* BCC strains failed to be translocated to the phagolysosome while the mutant lacking PknG was easily cleared by the macrophage. This impressive discovery propelled us to try and decipher the mechanisms that PknG uses to block phagosome-lysosome fusion. The logical experiment would be one that identified those proteins phosphorylated by PknG after mycobacteria have been phagocytosed. To this end, we carried out a label-free phosphoproteomic approach that we and others have shown to be high throughput platform to identify substrates of kinases. The functions of the identified substrates shed new light on the possible mechanisms that PknG uses to regulate and reprogram macrophage's signalling pathways that enable the bacterium's survival, as discussed below and summarised in **Figure 5.7**.

Intracellular trafficking via the actin cytoskeleton

Figure 5.4 shows the Gene Ontology terms that were enriched in this data and a closer look at the pathways that these substrates are involved in, even though there were no significantly enriched pathways, start to add missing links and fill gaps on how pathogenic mycobacteria survive inside the host macrophages through the regulation of actin cytoskeleton in the presence of PknG. The idea that pathogenic mycobacteria can manipulate the host's cytoskeleton through, until now, unknown mechanisms was first described by Gue´rin and colleagues where they noticed that pathogenic mycobacteria caused a marked disorganization of the F-actin network [228].

The cytoskeleton plays an important role in phagosome maturation and membrane trafficking events. Actin cytoskeleton reorganization is needed by eukaryotic cells to change shape, divide, move, and take up nutrients for survival. For any type of cell to migrate, the cell membrane has to protrude first. Protrusions are made up of lamellipodia and filopodia which binds to the actin cytoskeleton and strengthened by adhesins [229,230]. This causes traction forces that allow the cell to migrate on the cytoskeleton with adhesins being detached as the cell migrates. Cytoskeletal polymers like actin and tubulin, need to polymerize to be active. Actin polymerization and assembly has been reported to be able to stimulate or inhibit phagosome fusion with lysosomes [231].

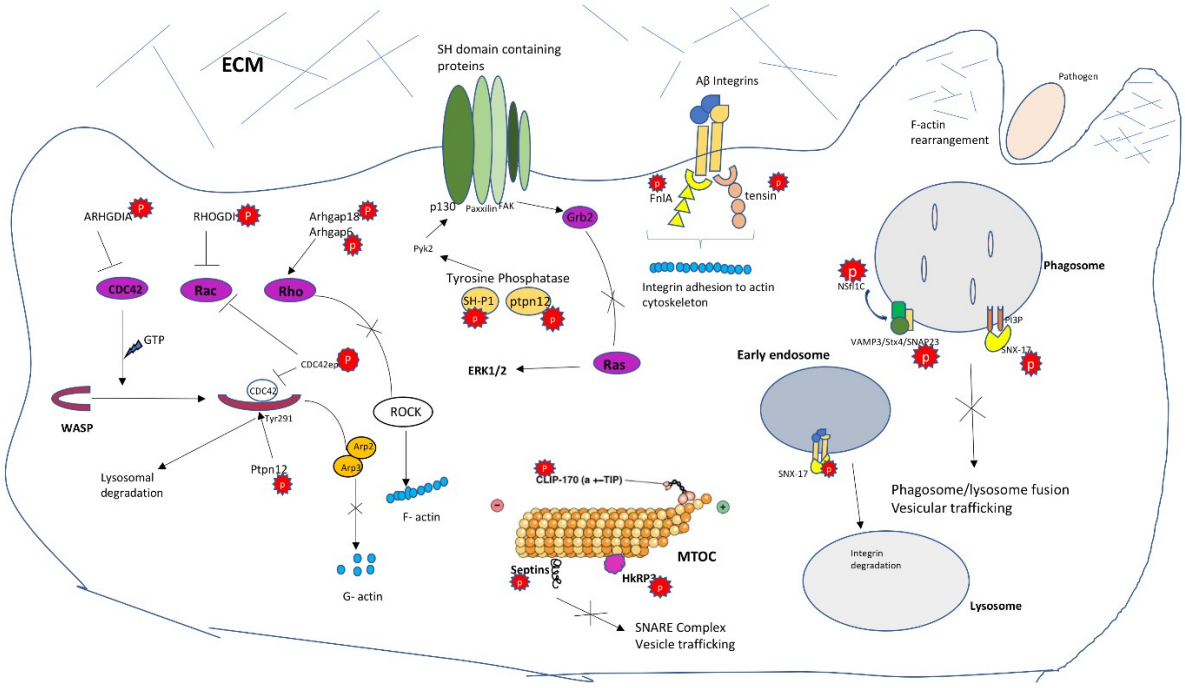

Figure 5-26: A schematic figure showing substrates phosphorylated in the presence of PknG and a summary of actin polymerization signalling pathways that the kinase may interfere.

Cytoskeletal disruption through the Rho signalling pathway

The Rac-Rho signalling pathway is one of the best-studied pathways that regulate the integrity of the actin cytoskeleton through regulation of Rho GTPase activity. The Rho-family guanosine triphosphatases (GTPases), for example, RhoA, Rac1 and Cdc42, are the most important members of this family. They regulate crucial processes that are dependent on the actin cytoskeleton such as cytokinesis, transcriptional activation, phagocytosis, morphology and migration [232,233]. They are also known to produce distinct changes to the actin cytoskeleton when expressed in all eukaryotic cells, leading to important cellular functions like phagocytosis and vesicular trafficking [234,235].

The importance of these Rho GTPases to actin cytoskeleton dynamics would require not only one mechanism that regulates them to ensure that the cells perform optimally in terms of motility and contractility. In a physiological state, all eukaryotic cells have multiple pathways that regulate Rho GTPases by switching their activity on and off. Rho-family GTPases homeostasis is strictly regulated through several layers. Rho GTPases are regulated post-translationally by modifications on their C-terminus, and that enables protein-protein interactions with their effector to activate them [236]. Secondly, signalling events induces their activation (GTP-bound) through the GDP/GTP exchange catalysed by GEFs (guanine nucleotide-exchange factors) and promotes downstream signalling [237]. Thirdly, they are maintained in an inactive (GDP-bound) form and protected from degradation in the cytosol by Rho GDP-dissociation inhibitor (RhoGDI), which we identified as a phosphorylated in the presence of PknG in this work. The negative regulation of Rho GTPases by RhoGDI maintains their homeostasis by preventing nucleotide exchange and membrane association and solubilizing them in the cytosol [238]. Gene knock-out studies of RhoGDI showed decreased actin polymerization and disrupted actin cytoskeleton [239,240].

Two Rho GTPase activating proteins (RhoGAP), Arhgap18 and Arhgap6, are host substrates phosphorylated in the presence of PknG, as determined by this study. They regulate the GTP hydrolysis activity of RohA by switching it to its inactive form and a still unclear mechanism [236,241]. Activated RhoA regulates the cytoskeletal dynamics effectors such as Rho kinases/ROCKs. Overexpression of RhoGAP resulted in human osteosarcoma SaOS-2 cells resulted in a decreased RhoA activation and disruption of actin stress fibres[242], whilst gene knockdown of Arhgap18 enhances focal adhesion and stress fibre formation [241]. In addition to its GAP specificity towards RohA, Arhgap6 also co-localizes with actin filaments through an N-terminal domain and recruits F-actin to promote actin remodelling [243]. These studies combined with our results lead to the hypothesis that PknG's phosphorylation of RhoGAP may increase its activity to block the activity of RhoA, which is beneficial to the bacterium through disruption of actin stress fibres and thereby blocking phagosome migration.

The Rho GTPase family member Cdc42 is a master regulator of actin nucleation and cytoskeleton remodelling. As like other Rho proteins, it is kept inactive by association with RhoGDIs [238,239,244]. ARHGDIA is a RhoGDI that we identified phosphorylated in the presence of PknG in this work. Mutations in ARHGDI leads to dissociation from and activation of Cdc42 and Rac [245], whilst knockdown studies of ARHGDI resulted in hyperactivation of RhoA, Rac1, and Cdc42[246]. These studies and our results together show one of the possible ways PknG may maintain these Rho GTPases in an inactive form through phosphorylation and regulation of RhoGDI, blocking downstream pathways that maintain the integrity of the actin cytoskeleton.

Activation of Cdc42 leads to its regulatory function through a conformation-specific interaction with target (effector) proteins containing a Cdc42/Rac interactive binding (CRIB) motif. One such group of Cdc42 effectors belong to the less studied Borg (binder of Rho GTPases) family of proteins. They have been proposed to be negative regulators of GTP bound Cdc42 [247,248]. In mammalian breast cell lines, Borg protein Cdc42ep4 is a substrate of Protein Kinase C (PKC), and the resultant phosphorylation diminishes its binding to Cdc42. Dissociation of Cdc42ep4 from activated Cdc42 allows its interaction with TEM4 thereby promoting Rac activation and filopodia formation[249]. We propose a model where

pathogenic mycobacteria interferes with this signalling pathway through PknG phosphorylation of Cdc42ep4, that increases its binding affinity to activated Cdc42, thereby negatively regulating the downstream functions of Cdc42 and concurrently inhibiting Rac activation in actin polymerization and cytoskeleton remodelling pathways.

Actin nucleation interference through the WASp-Arp2/3 complex

Macrophages ability to control pathogens depends on its structural rigidity and plasticity. Its architecture is mediated through the actin polymerization and Rho GTPase activation [250]. The functional effects of this structural and mechanical regulation are mobility and maturation that are key steps in pathogen elimination. Like other cells of the monocytic lineage, macrophages have actin-rich structures called podosomes that elongate and bind to the ECM through integrins[251]. De novo synthesis of new actin filaments is critical to actin cytoskeleton reassembly and rearrangement. The actin-related protein (Arp) 2/3 complex is one of the conserved actin cytoskeletal nucleation mechanism that assembles and polymerises actin filaments. It is a tightly regulated process that requires a co-stimulatory factor, nucleation-promoting factor (NPF), the well-studied being the proteins belonging to the WASp-like family (Wiskott–Aldrich syndrome protein). These WASp-like proteins are key regulators of actin polymerization, are scaffolds that link upstream signals to the activation of the ARP2/3 complex. Activated Cdc42 regulates WASp by binding to GTPase-binding

domain, changing its conformation, facilitating the interaction of WASp and Arp2/3 complex [252]. WASp-like proteins have to be phosphorylated by a tyrosine kinase at position Y291 [253]. Our data suggest that PknG may be regulator of actin nucleation through regulating the phosphorylation state of WASp, since two substrates identified in this work as being phosphorylated in the presence of PknG (Upstream inactivation Cdc42 by ARHGDI and Ptpn12) are known key regulators of Wasp. Notably, Ptpn12 dephosphorylates WASp-like protein on Try 291, making it susceptible to cytosolic degradation. These data collectively suggest that PknG may block phagosome-lysosome fusion by negatively affecting the activation of Cdc42 through phosphorylation of RhoGDI, making it inaccessible to interact with WASp thereby blocking actin polymerization, and through phosphorylation of Ptpn12 that leads to WASp degradation.

Interference of Integrins adhesion to actin cytoskeleton

Macrophages adhere to the extracellular matrix (ECM) by using specific cell surface adhesive structures. Integrins (α and β) are transmembrane proteins that link the ECM to intracellular cytoskeletal and signalling networks that dictate a cell's ability to adhere to, spread and migrate over distinct surfaces [254]. Integrins are regulated in terms of cell-surface delivery, internalization and recycling by proteins belonging to the FERM-like domain–containing sorting nexins of the SNX17/SNX27/SNX31 family[255], which were observed to be phosphorylated in this work. In particular, we identified SNX-17 to be phosphorylated at Ser_7. Sorting nexin protein SNX-17 is found in early endosomes and mediates retrieval of transmembrane proteins from the lysosomal pathway [255,256]. Its FERM domain binds to the NPxY motif of β Integrins, triggering their recycling [257,258]. It is well established that mutations on the SNX-17 protein lead to lysosomal degradation of these integrins. SNX-17 has a pho (PX) domain that has been shown to interact with membranes containing phosphatidylinositol 3-phosphate (PtdIns(3P) [259,260], also known as PI3P and recruits them to specific membranes or vesicular structures within cells. PI3P has a versatile role in phagosome maturation, vesicular trafficking and ROS production [261–265]. One of the interesting interactors of SNX-17 through its FERM domain is Ras GTPase in a GTP dependent manner [266], one of Rho proteins that are central to actin cytoskeleton remodelling. Phosphorylation of SNX-17 in the presence PknG gives rise to an interesting hypothesis that one of the ways that pathogenic mycobacteria block phagosome

maturation is by preventing membrane protein recycling and blocking vesicular trafficking at the phagosome membrane through negative regulation of SNX-17, whilst at the same time interfering with the Ras signalling pathway for actin cytoskeleton remodelling.

Tensins are a family of cytoplasmic phosphoproteins that are localized to integrin-linked focal adhesions. They interact with the cytoplasmic tail of β-Integrin through their phosphotyrosine-binding domain (PTB), whilst the N-terminal region binds to actin, thereby linking the actin cytoskeleton to αβ integrin receptors [267]. Tensin is an important component linking the ECM, the actin cytoskeleton, and signal transduction. Knock-out studies in mice have demonstrated that lack of tensin leads to loss of cell migration [268,269]. Tensin -3 (Tns3) is a substrate that is regulated in the presence of PknG. This is another evidence of the possible role PknG plays on the actin cytoskeleton and all its associated proteins that result in the inability of the macrophage's phagosome to migrate and fuse with the lysosome, resulting in the survival of mycobacteria.

Actin filaments are cross-linked to form its dynamic three-dimensional structure [270]. This organization enables the F-actin flexibility and rigidity and is mediated by filamins and other filament-forming proteins [271,272]. The interaction between filamins and actin creates the mechanical and dynamical properties of the cytoskeleton [273]. Filamin A is an actin-binding protein that plays a critical role in cytoskeleton remodelling by cross-linking actin filaments and attaches them to membrane proteins and the extracellular matrix through adhesion molecules such as integrins [274]. Filamin A is a negative regulator of integrins activation, through its binding to talin in response to mechanical force [275]. Mutations in FLNa and FLNb have been associated with several developmental malfunctions in human genetic disorders [276]. The FLNa partner binding capabilities are regulated by phosphorylation and mechanical stress. One of the host candidate substrates we identified in the study is FNLa. This is another layer of evidence that identifies a network of proteins that strongly suggest the role PknG play in interfering with macrophagic cytoskeleton remodelling.

Interference of actin-myosin interactions

The crucial step in cell motility and adherence is the actomyosin cortex beneath the cell membrane, which produces contractile forces that squeeze the cell forward during migration or constrict it during division [277,278]. A thin network of actin-attached tightly to below the cell surface acts as the cell cortex and myosin II motor proteins generate contractile forces which pull the actin filaments in the presence of ATP from regions of relaxation to regions of contraction [279,280]. Actomyosin contractility is required for the translocation of integrins in specialized cell-matrix adhesions along actin stress fibres, a process that stretches folded fibronectin dimers to facilitate their assembly[281]. Cells and tissue tension is generated by actin-myosin interaction. YAP (Transcriptional coactivator YAP1) has been shown to be important in regulating tissue tension in human cells, acting through ARHGAP18 to regulate cortical actomyosin network formation [282]. This work, ARGAP18 was identified substrate phosphorylated in the presence of PknG, suggesting that F-actin polymerization suppression and downstream actinomyosin network formation through YAP is one of the mechanisms PknG could possibly employ to block membrane fusion between the phagosome and lysosome.

Interference with microtubule dynamics

Microtubule (MT) stability is important for podosome formation in macrophages [283]. The absence of podosome is associated with a disturbed microtubule cytoskeleton, both in its overall shape and also on the level of orientation of individual microtubules [283]. Microtubules have minus and plus ends that binds to the microtubule organizing centre (MTOC) and explore the cell periphery respectively. In this section of the thesis, we will discuss the evidence that directs us to the possible role that PknG plays in destabilizing MT dynamics through phosphorylation of different proteins that are involved in signalling pathways that polymerizes MT.

MT cytoskeletal dynamics and their functionality in anchoring to other structures are mediated by proteins that interact and bind to their growing ends called plus-end tracking proteins (+TIPs) [284]. CAP-Gly domain-containing linker protein 1 (also known as Clip1 or Clip-170) belongs to a family cytoplasmic linker proteins (CLIPs), that links organelles with microtubules [285,286]. Clip-170 is localized at the plus end of growing MT and is associated with MT assembly and growing length

[286,287]. Its ability to bind to the growing ends of MT is regulated post-translationally through phosphorylation by PLK1 and CK2 [288–290]. In yeast cells, genetic analysis of the knock-out CLIP-170 homolog showed destabilization of MT plus ends in all regions [291]. CLIP-associating proteins (CLASPs) 1 and 2 attaches to CLIP-170 to promote turnover of attached MTs and they are phosphorylated by cyclin-dependent protein kinases 1 (Cdk1) [292]. This phosphorylation primes CLASPs to associate and recruit PLK1 to the growing ends of MT to phosphorylate and regulate Clip-170 in MT dynamics [292]. It was interesting to note that Cdc25b was phosphorylated in this work, a tyrosine protein phosphatase that dephosphophorytes Cdk1 and activates its kinase activity [293]. We also identified Clip1 as one of the substrates that are phosphorylated in the presence of PknG in this work. The regulation of Clip1 directly and through its effectors in the presence of PknG suggests negative regulation that results in a decreased ability of Clip1 to effectively interact and bind to growing ends of MT, leading to loss of MT organization and functions.

Ccdc88b, Hook-related protein 3 (HkRP3) is a microtubule binding hook protein that is localized at microtubule-organizing centre (MTOC) in macrophages [294]. The function of these proteins is unclear, but they seem to functionally couple elements of the cytoskeleton with different cellular processes, such as vesicular transport and cell movement. In studies using B cells and T cells, HkRP3 interacts with DOCK-8[294] (dedicator of cytokinesis 8), a protein that functions as GEF for the Rho family of GTPase Cdc42 [295]. Individual Guanine nucleotide exchange factors (GEFs) are thought to help recruit specific effectors to the monomeric GTPases they activate, thereby assembling compartmentalized signalling complexes. DOCK-8 has been shown to be involved in regulating F-actin and integrin accumulation at the immune synapse and its loss leads to halted macrophage migration[296,297]. We identified HkRP3 as one of the substrates phosphorylated in the presence of PknG. In NK cells, the interaction of HkRP3 with DOCK-8 is essential for NK cell-mediated cytotoxicity through its effects on lytic granule transport and MTOC polarization[294,298]. The regulation of HkRP3 in the presence of PknG, presumably negatively, demonstrate that PknG could interfere with microtubule stability by blocking MTOC polarization through a pathway that involves Cdc42 GEF DOCK-8 [299].

Septins are GTP-binding, filament-forming proteins that have been called the fourth component of the cytoskeleton [300]. They have been shown to play a crucial role in microtubule stability. They form filament structures and associate with other cytoskeletal components like actin filaments and microtubules. Their active core is homologous to the *Ras* family of GTPases which play an integral role in cytokinesis. The loss or inhibition of these septins leads to adverse effects on the actin cytoskeleton, the SNARE complex and vesicle trafficking [301]. Imaging studies have shown that Sept7, Sept9b, and Sept11 are distributed as a filamentous pattern along actin stress fibres in an actin filament-dependent manner; demonstrating the role of the Sept proteins in scaffolding the actin filaments for the cytoskeletal organisation [302,303]. We identified Sep7 as one of the candidate substrates phosphorylated in the presence of PknG, at Ser_1. Phosphorylation of these integral actin-binding proteins adds another layer of proof of the possible role that PknG may play in disrupting cytoskeletal organisation.

Interference with intracellular protein trafficking

Eukaryotic cells are highly organised. This organisation and tightly regulated signalling events are part of the cells precise mechanisms to maintain functionality. Trafficking of intracellular proteins is one of the ways that cells maintain homeostasis and respond to signals accordingly. The process is facilitated by vesicles transport or sorting proteins called SNARE (soluble *N*-ethylmaleimide-sensitive factor attachment protein receptor)[304]. SNARE complex mediates all intracellular membrane fusion trafficking events except for the mitochondrial fusion [305,306]. The hypothesis is that vesicle proteins that harbour proteins on their cell surface (v-SNARE) recognise target interactor proteins on the cell membrane (t-SNARE) that bind to the v-SNARE [307]. This is followed by the binding of SNAPs (soluble N-ethylmaleimide-sensitive factor attachment proteins) and NSF (N-ethylmaleimide-sensitive factor), an ATPase that triggers the break-up of the SNARE complex, leading to fusion of the two organelles [308]. One of the SNARE complexes that regulate macrophage adhesion, spreading and migration on fibronectin is the Q-SNARE complex: VAMP3/Stx4/SNAP23 [304]. The presence of PknG results phosphorylation of SNAP23, as identified in this work. VAMP3 is the t-SNARE that must bind to Stx4/SNAP23 v-SNARE and altered levels of any component of this complex have previously been reported to disrupt the

polarised localisation of podosome clusters [309]. Our data further identified NSFL cofactor p47 (Nsfl1c), an ATPase that dissociates the SNARE complex to facilitate membrane fusion[310], as also a possible substrate of PknG. Our results are further confirmation that irregularities in the components of the SNARE complex VAMP3/Stx4/SNAP23 blocks phagosome-lysosome fusion and suggest that PknG may play an important role in manipulating this well-organised host's system to the mycobacteria's advantage.

Cytoskeleton disruption through inactivation of tyrosine phosphatases

Tyrosine phosphorylation is at the centre of actin cytoskeletal organisation and signalling. SH (*Src* homology) domain-containing proteins at the cell membrane are primed for downstream protein-protein interactions through phosphorylation of the SH domain by a number of tyrosine kinases [311]. Actin polymerization pathways are induced by stimulation of SH proteins that gets auto-phosphorylated at specific tyrosine residues, that acts as a molecular switch, enabling them to undergo further tyrosine phosphorylation [311]. The resultant tyrosine phosphorylation enables protein-protein interaction with cytoplasmic interactors that are enzymes in a few pathways discussed in this section that ends in actin polymerisation.

Tyrosine-protein phosphatase non-receptor type 12 (Ptpn12), also known as PTP-PEST, is one of the substrates that are possibly under the regulation of PknG, as determined by the present study. It plays a role in regulation and dephosphorylation of cell adhesion tyrosine kinase β like PTK2B/PYK2 and the adaptor paxillin[312,313]. The cytoplasmic proline-rich tyrosine kinase 2 (Pyk2) is implicated in the regulation of actin cytoskeleton organization, in a process that is dependent on its autophosphorylation. Phosphorylated (activated) Pyk2 facilitates tyrosine phosphorylation of focal adhesion protein (Crk associated protein) p130[CAS314], priming it for protein-protein interactions with Crk, which is required for further activation of the GTP-binding protein, Rac1, which promotes actin cytoskeleton reorganisation [315]. The loss of Pyk2 activity leads to loss of macrophage motility and dendritic cells migration [313,316]. In this work, Pyk2 was found to be dephosphorylated, suggesting that possible PknG’s upstream

regulation of Ptpn12 results in dephosphorylation of Pyk2, therefore, restricting macrophage motility and normal functions.

Another substrate of Ptpn12 is Focal Adhesion Protein (FAK). Its shares sequence similarity to Pyk2, however, it is located at focal points with other cytoskeletal proteins like paxillin [317]. The close proximity of FAK and Paxillin has been suggested to mediate focal contact localization and activation of FAK [317]. Through its association with *c-Src,* it undergoes tyrosine phosphorylation, resulting in FAK binding to Grb2, Sos, and Ras, leading to ERK1/2 pathway activation. Since we have shown evidence that Ptpn12 is probably regulated by PknG, it follows that the dephosphorylation of FAK by Ptpn12 may block the ERK1/2 pathway for cytoskeletal remodelling. Furthermore, the special localization of these substrates of PknG supports our hypothesis that PknG is secreted out of the bacterium in response to the phagosome signals, thereby being able to phosphorylate substrates at different subcellular locations.

Tyrosine-protein phosphatase non-receptor type 6 (SH-P1) is expressed mostly in hematopoietic cells. SH-P1 is an SH domain phosphatase that is regulated through tyrosine phosphorylation by *Src* kinase and elevated intracellular calcium levels. Much of the work on the activity of tyrosine phosphatase function has been carried out in platelets [318]. It has been shown to be translocated into the cytoskeleton, where it interacts (through dephosphorylation) with adapter protein Grb2 [319]. Our data identified SH-P1 as one of the substrates that are phosphorylated in the presence of PknG to facilitate phagosome maturation arrest. These data demonstrate the possible mechanism that PknG phosphorylates SH-P1, thereby inhibiting its activity and interaction with Grb2, thereby inhibiting the *Ras* signalling pathway for actin cytoskeleton polymerization and lamellipodia formation. SH-P1 also regulates macrophage adhesion and motility mediated by integrins. Gene knock-out studies showed a decreased attachment of αβ Integrins, which is linked to chronic inflammatory diseases [320] and a decreased ability of immune cells to control bacterial infection [321]. SHP-1 activation was also shown to be important for downstream CD45 regulated adhesion of integrins and also regulates PIK3 mediated adhesion and macrophage spreading [320]. The suggested phosphorylation of SHP-1 by PknG

demonstrate the effect of phosphorylation of one effector that have severe phenotypic consequences for the host but that is to the benefit of the bacteria.

5.5 Conclusions and future perspectives

This chapter provided a high throughput identification of PknG kinase candidate substrates and the consequences of the phosphorylation on the host's ability to control mycobacterial infection. We identified a network of phosphoproteins phosphorylated in the presence of PknG that are involved in the actin cytoskeleton polymerization signalling pathways. We have described the possible mechanisms that PknG may employ to reprogram the host's signalling pathways to be able to block phagosome-lysosome fusion during the early events leading to latent TB infection.

The next planned experiments will be the validation of these phosphorylation events. Firstly, we will perform biochemical kinase-substrate assays with key proteins identified as phosphorylated in this study to confirm if they are candidate substrates of PknG. Secondly, our data point towards remodelling of the actin cytoskeleton, we plan to use state of the art microscopy to see any irregularities in the structural integrity of the cytoskeleton. This will be an on-going work that is beyond the scope of the present PhD thesis.

6. THESIS SUMMARY AND GENERAL CONCLUSIONS

The biological functionality of protein expression of a given system in response to stimuli is regulated through post-translational modifications. The regulation is bidirectional, it can either be negative or positive regulation depending on what the cell needs in response to stimuli. The study of post-translational modifications of proteins gives us an in-depth knowledge of the complex mechanisms governing molecular phenotypes of the cell. To this end, the aim of this thesis was to uncover how mycobacterial proteins are regulated by studying phosphorylation dynamics of mycobacteria in different environments, our goal being to better understand their physiology and the functional consequences of the phosphorylation in terms of survival and pathogenicity.

In the third chapter, we explored how the phosphorylation landscape differed between mycobacterial species. Until a few years ago, the mycobacterial phosphoproteome literature was lacking and our data has increased that catalogue. We compared two species of mycobacteria, focusing on growth rate. The physiological state of actively growing bacterial cells is characterised by the growth rate, and the expression and regulation of proteins in that state are often growth rate dependant. Cell growth is an intricate phenomenon which involves a well-orchestrated and carefully coordinated function of the cellular components and in this chapter, we aimed to correlate the differences in the proteins phosphorylated between the fast-growing and slow-growing mycobacterial species with the mechanisms different mycobacteria regulate growth. We observed phosphorylation events in proteins that that regulates mechanisms of cell division and elongation, including Wag31 and well-studied proteins that form divisome complex. The phosphorylation landscape of the fast-growing *M. smegmatis* was less complex than that of the slow-growing *M. bovis* BCG. It is interesting to note that pathogenic mycobacteria at any given state requires and regulates through phosphorylation a higher number of proteins that enables them to survive and to cause disease compared the non-pathogenic *M. smegmatis*. This complex and sophisticated protein phosphorylation network, regulating important cellular cycle events such as cell wall biosynthesis,

elongation, and cell division, as well response to stress, would allow a quick cellular response to abrupt environmental changes. However, this regulatory advantage might be associated with a cost, reflected by reduced metabolic fitness and slower growth rate.

The last two chapters of this thesis focused solely on Protein Kinase G. We set out to identify its regulatory role both in actively growing cultures and in the host by identifying the substrates it phosphorylates in both systems. We employed label-free quantitative phosphoproteomic workflow with subsequent MS based and *in silico* validation assays. This approach and the subsequent validation steps proved to be invaluable when it comes to correctly identifying kinase substrates and opens up the platform to study other mycobacterial kinases to understand their functions. Although there were no phenotypic differences observed in culture in the absence of *M. bovis* BCG PknG, unlike the reported growth defects in *M. tuberculosis* mutants lacking PknG, we identified substrates that gave us clues into the functions of this kinase. In actively growing cultures, there is a theme on the regulatory role of PknG to maintain the bacterial cell's homeostasis. Our results showed that PknG is a transcription and translation regulator, and that theme also extended to some of the host substrates phosphorylated by PknG.

The most important role of PknG in respect to *M. tuberculosis* pathogenesis is its ability to block phagosome-lysosome fusion, thereby mediating survival of pathogenic mycobacteria in macrophages. We set out to describe the mechanisms PknG uses that results in the phenotype that has been associated with latent TB infection. Since kinase functions depend solely on the substrates they phosphorylate, we started this work by hypothesising that PknG phosphorylates host substrates, thereby reprogramming normal macrophage functions. Our results revealed interesting host substrates that strongly indicate that PknG interferes with the actin polymerization signalling and resulting in dire consequences to the cytoskeleton integrity. It is well established in the literature the different signalling cascades and their regulators that respond to stimuli by polymerizing different cytoskeletal polymers. The cytoskeleton gives cells and organelles mobility to be able to migrate in response to signals. Macrophages ability to control pathogens depends on its structural rigidity and plasticity, that is a function of the cytoskeleton integrity. We showed that the regulators of Rho

GTPases (RhoGDI and GEF) are phosphorylated in the presence of PknG. These Rho GTPases are central to actin signalling and the phosphorylation of RhoGDI and GEF in the presence of PknG strongly suggests that they are kept inactive and actin polymerization is interrupted. We also identified candidate host substrates of PknG that are involved in organelle fusion. In this last chapter, we therefore identified intricate and inter-linked PknG candidate substrates that points us in the direction to be able to answer the questions we set out to elucidate with this thesis, namely to describe the mechanisms that PknG employs to block phagosome maturation: those mechanisms include phosphorylating and, therefore, interfering with key regulators of proteins involved in actin polymerization, integrins, organelle fusion, actin-myosin interactions and microtubule stability.

7. REFRENCES

1. Stock JB, Ninfa a J, Stock a M. Protein phosphorylation and regulation of adaptive responses in bacteria. Vol. 53, Microbiological reviews. 1989. 450-490 p.

2. Hunter T. A thousand and one protein kinases. Cell [Internet]. 1987 Sep [cited 2017 Mar 8];50(6):823–9. Available from: http://linkinghub.elsevier.com/retrieve/pii/0092867487905095

3. Hanks SK, Quinn AM, Hunter T. The protein kinase family: conserved features and deduced phylogeny of the catalytic domains. Science (80-) [Internet]. 1988 Jul 1;241(4861):42 LP-52. Available from: http://science.sciencemag.org/content/241/4861/42.abstract

4. Hunter T, Wang Y, Fallen C., Ihle J., Weber M., Sturgill T., et al. Protein kinases and phosphatases: the yin and yang of protein phosphorylation and signaling. Cell [Internet]. 1995 Jan 27 [cited 2017 Mar 8];80(2):225–36. Available from: http://www.ncbi.nlm.nih.gov/pubmed/7834742

5. Jers C, Soufi B, Grangeasse C, Deutscher J, Mijakovic I. Phosphoproteomics in bacteria: towards a systemic understanding of bacterial phosphorylation

networks. Expert Rev Proteomics [Internet]. 2008 Aug 1;5(4):619–27. Available from: http://dx.doi.org/10.1586/14789450.5.4.619

6. Deutscher J, Saier Jr. MH. Ser/Thr/Tyr Protein Phosphorylation in Bacteria – For Long Time Neglected, Now Well Established. J Mol Microbiol Biotechnol [Internet]. 2005;9(3–4):125–31. Available from: http://www.karger.com/DOI/10.1159/000089641

7. Ge R, Shan W. Bacterial phosphoproteomic analysis reveals the correlation between protein phosphorylation and bacterial pathogenicity. Genomics Proteomics Bioinformatics [Internet]. 2011 Oct [cited 2014 Oct 24];9(4–5):119–27. Available from: http://www.sciencedirect.com/science/article/pii/S1672022911600156

8. Molle V, Zanella-Cleon I, Robin J-P, Mallejac S, Cozzone AJ, Becchi M. Characterization of the phosphorylation sites of Mycobacterium tuberculosis serine/threonine protein kinases, PknA, PknD, PknE, and PknH by mass spectrometry. Proteomics [Internet]. 2006 Jul [cited 2014 Nov 29];6(13):3754–66. Available from: http://www.ncbi.nlm.nih.gov/pubmed/16739134

9. Fiuza M, Canova MJ, Zanella-Cléon I, Becchi M, Cozzone AJ, Mateos LM, et al. From the characterization of the four serine/threonine protein kinases (PknA/B/G/L) of Corynebacterium glutamicum toward the role of PknA and PknB in cell division. J Biol Chem [Internet]. 2008 Jun 27 [cited 2014 Nov 29];283(26):18099–112. Available from: http://www.ncbi.nlm.nih.gov/pubmed/18442973

10. Canova MJ, Veyron-Churlet R, Zanella-Cleon I, Cohen-Gonsaud M, Cozzone AJ, Becchi M, et al. The Mycobacterium tuberculosis serine/threonine kinase PknL phosphorylates Rv2175c: Mass spectrometric profiling of the activation loop phosphorylation sites and their role in the recruitment of Rv2175c. Proteomics [Internet]. 2008;8(3):521–33. Available from: http://dx.doi.org/10.1002/pmic.200700442

11. Soares NC, Spät P, Méndez JA, Nakedi K, Aranda J, Bou G. Ser/Thr/Tyr phosphoproteome characterization of Acinetobacter baumannii: comparison between a reference strain and a highly invasive multidrug-resistant clinical isolate. J Proteomics [Internet]. 2014 May 6 [cited 2014 Nov 25];102:113–24. Available from:

http://www.sciencedirect.com/science/article/pii/S1874391914001316

12. Soares NC, Spät P, Krug K, Macek B. Global Dynamics of the Escherichia coli Proteome and Phosphoproteome During Growth in Minimal Medium. J Proteome Res [Internet]. 2013 Apr 16;12(6):2611–21. Available from: http://dx.doi.org/10.1021/pr3011843

13. Pérez J, Castañeda-García A, Jenke-Kodama H, Müller R, Muñoz-Dorado J. Eukaryotic-like protein kinases in the prokaryotes and the myxobacterial kinome. Proc Natl Acad Sci [Internet]. 2008 Oct 14;105(41):15950–5. Available from: http://www.pnas.org/content/105/41/15950.abstract

14. Pereira SFF, Goss L, Dworkin J. Eukaryote-Like Serine/Threonine Kinases and Phosphatases in Bacteria. Microbiol Mol Biol Rev [Internet]. 2011 Mar 1;75(1):192–212. Available from: http://mmbr.asm.org/content/75/1/192.abstract

15. Hansen A-M, Chaerkady R, Sharma J, Díaz-Mejía JJ, Tyagi N, Renuse S, et al. The Escherichia coli phosphotyrosine proteome relates to core pathways and virulence. PLoS Pathog [Internet]. 2013 Jan [cited 2014 Nov 25];9(6):e1003403. Available from: http://www.pubmedcentral.nih.gov/articlerender.fcgi?artid=3681748&tool=pmcentrez&rendertype=abstract

16. Fernandez P, Saint-Joanis B, Barilone N, Jackson M, Gicquel B, Cole ST, et al. The Ser/Thr protein kinase PknB is essential for sustaining mycobacterial growth. J Bacteriol [Internet]. 2006 Nov [cited 2014 Nov 29];188(22):7778–84. Available from: http://www.pubmedcentral.nih.gov/articlerender.fcgi?artid=1636329&tool=pmcentrez&rendertype=abstract

17. Calder B, Albeldas C, Blackburn JM, Soares NC. Mass Spectrometry Offers Insight into the Role of Ser/Thr/Tyr Phosphorylation in the Mycobacteria [Internet]. Vol. 7, Frontiers in Microbiology . 2016. p. 141. Available from: http://journal.frontiersin.org/article/10.3389/fmicb.2016.00141

18. Wehenkel A, Bellinzoni M, Graña M, Duran R, Villarino A, Fernandez P, et al. Mycobacterial Ser/Thr protein kinases and phosphatases: Physiological roles and therapeutic potential. Biochim Biophys Acta - Proteins Proteomics [Internet]. 2008 [cited 2017 Apr 8];1784(1):193–202. Available from: http://www.sciencedirect.com/science/article/pii/S1570963907001902

19. Ravichandran A, Sugiyama N, Tomita M, Swarup S, Ishihama Y. Ser/Thr/Tyr phosphoproteome analysis of pathogenic and non-pathogenic Pseudomonas species. Proteomics [Internet]. 2009 May [cited 2014 Nov 20];9(10):2764–75. Available from: http://www.ncbi.nlm.nih.gov/pubmed/19405024

20. Lin M-H, Hsu T-L, Lin S-Y, Pan Y-J, Jan J-T, Wang J-T, et al. Phosphoproteomics of Klebsiella pneumoniae NTUH-K2044 Reveals a Tight Link between Tyrosine Phosphorylation and Virulence. Mol Cell Proteomics [Internet]. 2009 Dec 20;8(12):2613–23. Available from: http://www.ncbi.nlm.nih.gov/pmc/articles/PMC2816022/

21. Deol P, Vohra R, Saini AK, Singh A, Chandra H, Chopra P, et al. Role of Mycobacterium tuberculosis Ser/Thr kinase PknF: implications in glucose transport and cell division. J Bacteriol [Internet]. 2005 May;187(10):3415–20. Available from: http://www.pubmedcentral.nih.gov/articlerender.fcgi?artid=1112024&tool=pmcentrez&rendertype=abstract

22. Av-gay Y, Everett M. The eukaryotic-like Ser / Thr protein kinases of Mycobacterium tuberculosis. Trends Microbiol Rev. 2000;8(5):238–44.

23. Han G, Zhang CC. On the origin of Ser/Thr kinases in a prokaryote. FEMS Microbiol Lett. 2001;200(1):79–84.

24. Ochman H, Lawrence JG, Groisman EA. Lateral gene transfer and the nature of bacterial innovation. Nature [Internet]. 2000 May 18;405(6784):299–304. Available from: http://dx.doi.org/10.1038/35012500

25. Stancik IA, Šestak MS, Ji B, Axelson-Fisk M, Franjevic D, Jers C, et al. Serine/Threonine Protein Kinases from Bacteria, Archaea and Eukarya Share a Common Evolutionary Origin Deeply Rooted in the Tree of Life. J Mol Biol. 2018;430(1):27–32.

26. AV-GAY Y, DAVIES J. Components of Eukaryotic-like Protein Signaling Pathways in Mycobacterium tuberculosis. Microb Comp Genomics [Internet]. 1997 Jan 1;2(1):63–73. Available from: http://dx.doi.org/10.1089/omi.1.1997.2.63

27. Cole ST, Brosch R, Parkhill J, Garnier T, Churcher C, Harris D, et al. Deciphering the biology of Mycobacterium tuberculosis from the complete genome sequence. Nature [Internet]. 1998 Jun 11;393(6685):537–44.

Available from: http://dx.doi.org/10.1038/31159

28. Alber T. Signaling mechanisms of the Mycobacterium tuberculosis receptor Ser/Thr protein kinases. Curr Opin Struct Biol [Internet]. 2009 Dec 14;19(6):650–7. Available from: http://www.ncbi.nlm.nih.gov/pmc/articles/PMC2790423/

29. Prisic S, Dankwa S, Schwartz D, Chou MF, Locasale JW, Kang C-M, et al. Extensive phosphorylation with overlapping specificity by Mycobacterium tuberculosis serine/threonine protein kinases. Proc Natl Acad Sci U S A [Internet]. 2010 Apr 20 [cited 2014 Oct 21];107(16):7521–6. Available from: http://www.pubmedcentral.nih.gov/articlerender.fcgi?artid=2867705&tool=pmcentrez&rendertype=abstract

30. Nakedi KC, Nel AJM, Garnett S, Blackburn JM, Soares NC. Comparative Ser/Thr/Tyr phosphoproteomics between two mycobacterial species: The fast growing Mycobacterium smegmatis and the slow growing Mycobacterium bovis BCG. Front Microbiol. 2015;6(APR):1–12.

31. Kusebauch U, Ortega C, Ollodart A, Rogers RS, Sherman DR, Moritz RL, et al. Mycobacterium tuberculosis supports protein tyrosine phosphorylation. Proc Natl Acad Sci [Internet]. 2014 Jun 24;111(25):9265–70. Available from: http://www.pnas.org/content/111/25/9265.abstract

32. Fortuin S, Tomazella GG, Nagaraj N, Sampson SL, van Pittius NCG, Soares NC, et al. Phosphoproteomics analysis of a clinical Mycobacterium tuberculosis Beijing isolate: expanding the mycobacterial phosphoproteome catalog. Front Microbiol. 2015;6.

33. Martinez M, Alzari PM, André-Leroux G. 12 Signalling Mechanisms in Prokaryotes. Bact Membr Struct Mol Biol. 2014;387.

34. Zhou P, Wong D, Li W, Xie J, Av-Gay Y. Phosphorylation of Mycobacterium tuberculosis protein tyrosine kinase A PtkA by Ser/Thr protein kinases [Internet]. Vol. 467, Biochemical and Biophysical Research Communications. 2015 [cited 2017 Apr 27]. Available from: http://www.sciencedirect.com/science/article/pii/S0006291X15306410

35. Chow K, Ng D, Stokes R, Johnson P. Protein tyrosine phosphorylation in Mycobacterium tuberculosis. FEMS Microbiol Lett [Internet]. 1994;124(2):203–7. Available from:

http://www.sciencedirect.com/science/article/pii/037810979490250X

36. Walburger A, Koul A, Ferrari G, Nguyen L, Prescianotto-baschong C, Huygen K, et al. Protein Kinase G from Pathogenic Mycobacteria Promotes Survival Within Macrophages. 2004;304(June).

37. Cowley S, Ko M, Pick N, Chow R, Downing KJ, Gordhan BG, et al. The Mycobacterium tuberculosis protein serine/threonine kinase PknG is linked to cellular glutamate/glutamine levels and is important for growth in vivo. Mol Microbiol [Internet]. 2004 Jun [cited 2014 Nov 29];52(6):1691–702. Available from: http://www.ncbi.nlm.nih.gov/pubmed/15186418

38. Chopra P, Singh B, Singh R, Vohra R, Koul A, Meena LS, et al. Phosphoprotein phosphatase of Mycobacterium tuberculosis dephosphorylates serine–threonine kinases PknA and PknB. Biochem Biophys Res Commun [Internet]. 2003 Nov [cited 2014 Nov 29];311(1):112–20. Available from: http://linkinghub.elsevier.com/retrieve/pii/S0006291X03020011

39. Park ST, Kang C-M, Husson RN. Regulation of the SigH stress response regulon by an essential protein kinase in Mycobacterium tuberculosis. Proc Natl Acad Sci U S A [Internet]. 2008 Sep 2;105(35):13105–10. Available from: http://www.pubmedcentral.nih.gov/articlerender.fcgi?artid=2529121&tool=pmcentrez&rendertype=abstract

40. Kang C, Abbott DW, Park ST, Dascher CC, Cantley LC, Husson RN. serine / threonine kinases PknA and PknB : substrate identification and regulation of cell shape. 2005;1692–704.

41. Signoretto C, Di Stefano F, Canepari P. Modified peptidoglycan chemical composition in shape-altered Escherichia coli. Microbiology. 1996;142(8):1919–26.

42. Jani C, Eoh H, Lee JJ, Hamasha K, Sahana MB, Han J-S, et al. Regulation of polar peptidoglycan biosynthesis by Wag31 phosphorylation in mycobacteria. BMC Microbiol [Internet]. 2010 Jan [cited 2014 Nov 20];10(1):327. Available from: http://www.pubmedcentral.nih.gov/articlerender.fcgi?artid=3019181&tool=pmcentrez&rendertype=abstract

43. Nguyen L, Scherr N, Gatfield J, Walburger A, Pieters J, Thompson CJ. Antigen

84, an Effector of Pleiomorphism in Mycobacterium smegmatis . J Bacteriol [Internet]. 2007 Nov 1;189(21):7896–910. Available from: http://jb.asm.org/content/189/21/7896.abstract

44. Young TA, Delagoutte B, Endrizzi JA, Falick AM, Alber T. Structure of Mycobacterium tuberculosis PknB supports a universal activation mechanism for Ser/Thr protein kinases. Nat Struct Biol [Internet]. 2003 Jan 27;10:168. Available from: http://dx.doi.org/10.1038/nsb897

45. Roumestand C, Leiba J, Galophe N, Margeat E, Padilla A, Bessin Y, et al. Structural insight into the Mycobacterium tuberculosis Rv0020c protein and its interaction with the PknB kinase. Structure. 2011;19(10):1525–34.

46. Braibant M, Gilot P, Content J. The ATP binding cassette (ABC) transport systems of Mycobacterium tuberculosis. FEMS Microbiol Rev [Internet]. 2000 Oct 1;24(4):449–67. Available from: http://dx.doi.org/10.1111/j.1574-6976.2000.tb00550.x

47. Kumar D, Narayanan S. PknE, a serine/threonine kinase of Mycobacterium tuberculosis modulates multiple apoptotic paradigms. Infect Genet Evol [Internet]. 2012;12(4):737–47. Available from: http://dx.doi.org/10.1016/j.meegid.2011.09.008

48. Parandhaman DK, Sharma P, Bisht D, Narayanan S. Proteome and phosphoproteome analysis of the serine/threonine protein kinase E mutant of Mycobacterium tuberculosis. Life Sci [Internet]. 2014 Jul 30 [cited 2014 Oct 24];109(2):116–26. Available from: http://www.sciencedirect.com/science/article/pii/S002432051400544X

49. Hofmann K, Bucher P. The FHA domain: a putative nuclear signalling domain found in protein kinases and transcription factors. Trends Biochem Sci [Internet]. 2017 Dec 7;20(9):347–9. Available from: http://dx.doi.org/10.1016/S0968-0004(00)89072-6

50. Durocher D, Taylor IA, Sarbassova D, Haire LF, Westcott SL, Jackson SP, et al. The Molecular Basis of FHA Domain:Phosphopeptide Binding Specificity and Implications for Phospho-Dependent Signaling Mechanisms. Mol Cell [Internet]. 2000 Nov;6(5):1169–82. Available from: https://www.sciencedirect.com/science/article/pii/S1097276500001143

51. Durocher D, Henckel J, Fersht AR, Jackson SP. The FHA Domain Is a Modular

Phosphopeptide Recognition Motif. Mol Cell [Internet]. 1999 Sep;4(3):387–94. Available from: https://www.sciencedirect.com/science/article/pii/S1097276500803408

52. Molle V, Soulat D, Jault JM, Grangeasse C, Cozzone AJ, Prost JF. Two FHA domains on an ABC transporter, Rv1747, mediate its phosphorylation by PknF, a Ser/Thr protein kinase from Mycobacterium tuberculosis. FEMS Microbiol Lett. 2004;234(2):215–23.

53. Koul A, Choidas A, Tyagi AK, Drlica K, Singh Y, Ullrich A. Serine/threonine protein kinases PknF and PknG of Mycobacterium tuberculosis: Characterization and localization. Microbiology. 2001;147(8):2307–14.

54. Papavinasasundaram KG, Chan B, Chung J, Colston J, Davis EO, Av-gay Y, et al. Deletion of the Mycobacterium tuberculosis pknH Gene Confers a Higher Bacillary Load during the Chronic Phase of Infection in BALB / c Mice Deletion of the Mycobacterium tuberculosis pknH Gene Confers a Higher Bacillary Load during the Chronic Phase of In. Society. 2005;187(16):5751–60.

55. Zheng X, Papavinasasundaram KG, Av-Gay Y. Novel substrates of Mycobacterium tuberculosis PknH Ser/Thr kinase. Biochem Biophys Res Commun [Internet]. 2007 Mar 30 [cited 2014 Nov 30];355(1):162–8. Available from: http://www.sciencedirect.com/science/article/pii/S0006291X07001805

56. Molle V, Kremer L, Girard-Blanc C, Besra GS, Cozzone AJ, Prost JF. An FHA Phosphoprotein Recognition Domain Mediates Protein EmbR Phosphorylation by PknH, a Ser/Thr Protein Kinase from Mycobacterium tuberculosis. Biochemistry. 2003;42(51):15300–9.

57. Malhotra V, Arteaga-Cortés LT, Clay G, Clark-Curtiss JE. Mycobacterium tuberculosis protein kinase K confers survival advantage during early infection in mice and regulates growth in culture and during persistent infection: Implications for immune modulation. Microbiology. 2010;156(9):2829–41.

58. Malhotra V, Okon BP, Clark-Curtiss JE. Mycobacterium tuberculosis protein kinase K enables growth adaptation through translation control. J Bacteriol. 2012;194(16):4184–96.

59. Lakshminarayan H, Narayanan S, Bach H, Sundaram KGP, Av-Gay Y. Molecular cloning and biochemical characterization of a serine threonine protein kinase, PknL, from Mycobacterium tuberculosis. Protein Expr Purif. 2008;58(2):309–17.

60. Refaya AK, Sharma D, Kumar V, Bisht D, Narayanan S. A Serine/threonine kinase PknL, is involved in the adaptive response of Mycobacterium tuberculosis. Microbiol Res [Internet]. 2016;190:1–11. Available from: http://dx.doi.org/10.1016/j.micres.2016.02.005

61. Scherr N, Honnappa S, Kunz G, Mueller P, Jayachandran R, Winkler F, et al. Structural basis for the specific inhibition of protein kinase G , a virulence factor of Mycobacterium tuberculosis. 2007;104(41).

62. Lisa MN, Gil M, Andr??-Leroux G, Barilone N, Dur??n R, Biondi RM, et al. Molecular Basis of the Activity and the Regulation of the Eukaryotic-like S/T Protein Kinase PknG from Mycobacterium tuberculosis. Structure. 2015;1039–48.

63. van der Woude AD, Stoop EJM, Stiess M, Wang S, Ummels R, van Stempvoort G, et al. Analysis of secA2-dependent substrates in mycobacterium marinum identifies protein kinase G (PknG) as a virulence effector. Cell Microbiol. 2014;16(2):280–95.

64. Wolff KA, de la Peña AH, Nguyen HT, Pham TH, Amzel LM, Gabelli SB, et al. A Redox Regulatory System Critical for Mycobacterial Survival in Macrophages and Biofilm Development. PLoS Pathog. 2015;11(4):1–20.

65. Wolff KA, Nguyen HT, Cartabuke RH, Singh A, Ogwang S, Nguyen L. Protein kinase G is required for intrinsic antibiotic resistance in mycobacteria. Antimicrob Agents Chemother. 2009;53(8):3515–9.

66. Reckel S, Hantschel O. Kinase Regulation in Mycobacterium tuberculosis: Variations on a Theme. Structure [Internet]. 2015 Jun [cited 2016 Jan 14];23(6):975–6. Available from: http://www.sciencedirect.com/science/article/pii/S0969212615001835

67. Scherr N, Mu P, Perisa D, Combaluzier B, Jeno P, Pieters J. Survival of Pathogenic Mycobacteria in Macrophages Is Mediated through Autophosphorylation of Protein Kinase G □ †. 2009;191(14):4546–54.

68. Johnson LN, Noble MEM, Owen DJ. Active and inactive protein kinases: Structural basis for regulation. Cell. 1996;85(2):149–58.

69. Taylor SS, Radzio-Andzelm E. Three protein kinase structures define a common motif. Structure. 1994;2(5):345–55.

70. O'Hare HM, Durán R, Cerveñansky C, Bellinzoni M, Wehenkel AM, Pritsch O, et al. Regulation of glutamate metabolism by protein kinases in mycobacteria. Mol Microbiol. 2008;70(6):1408–23.

71. Schlessinger J, Lemmon MA. SH2 and PTB Domains in Tyrosine Kinase Signaling. Sci STKE [Internet]. 2003 Jul 15;2003(191):re12 LP-re12. Available from: http://stke.sciencemag.org/content/2003/191/re12.abstract

72. Martin K, Steinberg TH, Cooley LA, Gee KR, Beechem JM, Patton WF. Quantitative analysis of protein phosphorylation status and protein kinase activity on microarrays using a novel fluorescent phosphorylation sensor dye. Proteomics [Internet]. 2003 Jul 1;3(7):1244–55. Available from: http://dx.doi.org/10.1002/pmic.200300445

73. Fukunaga R, Hunter T. MNK1, a new MAP kianse-activated protein kianse, isolated by a novel expression screening method for idenifying protein kinase substrates. Embo J. 1997;16(8):1921–33.

74. Y. Jia, C.M. Quinn, S. Kwak RVT. Current in vitro kinase assay technologies: the quest for a universal format. Curr Drug Discov Technol. 2008;5:59–66.

75. Rush J, Moritz A, Lee KA, Guo A, Goss VL, Spek EJ, et al. Immunoaffinity profiling of tyrosine phosphorylation in cancer cells. Nat Biotech [Internet]. 2005 Jan;23(1):94–101. Available from: http://dx.doi.org/10.1038/nbt1046

76. De Corte V, Demol H, Goethals M, Van Damme J, Gettemans J, Vandekerckhove J. Identification of Tyr438 as the major in vitro c-Src phosphorylation site in human gelsolin: a mass spectrometric approach. Protein Sci [Internet]. 1999;8(1):234–41. Available from: http://www.pubmedcentral.nih.gov/articlerender.fcgi?artid=2144107&tool=pmcentrez&rendertype=abstract

77. Pandey A, Podtelejnikov A V, Blagoev B, Bustelo XR, Mann M, Lodish HF. Analysis of receptor signaling pathways by mass spectrometry: Identification of Vav-2 as a substrate of the epidermal and platelet-derived

growth factor receptors. Proc Natl Acad Sci [Internet]. 2000 Jan 4;97(1):179–84. Available from: http://www.pnas.org/content/97/1/179.abstract

78. Hunter T. Cold Spring Harbor Perspect. Biol. 2014;6:a020644.

79. Poss ZC, Ebmeier CC, Odell AT, Tangpeerachaikul A, Lee T, Pelish HE, et al. Identification of Mediator Kinase Substrates in Human Cells using Cortistatin A and Quantitative Phosphoproteomics. Cell Rep [Internet]. 2016 Mar 29 [cited 2016 Apr 11];15(2):436–50. Available from: http://www.sciencedirect.com/science/article/pii/S2211124716302868

80. Sharma K, D'Souza RCJ, Tyanova S, Schaab C, Wiśniewski JR, Cox J, et al. Ultradeep Human Phosphoproteome Reveals a Distinct Regulatory Nature of Tyr and Ser/Thr-Based Signaling. Cell Rep [Internet]. 2014 Aug [cited 2014 Aug 26];8(5):1583–94. Available from: http://www.sciencedirect.com/science/article/pii/S2211124714006202

81. Xue L, Geahlen RL, Tao WA. Identification of direct tyrosine kinase substrates based on protein kinas assay-linked phoshpoproteomics. Mcp. 2013;2969–80.

82. Russell H, Siuzdak G. A Mass Spec Timeline. Today'S Chem Work [Internet]. 2003;47–9. Available from: http://masspec.scripps.edu/publications/public_pdf/90_art.pdf

83. Chen X, Wu D, Zhao Y, Wong BHC, Guo L. Increasing phosphoproteome coverage and identification of phosphorylation motifs through combination of different HPLC fractionation methods. J Chromatogr B Anal Technol Biomed Life Sci. 2011;879(1):25–34.

84. Swaney D, Wenger C, Coon J. Value of using multiple proteases for large-scale mass spectrometry-based proteomics. J Proteome Res [Internet]. 2010;1323–9. Available from: http://pubs.acs.org/doi/abs/10.1021/pr900863u

85. Bian Y, Ye M, Song C, Cheng K, Wang C, Wei X, et al. Improve the coverage for the analysis of phosphoproteome of HeLa cells by a tandem digestion approach. J Proteome Res. 2012;11(5):2828–37.

86. Klammer AA, MacCoss MJ. Effects of modified digestion schemes on the

identification of proteins from complex mixtures. J Proteome Res. 2006;5(3):695–700.

87. Mann M, Ong S, Gr M, Steen H, Jensen ON, Pandey A. Analysis of protein phosphorylation using mass spectrometry : deciphering the phosphoproteome. 2002;20(6):261–8.

88. Steen H, Jebanathirajah JA, Rush J, Morrice N, Kirschner MW. Phosphorylation Analysis by Mass Spectrometry. Mol Cell Proteomics [Internet]. 2006;5(1):172–81. Available from: http://www.mcponline.org/lookup/doi/10.1074/mcp.M500135-MCP200

89. Hunter AP, Games DE. Chromatographic and mass spectrometric methods for the identification of phosphorylation sites in phosphoproteins. Rapid Commun Mass Spectrom [Internet]. 1994 Jul 1;8(7):559–70. Available from: http://dx.doi.org/10.1002/rcm.1290080713

90. Nagaraj N, D'Souza RCJ, Cox J, Olsen J V, Mann M. Feasibility of Large-Scale Phosphoproteomics with Higher Energy Collisional Dissociation Fragmentation. J Proteome Res [Internet]. 2010 Dec 3;9(12):6786–94. Available from: https://doi.org/10.1021/pr100637q

91. DeGnore J, Qin J. Fragmentation of phosphopeptides in an ion trap mass spectrometer. J Am Soc Mass Spectrom [Internet]. 1998;9(11):1175–88. Available from: https://www.ncbi.nlm.nih.gov/pubmed/9794085%5Cnhttp://www.sciencedirect.com/science/article/pii/S1044030598000889

92. Syka JEP, Coon JJ, Schroeder MJ, Shabanowitz J, Hunt DF. Peptide and protein sequence analysis by electron transfer dissociation mass spectrometry. Proc Natl Acad Sci U S A [Internet]. 2004;101(26):9528–33. Available from: http://www.pubmedcentral.nih.gov/articlerender.fcgi?artid=470779&tool=pmcentrez&rendertype=abstract

93. Simons J. Mechanisms for S-S and N-C?? bond cleavage in peptide ECD and ETD mass spectrometry. Chem Phys Lett [Internet]. 2010;484(4–6):81–95. Available from: http://dx.doi.org/10.1016/j.cplett.2009.10.062

94. Gunawardena HP, Gorenstein L, Erickson DE, Xia Y, McLuckey SA. Electron transfer dissociation of multiply protonated and fixed charge disulfide linked polypeptides. Int J Mass Spectrom. 2007;265(2–3):130–8.

95. Frese CK, Altelaar AFM, Hennrich ML, Nolting D, Zeller M, Griep-Raming J, et al. Improved Peptide Identification by Targeted Fragmentation Using CID, HCD and ETD on an LTQ-Orbitrap Velos. J Proteome Res. 2011;10(5):2377–88.

96. Sweet SMM, Creese AJ, Cooper HJ. Strategy for the Identification of Sites of Phosphorylation in Proteins: Neutral Loss Triggered Electron Capture Dissociation. Anal Chem [Internet]. 2006 Nov 1;78(21):7563–9. Available from: http://dx.doi.org/10.1021/ac061331i

97. Collins MO, Wright JC, Jones M, Rayner JC, Choudhary JS. ScienceDirect Confident and sensitive phosphoproteomics using combinations of collision induced dissociation and electron transfer dissociation ☆. J Proteomics [Internet]. 2014;103:1–14. Available from: http://dx.doi.org/10.1016/j.jprot.2014.03.010

98. Cox J, Neuhauser N, Michalski A, Scheltema RA, Olsen J V, Mann M. Andromeda: A Peptide Search Engine Integrated into the MaxQuant Environment. J Proteome Res [Internet]. 2011 Apr 1;10(4):1794–805. Available from: http://dx.doi.org/10.1021/pr101065j

99. Eng JK, Searle BC, Clauser KR, Tabb DL. A Face in the Crowd: Recognizing Peptides Through Database Search. Mol Cell Proteomics [Internet]. 2011;10(11):R111.009522-R111.009522. Available from: http://www.mcponline.org/cgi/doi/10.1074/mcp.R111.009522

100. Craig R, Beavis RC. TANDEM: matching proteins with tandem mass spectra. Bioinformatics [Internet]. 2004 Jun 12;20(9):1466–7. Available from: http://dx.doi.org/10.1093/bioinformatics/bth092

101. Perkins DN, Pappin DJC, Creasy DM, Cottrell JS. Probability-based protein identification by searching sequence databases using mass spectrometry data. Electrophoresis [Internet]. 1999;20(18):3551–67. Available from: http://doi.wiley.com/10.1002/%28SICI%291522-2683%2819991201%2920%3A18%3C3551%3A%3AAID-ELPS3551%3E3.0.CO%3B2-2

102. Eng JK, Mccormack AL, Yates JR. An Approach to Correlate Tandem Mass Spectral Data of Peptides with Amino Acid Sequences in a Protein Database. Am Soc Mass Spectrom. 1994;5:976–89.

103. Geer LY, Markey SP, Kowalak JA, Wagner L, Xu M, Maynard DM, et al. Open Mass Spectrometry Search Algorithm. J Proteome Res [Internet]. 2004 Oct 1;3(5):958–64. Available from: http://dx.doi.org/10.1021/pr0499491

104. Ma ZQ, Dasari S, Chambers MC, Litton MD, Sobecki SM, Zimmerman LJ, et al. IDPicker 2.0: Improved protein assembly with high discrimination peptide identification filtering. J Proteome Res. 2009;8(8):3872–81.

105. Wang D, Dasari S, Chambers MC, Holman JD, Chen K, Liebler DC, et al. Basophile: Accurate Fragment Charge State Prediction Improves Peptide Identification Rates. Genomics, Proteomics Bioinforma [Internet]. 2013;11(2):86–95. Available from: http://dx.doi.org/10.1016/j.gpb.2012.11.004

106. Kleiman LB, Maiwald T, Conzelmann H, Lauffenburger DA, Sorger PK. Rapid Phospho-Turnover by Receptor Tyrosine Kinases Impacts Downstream Signaling and Drug Binding. Mol Cell [Internet]. 2011;43(5):723–37. Available from: http://dx.doi.org/10.1016/j.molcel.2011.07.014

107. Soares NC, Spät P, Méndez JA, Nakedi K, Aranda J, Bou G. Ser/Thr/Tyr phosphoproteome characterization of Acinetobacter baumannii: Comparison between a reference strain and a highly invasive multidrug-resistant clinical isolate. J Proteomics. 2014;102.

108. Johnson H. Uncovering dynamic phosphorylation signaling using mass spectrometry. Int J Mass Spectrom [Internet]. 2015;391:123–38. Available from: http://dx.doi.org/10.1016/j.ijms.2015.08.002

109. Krug K, Macek B. Global Dynamics of the Escherichia coli Proteome and Phosphoproteome During Growth in Minimal Medium. 2013;

110. Ravikumar V, Shi L, Krug K, Derouiche A, Jers C, Cousin C, et al. Quantitative phosphoproteome analysis of bacillus subtilis reveals novel substrates of the kinase PrkC and phosphatase PrpC. Mol Cell Proteomics [Internet]. 2014 Aug [cited 2014 Nov 10];13(8):1965–78. Available from: http://www.ncbi.nlm.nih.gov/pubmed/24390483

111. Montoya A, Beltran L, Casado P, Rodríguez-Prados J-C, Cutillas PR. Characterization of a TiO2 enrichment method for label-free quantitative phosphoproteomics. Methods [Internet]. 2011 [cited 2017 Apr 8];54(4):370–8. Available from:

http://www.sciencedirect.com/science/article/pii/S1046202311000399

112. Olsen, JV Miller ML, Brunak S, Vermeulen M, Santamaria A, Kumar C, Jensen LJ, et al. Quantitative phosphoproteomics reveals widespread full phosphorylation site occupancy during mitosis. Sci Signal. 2010;3(104).

113. Andersson L, Porath J. Isolation of phosphoproteins by immobilized metal (Fe3+) affinity chromatography. Anal Biochem [Internet]. 1986;154(1):250–4. Available from: http://www.sciencedirect.com/science/article/pii/0003269786905233

114. Posewitz MC, Tempst P. Immobilized gallium(III) affinity chromatography of phosphopeptides. Anal Chem. 1999;71(14):2883–92.

115. Boersema PJ, Divecha N, Heck AJR, Mohammed S. Evaluation and optimization of ZIC-HILIC-RP as an alternative MudPIT strategy. J Proteome Res. 2007;6(3):937–46.

116. McNulty DE, Annan RS. Hydrophilic Interaction Chromatography Reduces the Complexity of the Phosphoproteome and Improves Global Phosphopeptide Isolation and Detection. Mol Cell Proteomics [Internet]. 2008;7(5):971–80. Available from: http://www.mcponline.org/lookup/doi/10.1074/mcp.M700543-MCP200

117. Lu J, Li Y, Deng C. Facile synthesis of zirconium phosphonate-functionalized magnetic mesoporous silica microspheres designed for highly selective enrichment of phosphopeptides. Nanoscale [Internet]. 2011;3(3):1225–33. Available from: http://dx.doi.org/10.1039/C0NR00896F

118. Ma W, Zhang Y, Li L, Zhang Y, Yu M, Guo J, et al. Ti4+-Immobilized Magnetic Composite Microspheres for Highly Selective Enrichment of Phosphopeptides. Adv Funct Mater [Internet]. 2012 Aug 10;23(1):107–15. Available from: https://doi.org/10.1002/adfm.201201364

119. Huang J, Wang F, Ye M, Zou H. Enrichment and separation techniques for large-scale proteomics analysis of the protein post-translational modifications. J Chromatogr A [Internet]. 2014;1372:1–17. Available from: http://dx.doi.org/10.1016/j.chroma.2014.10.107

120. Pinkse MWH, Uitto PM, Hilhorst MJ, Ooms B, Heck AJR. Selective Isolation at the Femtomole Level of Phosphopeptides from Proteolytic Digests Using

2D-NanoLC-ESI-MS / MS and Titanium Oxide Precolumns peptides by trapping them under acidic conditions on a. 2004;76(14):3935–43.

121. Sano A, Nakamura H. Titania as a chemo-affinity support for the column-switching HPLC analysis of phosphopeptides: application to the characterization of phosphorylation sites in proteins by combination with protease digestion and electrospray ionization mass spectrometry. Anal Sci. 2004;20(5):861–4.

122. Ikeguchi Y, Nakamura H. Determination of organic phosphates by column-switching high performance anion-exchange chromatography using on-line preconcentration on titania. Anal Sci [Internet]. 1997;13(June):479–83. Available from: http://pdf.lookchem.com/pdf/22/4c92d717-24ca-4fd7-a7f6-82ca0b3aee43.pdf

123. Larsen MR, Thingholm TE, Jensen ON, Roepstorff P, Jørgensen TJD. Highly Selective Enrichment of Phosphorylated Peptides from Peptide Mixtures Using Titanium Dioxide Microcolumns *. 2005;873–86.

124. Chen C, Chen Y. Fe 3 O 4 / TiO 2 Core / Shell Nanoparticles as Affinity Probes for the Analysis of Phosphopeptides Using TiO 2 Surface-Assisted Laser Desorption / Ionization Mass Spectrometry. 2005;77(18):5912–9.

125. Ficarro SB, McCleland ML, Stukenberg PT, Burke DJ, Ross MM, Shabanowitz J, et al. Phosphoproteome analysis by mass spectrometry and its application to Saccharomyces cerevisiae. Nat Biotech [Internet]. 2002 Mar;20(3):301–5. Available from: http://dx.doi.org/10.1038/nbt0302-301

126. Thingholm TE, Jensen ON, Robinson PJ, Larsen MR. SIMAC (sequential elution from IMAC), a phosphoproteomics strategy for the rapid separation of monophosphorylated from multiply phosphorylated peptides. Mol Cell Proteomics. 2008;7(4):661–71.

127. Cox J, Mann M. MaxQuant enables high peptide identification rates, individualized p.p.b.-range mass accuracies and proteome-wide protein quantification. Nat Biotechnol [Internet]. 2008 Nov 30;26:1367. Available from: http://dx.doi.org/10.1038/nbt.1511

128. Eng JK, Jahan TA, Hoopmann MR. Comet: An open-source MS/MS sequence database search tool. Proteomics [Internet]. 2013 Jan 1;13(1):22–4. Available from: http://dx.doi.org/10.1002/pmic.201200439

129. Savitski MM, Lemeer S, Boesche M, Lang M, Mathieson T, Bantscheff M, et al. Confident Phosphorylation Site Localization Using the Mascot Delta Score. Mol Cell Proteomics [Internet]. 2011 Feb 1;10(2). Available from: http://www.mcponline.org/content/10/2/M110.003830.abstract

130. Beausoleil SA, Villén J, Gerber SA, Rush J, Gygi SP. A probability-based approach for high-throughput protein phosphorylation analysis and site localization. Nat Biotechnol [Internet]. 2006 Sep 10;24:1285. Available from: http://dx.doi.org/10.1038/nbt1240

131. Chalkley RJ, Clauser KR. Modification Site Localization Scoring: Strategies and Performance. Mol Cell Proteomics [Internet]. 2012 May 1;11(5):3–14. Available from: http://www.mcponline.org/content/11/5/3.abstract

132. Ruttenberg BE, Pisitkun T, Knepper MA, Hoffert JD. PhosphoScore: An Open-Source Phosphorylation Site Assignment Tool for MSn Data. J Proteome Res [Internet]. 2008 Jul 1;7(7):3054–9. Available from: http://dx.doi.org/10.1021/pr800169k

133. Taus T, Köcher T, Pichler P, Paschke C, Schmidt A, Henrich C, et al. Universal and Confident Phosphorylation Site Localization Using phosphoRS. J Proteome Res [Internet]. 2011 Dec 2;10(12):5354–62. Available from: http://dx.doi.org/10.1021/pr200611n

134. Mayya V, Han DK. Phosphoproteomics by mass spectrometry: insights, implications, applications and limitations. Expert Rev Proteomics [Internet]. 2009;6(6):605–18. Available from: http://www.ncbi.nlm.nih.gov/pubmed/19929607%5Cnhttp://www.pubmedcentral.nih.gov/articlerender.fcgi?artid=PMC2931417

135. Potapova IA, El-Maghrabi MR, Doronin S V., Benjamin WB. Phosphorylation of recombinant human ATP:citrate lyase by cAMP-dependent protein kinase abolishes homotropic allosteric regulation of the enzyme by citrate and increases the enzyme activity. Allosteric activation of atp:citrate lyase by phosphorylated sug. Biochemistry. 2000;39(5):1169–79.

136. Viner RI, Zhang T, Second T, Zabrouskov V. Quantification of post-translationally modified peptides of bovine α-crystallin using tandem mass tags and electron transfer dissociation. J Proteomics [Internet]. 2009;72(5):874–85. Available from:

http://www.sciencedirect.com/science/article/pii/S1874391909000967

137. Dayon L, Hainard A, Licker V, Turck N, Kuhn K, Hochstrasser DF, et al. Relative Quantification of Proteins in Human Cerebrospinal Fluids by MS/MS Using 6-Plex Isobaric Tags. Anal Chem [Internet]. 2008 Apr 15;80(8):2921–31. Available from: http://dx.doi.org/10.1021/ac702422x

138. Choe L, D'Ascenzo M, Relkin NR, Pappin D, Ross P, Williamson B, et al. 8-Plex quantitation of changes in cerebrospinal fluid protein expression in subjects undergoing intravenous immunoglobulin treatment for Alzheimer's disease. Proteomics [Internet]. 2007 Oct 1;7(20):3651–60. Available from: http://dx.doi.org/10.1002/pmic.200700316

139. Thompson A, Schäfer J, Kuhn K, Kienle S, Schwarz J, Schmidt G, et al. Tandem Mass Tags: A Novel Quantification Strategy for Comparative Analysis of Complex Protein Mixtures by MS/MS. Anal Chem [Internet]. 2003 Apr 1;75(8):1895–904. Available from: http://dx.doi.org/10.1021/ac0262560

140. Ross PL, Huang YN, Marchese JN, Williamson B, Parker K, Hattan S, et al. Multiplexed Protein Quantitation in Saccharomyces cerevisiae Using Amine-reactive Isobaric Tagging Reagents. Mol Cell Proteomics [Internet]. 2004 Dec 1;3(12):1154–69. Available from: http://www.mcponline.org/content/3/12/1154.abstract

141. Schwämmle V, Verano-Braga T, Roepstorff P. Computational and statistical methods for high-throughput analysis of post-translational modifications of proteins. J Proteomics [Internet]. 2015;129:3–15. Available from: http://dx.doi.org/10.1016/j.jprot.2015.07.016

142. Oh S, Kang DD, Brock GN, Tseng GC. Biological impact of missing-value imputation on downstream analyses of gene expression profiles. Bioinformatics [Internet]. 2011 Jan 1;27(1):78–86. Available from: http://dx.doi.org/10.1093/bioinformatics/btq613

143. Little RJA, Rubin DB. Statistical analysis with missing data. New York: John Willey & Sons. Inc; 2002.

144. Wang P. Normalization regarding non-random missing values in high-throughput mass spectrometry data pei wang, hua tang, heidi zhang, jeffrey whiteaker, amanda g. paulovich, and martin mcintosh pacific symposium on biocomputing 11: 315-326 (2006). In: Pacific Symposium on

Biocomputing. 2006. p. 315–26.

145. Kauko O, Laajala TD, Jumppanen M, Hintsanen P, Suni V, Haapaniemi P, et al. Label-free quantitative phosphoproteomics with novel pairwise abundance normalization reveals synergistic RAS and CIP2A signaling. Sci Rep [Internet]. 2015;5(August):13099. Available from: http://www.pubmedcentral.nih.gov/articlerender.fcgi?artid=4642524&tool=pmcentrez&rendertype=abstract

146. Macek B, Mijakovic I, Olsen J V, Gnad F, Kumar C, Jensen PR, et al. The Serine/Threonine/Tyrosine Phosphoproteome of the Model Bacterium Bacillus subtilis. Mol Cell Proteomics [Internet]. 2007 Apr 1;6(4):697–707. Available from: http://www.mcponline.org/content/6/4/697.abstract

147. Shi L, Pigeonneau N, Ravikumar V, Dobrinic P, Macek B, Franjevic D, et al. Cross-phosphorylation of bacterial serine/threonine and tyrosine protein kinases on key regulatory residues. Front Microbiol [Internet]. 2014 Jan [cited 2014 Nov 29];5(September):495. Available from: http://www.pubmedcentral.nih.gov/articlerender.fcgi?artid=4166321&tool=pmcentrez&rendertype=abstract

148. Litchfield DW, Shilton BH, Brandl CJ, Gyenis L. Pin1: Intimate involvement with the regulatory protein kinase networks in the global phosphorylation landscape. Biochim Biophys Acta - Gen Subj. 2015;1850(10):2077–86.

149. Ducommun S, Deak M, Sumpton D, Ford RJ, Núñez Galindo A, Kussmann M, et al. Motif affinity and mass spectrometry proteomic approach for the discovery of cellular AMPK targets: Identification of mitochondrial fission factor as a new AMPK substrate. Cell Signal [Internet]. 2015;27(5):978–88. Available from: http://dx.doi.org/10.1016/j.cellsig.2015.02.008

150. Romanov N, Hollenstein DM, Janschitz M, Ammerer G, Anrather D, Reiter W. Identifying protein kinase – specific effectors of the osmostress response in yeast. 2017;2435.

151. Peterson AC, Russell JD, Bailey DJ, Westphall MS, Coon JJ. Parallel Reaction Monitoring for High Resolution and High Mass Accuracy Quantitative, Targeted Proteomics. Mol Cell Proteomics [Internet]. 2012;11(11):1475–88. Available from: http://www.mcponline.org/cgi/doi/10.1074/mcp.O112.020131

152. Albeldas C, Ganief N, Calder B, Nakedi KC, Garnett S, Nel AJM, et al. Global proteome and phosphoproteome dynamics indicate novel mechanisms of vitamin C induced dormancy in Mycobacterium smegmatis. J Proteomics. 2017;

153. Saidi M, Beaudry F. Targeted high-resolution quadrupole-Orbitrap mass spectrometry analyses reveal a significant reduction of tachykinin and opioid neuropeptides level in PC1 and PC2 mutant mouse spinal cords. Neuropeptides [Internet]. 2017;(November 2016):0–1. Available from: http://linkinghub.elsevier.com/retrieve/pii/S0143417916301974

154. Osinalde N, Aloria K, Omaetxebarria MJ, Kratchmarova I. Targeted mass spectrometry: an emerging powerful approach to unblock the bottleneck in phosphoproteomics. J Chromatogr B [Internet]. 2017;1055–1056(April):29–38. Available from: http://www.sciencedirect.com/science/article/pii/S1570023217306682

155. Huang Q, Yang L, Luo J, Guo L, Wang Z, Yang X, et al. SWATH enables precise label-free quantification on proteome scale. Proteomics. 2015;15(7):1215–23.

156. Prisic S, Husson RN. Mycobacterium tuberculosis Serine/Threonine Protein Kinases. Microbiol Spectr [Internet]. 2014;2(5). Available from: http://www.pubmedcentral.nih.gov/articlerender.fcgi?artid=4242435&tool=pmcentrez&rendertype=abstract

157. Strober W. Trypan Blue Exclusion Test of Cell Viability. In: Current Protocols in Immunology [Internet]. John Wiley & Sons, Inc.; 2001. Available from: http://dx.doi.org/10.1002/0471142735.ima03bs21

158. Wessel D, Flügge UI. A method for the quantitative recovery of protein in dilute solution in the presence of detergents and lipids. Anal Biochem [Internet]. 1984 Apr [cited 2014 Nov 24];138(1):141–3. Available from: http://www.sciencedirect.com/science/article/pii/0003269784907826

159. Ramagli LS. Quantifying protein in 2-D PAGE solubilization buffers. [Internet]. Vol. 112, Methods in molecular biology (Clifton, N.J.). 1999. p. 99–103. Available from: http://www.scopus.com/inward/record.url?eid=2-s2.0-0032603137&partnerID=tZOtx3y1

160. Friedenauer S, Berlet HH. Sensitivity and variability of the Bradford protein

assay in the presence of detergents. Anal Biochem [Internet]. 1989;178(2):263–8. Available from: http://www.sciencedirect.com/science/article/pii/0003269789906362

161. Kurcinski M, Kolinski A, Kmiecik S. Mechanism of folding and binding of an intrinsically disordered protein as revealed by ab initio simulations. J Chem Theory Comput. 2014;10(6):2224–31.

162. Blaszczyk M, Kurcinski M, Kouza M, Wieteska L, Debinski A, Kolinski A, et al. Modeling of protein-peptide interactions using the CABS-dock web server for binding site search and flexible docking. Methods [Internet]. 2016;93:72–83. Available from: http://dx.doi.org/10.1016/j.ymeth.2015.07.004

163. Marrero J, Rhee KY, Schnappinger D, Pethe K, Ehrt S. Gluconeogenic carbon flow of tricarboxylic acid cycle intermediates is critical for Mycobacterium tuberculosis to establish and maintain infection. Proc Natl Acad Sci U S A [Internet]. 2010 May 25 [cited 2014 Nov 29];107(21):9819–24. Available from: http://www.pubmedcentral.nih.gov/articlerender.fcgi?artid=2906907&tool=pmcentrez&rendertype=abstract

164. McKinney JD, zu Bentrup KH, Munoz-Elias EJ, Miczak A, Chen B, Chan W-T, et al. Persistence of Mycobacterium tuberculosis in macrophages and mice requires the glyoxylate shunt enzyme isocitrate lyase. Nature [Internet]. 2000 Aug 17;406(6797):735–8. Available from: http://dx.doi.org/10.1038/35021074

165. Corper, H. J. and Cohn ML. No Title The viability and virulence of old cultures of tubercle bacilli: studies on twelve year broth cultures maintained at incubator temperatures. Am Rev Tuberc. 1933;(28):856–874.

166. Wayne LG, Hayes LG. An In Vitro Model for Sequential Study of Shiftdown of Mycobacterium tuberculosis through Two Stages of Nonreplicating Persistence. 1996;64(6):2062–9.

167. Baek S-H, Li AH, Sassetti CM. Metabolic regulation of mycobacterial growth and antibiotic sensitivity. PLoS Biol [Internet]. 2011 May [cited 2014 Nov 4];9(5):e1001065. Available from: http://www.pubmedcentral.nih.gov/articlerender.fcgi?artid=3101192&tool=pmcentrez&rendertype=abstract

168. Kieser KJ, Rubin EJ. How sisters grow apart: mycobacterial growth and division. Nat Rev Micro [Internet]. 2014 Aug;12(8):550–62. Available from: http://dx.doi.org/10.1038/nrmicro3299

169. Sassetti CM, Boyd DH, Rubin EJ. Genes required for mycobacterial growth defined by high density mutagenesis. Mol Microbiol [Internet]. 2003 Mar 25;48(1):77–84. Available from: http://doi.wiley.com/10.1046/j.1365-2958.2003.03425.x

170. Molle V, Kremer L. Division and cell envelope regulation by Ser/Thr phosphorylation: Mycobacterium shows the way. Mol Microbiol [Internet]. 2010 Mar [cited 2014 Nov 27];75(5):1064–77. Available from: http://www.ncbi.nlm.nih.gov/pubmed/20487298

171. Behr MA, Wilson MA, Gill WP, Salamon H, Schoolnik GK, Rane S, et al. Comparative Genomics of BCG Vaccines by Whole-Genome DNA Microarray. Science (80-) [Internet]. 1999 May 28;284(5419):1520 LP-1523. Available from: http://science.sciencemag.org/content/284/5419/1520.abstract

172. Calmette A, Guérin G, Nègre L BA. Prémunition des nouveaux-nés contre la tuberculose par le vaccin BCG. Ann Inst Pasteur. 1921;(40):89–133.

173. Barry CEI. Mycobacterium smegmatis: an absurd model for tuberculosis? Response from Barry III. Trends Microbiol. 2001;(9):473–474.

174. Reyrat, J-M. and Kahn D. Mycobacterium smegmatis: an absurd model for tuberculosis? Trends Microbiol. 2001;(9):472–473.

175. Danilchanka O, Pavlenok M, Niederweis M. Role of Porins for Uptake of Antibiotics by Mycobacterium smegmatis . Antimicrob Agents Chemother [Internet]. 2008 Sep 1;52(9):3127–34. Available from: http://aac.asm.org/content/52/9/3127.abstract

176. Gupta M, Sajid A, Arora G, Tandon V, Singh Y. Forkhead-associated Domain-containing Protein Rv0019c and Polyketide-associated Protein PapA5, from Substrates of Serine/Threonine Protein Kinase PknB to Interacting Proteins of Mycobacterium tuberculosis. J Biol Chem [Internet]. 2009 Dec 11;284(50):34723–34. Available from: http://www.jbc.org/content/284/50/34723.abstract

177. Wells RM, Jones CM, Xi Z, Speer A, Danilchanka O, Doornbos KS, et al.

Discovery of a Siderophore Export System Essential for Virulence of <italic>Mycobacterium tuberculosis</italic>. PLoS Pathog [Internet]. 2013 Jan 31;9(1):e1003120. Available from: http://dx.doi.org/10.1371/journal.ppat.1003120

178. Schwartz D GS. An iterative statistical approach to the identification of protein phosphorylation motifs from large-scale data sets. Nat Biotechnol. 2005;1391–1398.

179. Freschi L, Osseni M, Landry CR. Functional divergence and evolutionary turnover in mammalian phosphoproteomes. PLoS Genet [Internet]. 2014 Jan [cited 2014 Nov 29];10(1):e1004062. Available from: http://www.pubmedcentral.nih.gov/articlerender.fcgi?artid=3900387&tool=pmcentrez&rendertype=abstract

180. Gee CL, Papavinasasundaram KG, Blair SR, Baer CE, Falick AM, King DS, et al. A Phosphorylated Pseudokinase Complex Controls Cell Wall Synthesis in Mycobacteria. Sci Signal [Internet]. 2012 Jan 24;5(208):ra7-ra7. Available from: http://www.ncbi.nlm.nih.gov/pmc/articles/PMC3664666/

181. Boitel B, Ortiz-Lombardía M, Durán R, Pompeo F, Cole ST, Cerveñansky C, et al. PknB kinase activity is regulated by phosphorylation in two Thr residues and dephosphorylation by PstP, the cognate phospho-Ser/Thr phosphatase, in Mycobacterium tuberculosis. Mol Microbiol [Internet]. 2003;49(6):1493–508. Available from: http://dx.doi.org/10.1046/j.1365-2958.2003.03657.x

182. Villarino a, Duran R, Wehenkel a, Fernandez P, England P, Brodin P, et al. Proteomic identification of M. tuberculosis protein kinase substrates: PknB recruits GarA, a FHA domain-containing protein, through activation loop-mediated interactions. J Mol Biol [Internet]. 2005 Jul 29 [cited 2014 Nov 29];350(5):953–63. Available from: http://www.ncbi.nlm.nih.gov/pubmed/15978616

183. Wybenga-Groot LE, Baskin B, Ong SH, Tong J, Pawson T, Sicheri F. Structural Basis for Autoinhibition of the EphB2 Receptor Tyrosine Kinase by the Unphosphorylated Juxtamembrane Region. Cell [Internet]. 2001 Sep [cited 2014 Nov 24];106(6):745–57. Available from: http://www.sciencedirect.com/science/article/pii/S0092867401004962

184. Thakur M, Chaba R, Mondal AK, Chakraborti PK. Interdomain interaction reconstitutes the functionality of PknA, a eukaryotic type Ser/Thr kinase from Mycobacterium tuberculosis. J Biol Chem [Internet]. 2008 Mar 21 [cited 2014 Nov 29];283(12):8023–33. Available from: http://www.ncbi.nlm.nih.gov/pubmed/18199749

185. Chawla Y, Upadhyay SK, Khan S, Nagarajan SN, Forti F, Nandicoori VK. Protein Kinase B (PknB) of Mycobacterium tuberculosis is essential for growth of the pathogen in vitro as well as for survival within the host. J Biol Chem [Internet]. 2014 Apr 4; Available from: http://www.jbc.org/content/early/2014/04/04/jbc.M114.563536.abstract

186. Macek B, Gnad F, Soufi B, Kumar C, Olsen J V, Mijakovic I, et al. Phosphoproteome Analysis of E. coli Reveals Evolutionary Conservation of Bacterial Ser/Thr/Tyr Phosphorylation. Mol Cell Proteomics [Internet]. 2008 Feb 1;7(2):299–307. Available from: http://www.mcponline.org/content/7/2/299.abstract

187. Sun X, Ge F, Xiao C-L, Yin X-F, Ge R, Zhang L-H, et al. Phosphoproteomic Analysis Reveals the Multiple Roles of Phosphorylation in Pathogenic Bacterium Streptococcus pneumoniae. J Proteome Res [Internet]. 2009 Nov 8;9(1):275–82. Available from: http://dx.doi.org/10.1021/pr900612v

188. Sajid A, Arora G, Gupta M, Upadhyay S, Nandicoori VK, Singh Y. Phosphorylation of Mycobacterium tuberculosis Ser/Thr phosphatase by PknA and PknB. PLoS One [Internet]. 2011 Jan [cited 2014 Nov 23];6(3):e17871. Available from: http://www.pubmedcentral.nih.gov/articlerender.fcgi?artid=3052367&tool=pmcentrez&rendertype=abstract

189. Pullen KE, Ng H-L, Sung P-Y, Good MC, Smith SM, Alber T. An alternate conformation and a third metal in PstP/Ppp, the M. tuberculosis PP2C-Family Ser/Thr protein phosphatase. Structure [Internet]. 2004 Nov [cited 2014 Nov 29];12(11):1947–54. Available from: http://www.ncbi.nlm.nih.gov/pubmed/15530359

190. Gupta M, Sajid A, Sharma K, Ghosh S, Arora G, Singh R, et al. HupB, a Nucleoid-Associated Protein of Mycobacterium tuberculosis, Is Modified by Serine/Threonine Protein Kinases In Vivo. J Bacteriol [Internet]. 2014 Jul 15;196(14):2646–57. Available from:

http://jb.asm.org/content/196/14/2646.abstract

191. Jers C, Kobir A, Søndergaard EO, Jensen PR, Mijakovic I. <italic>Bacillus subtilis</italic> Two-Component System Sensory Kinase DegS Is Regulated by Serine Phosphorylation in Its Input Domain. PLoS One [Internet]. 2011 Feb 3;6(2):e14653. Available from: http://dx.doi.org/10.1371%2Fjournal.pone.0014653

192. Lee JJ, Kang C, Lee JH, Park KS, Jeon JH, Lee SH. Phosphorylation-dependent interaction between a serine / threonine kinase PknA and a putative cell division protein Wag31 in Mycobacterium tuberculosis. 2014;525–33.

193. Matsumoto S, Yukitake H, Furugen M, Matsuo T, Mineta T, Yamada T. Identification of a Novel DNA-Binding Protein from Mycobacterium bovis Bacillus Calmette-Guérin. Microbiol Immunol [Internet]. 1999;43(11):1027–36. Available from: http://dx.doi.org/10.1111/j.1348-0421.1999.tb01232.x

194. Lee BH, Murugasu-Oei B, Dick T. Upregulation of a histone-like protein in dormant Mycobacterium smegmatis. Mol Gen Genet MGG [Internet]. 1998;260(5):475–9. Available from: http://dx.doi.org/10.1007/s004380050919

195. Katsube T, Matsumoto S, Takatsuka M, Okuyama M, Ozeki Y, Naito M, et al. Control of Cell Wall Assembly by a Histone-Like Protein in Mycobacteria . J Bacteriol [Internet]. 2007 Nov 14;189(22):8241–9. Available from: http://www.ncbi.nlm.nih.gov/pmc/articles/PMC2168677/

196. Cousin C, Derouiche A, Shi L, Pagot Y, Poncet S, Mijakovic I. Protein-serine/threonine/tyrosine kinases in bacterial signaling and regulation. FEMS Microbiol Lett. 2013;346(1):11–9.

197. Pérez J, Castañeda-García A, Jenke-Kodama H, Müller R, Muñoz-Dorado J. Eukaryotic-like protein kinases in the prokaryotes and the myxobacterial kinome. Proc Natl Acad Sci U S A [Internet]. 2008 Oct 14 [cited 2017 Mar 8];105(41):15950–5. Available from: http://www.ncbi.nlm.nih.gov/pubmed/18836084

198. Gopalaswamy R, Narayanan S, Chen B, Jacobs WR, Av-Gay Y. The serine/threonine protein kinase PknI controls the growth of Mycobacterium tuberculosis upon infection. FEMS Microbiol Lett. 2009;295(1):23–9.

199. Gómez-Velasco A, Bach H, Rana AK, Cox LR, Bhatt A, Besra GS, et al. Disruption of the serine/threonine protein kinase H affects phthiocerol dimycocerosates synthesis in Mycobacterium tuberculosis. Microbiol (United Kingdom). 2013;159(4):726–36.

200. Nguyen L, Walburger A, Houben E, Koul A, Muller S, Morbitzer M, et al. Role of Protein Kinase G in Growth and Glutamine Metabolism of Mycobacterium bovis BCG. 2005;187(16):5852–6.

201. Khan MZ, Bhaskar A, Upadhyay S, Kumari P, Rajmani RS, Jain P, et al. Protein Kinase G confers survival advantage to Mycobacterium tuberculosis during latency like conditions. J Biol Chem [Internet]. 2017;jbc.M117.797563. Available from: http://www.jbc.org/lookup/doi/10.1074/jbc.M117.797563

202. Mueller P, Pieters J. Identification of mycobacterial GarA as a substrate of protein kinase G from M. tuberculosis using a KESTREL-based proteome wide approach. J Microbiol Methods [Internet]. 2017; Available from: http://linkinghub.elsevier.com/retrieve/pii/S0167701217300519

203. Nakedi KC, Nel AJM, Garnett S, Blackburn JM, Soares NC. Comparative Ser/Thr/Tyr phosphoproteomics between two mycobacterial species: The fast growing Mycobacterium smegmatis and the slow growing Mycobacterium bovis BCG. Front Microbiol. 2015;6(APR).

204. England P, Wehenkel A, Martins S, Hoos S, André-Leroux G, Villarino A, et al. The FHA-containing protein GarA acts as a phosphorylation-dependent molecular switch in mycobacterial signaling. FEBS Lett [Internet]. 2009 Jan 22;583(2):301–7. Available from: http://dx.doi.org/10.1016/j.febslet.2008.12.036

205. Baer CE, Iavarone AT, Alber T, Sassetti CM. Biochemical and spatial coincidence in the provisional Ser/Thr protein kinase interaction network of Mycobacterium tuberculosis. J Biol Chem. 2014;289(30):20422–33.

206. Margenat M, Labandera A-M, Gil M, Carrion F, Purificação M, Razzera G, et al. New potential eukaryotic substrates of the mycobacterial protein tyrosine phosphatase PtpA: hints of a bacterial modulation of macrophage bioenergetics state. Sci Rep. 2015;5.

207. Plocinska R, Martinez L, Gorla P, Pandeeti E, Sarva K, Blaszczyk E, et al.

Mycobacterium tuberculosis MtrB sensor kinase interactions with FtsI and Wag31 proteins reveal a role for MtrB distinct from that regulating MtrA activities. J Bacteriol. 2014;196(23).

208. Chao JD, Papavinasasundaram KG, Zheng X, Chávez-Steenbock A, Wang X, Lee GQ, et al. Convergence of Ser/Thr and two-component signaling to coordinate expression of the dormancy regulon in Mycobacterium tuberculosis. J Biol Chem. 2010;285(38):29239–46.

209. Sassetti CM, Boyd DH, Rubin EJ. Genes required for mycobacterial growth defined by high density mutagenesis. Mol Microbiol [Internet]. 2003 Apr 1;48(1):77–84. Available from: http://dx.doi.org/10.1046/j.1365-2958.2003.03425.x

210. Berwick DC, Tavaré JM. Identifying protein kinase substrates: Hunting for the organ-grinder's monkeys. Trends Biochem Sci. 2004;29(5):227–32.

211. Mayya V, Rezual K, Wu L, Fong MB, Han DK. Absolute Quantification of Multisite Phosphorylation by Selective Reaction Monitoring Mass Spectrometry. Mol Cell Proteomics [Internet]. 2006;5(6):1146–57. Available from: http://www.ncbi.nlm.nih.gov/pubmed/16546994

212. Vogel WK, Gafken PR, Leid M, Filtz TM. Kinetic analysis of BCL11B multisite phosphorylation-dephosphorylation and coupled sumoylation in primary thymocytes by multiple reaction monitoring mass spectroscopy. J Proteome Res. 2014;13(12):5860–8.

213. Whiteaker JR, Zhao L, Yan P, Ivey RG, Voytovich UJ, Moore HD, et al. Peptide Immunoaffinity Enrichment and Targeted Mass Spectrometry Enables Multiplex, Quantitative Pharmacodynamic Studies of Phospho-Signaling. Mol Cell Proteomics [Internet]. 2015;14(8):2261–73. Available from: http://www.mcponline.org/lookup/doi/10.1074/mcp.O115.050351

214. Kennedy JJ, Yan P, Zhao L, Ivey RG, Voytovich UJ, Moore HD, et al. Immobilized Metal Affinity Chromatography Coupled to Multiple Reaction Monitoring Enables Reproducible Quantification of Phospho-signaling. Mol Cell Proteomics [Internet]. 2016;15(2):726–39. Available from: http://www.mcponline.org/lookup/doi/10.1074/mcp.O115.054940%5Cnhttp://www.ncbi.nlm.nih.gov/pubmed/26621847%5Cnhttp://www.pubmedcentral.nih.gov/articlerender.fcgi?artid=PMC4739685

215. Shi T, Gao Y, Gaffrey MJ, Nicora CD, Fillmore TL, Chrisler WB, et al. Sensitive targeted quantification of ERK phosphorylation dynamics and stoichiometry in human cells without affinity enrichment. Anal Chem. 2015;87(2):1103–10.

216. Lee S, Lin X, Nam NH, Parang K, Sun G. Determination of the substrate-docking site of protein tyrosine kinase C-terminal Src kinase. Proc Natl Acad Sci U S A [Internet]. 2003;100(25):14707–12. Available from: http://www.pubmedcentral.nih.gov/articlerender.fcgi?artid=299771&tool=pmcentrez&rendertype=abstract

217. Page R, Peti W. Toxin-antitoxin systems in bacterial growth arrest and persistence. Nat Chem Biol [Internet]. 2016 Apr;12(4):208–14. Available from: http://dx.doi.org/10.1038/nchembio.2044

218. Sala A, Bordes P, Genevaux P. Multiple toxin-antitoxin systems in Mycobacterium tuberculosis. Toxins (Basel). 2014;6(3):1002–20.

219. Stamm CE, Collins AC, Shiloh MU. Sensing of Mycobacterium tuberculosis and consequences to both host and bacillus. Immunol Rev. 2015;264(1):204–19.

220. O'Garra A, Redford PS, McNab FW, Bloom CI, Wilkinson RJ, Berry MPR. The immune response in tuberculosis. [Internet]. Vol. 31, Annual review of immunology. 2013. 475-527 p. Available from: http://dx.doi.org/10.1146/annurev-immunol-032712-095939%5Cnhttp://www.annualreviews.org/doi/pdf/10.1146/annurev-immunol-032712-095939%5Cnhttp://www.ncbi.nlm.nih.gov/pubmed/23516984

221. Via LE, Deretic D, Ulmer RJ, Hibler NS, Huber LA, Deretic V. Arrest of Mycobacterial Phagosome Maturation Is Caused by a Block in Vesicle Fusion between Stages Controlled by rab5 and rab7. J Biol Chem [Internet]. 1997 May 16;272(20):13326–31. Available from: http://www.jbc.org/content/272/20/13326.abstract

222. Clemens DL, Lee B-Y, Horwitz MA. Deviant Expression of Rab5 on Phagosomes Containing the Intracellular Pathogens Mycobacterium tuberculosis andLegionella pneumophila Is Associated with Altered Phagosomal Fate. Infect Immun [Internet]. 2000 May 1;68(5):2671–84.

Available from: http://iai.asm.org/content/68/5/2671.abstract

223. Nathan C, Shiloh MU. Reactive oxygen and nitrogen intermediates in the relationship between mammalian hosts and microbial pathogens. Pnas. 2000;97(16):8841–8.

224. Russell DG, Mwandumba HC, Rhoades EE. Mycobacterium and the coat of many lipids. J Cell Biol [Internet]. 2002 Aug 5;158(3):421 LP-426. Available from: http://jcb.rupress.org/content/158/3/421.abstract

225. Sturgill-Koszycki S, Schlesinger PH, Chakraborty P, Haddix PL, Collins HL, Fok AK, et al. Lack of acidification in Mycobacterium phagosomes produced by exclusion of the vesicular proton-ATPase. Science (80-) [Internet]. 1994 Feb 4;263(5147):678 LP-681. Available from: http://science.sciencemag.org/content/263/5147/678.abstract

226. Russell DG. The ins and outs of the Mycobacterium tuberculosis-containing vacuole. Cell Microbiol. 2016;18(8):1065–9.

227. Szklarczyk D, Franceschini A, Wyder S, Forslund K, Heller D, Huerta-Cepas J, et al. STRING v10: protein–protein interaction networks, integrated over the tree of life. Nucleic Acids Res [Internet]. 2015 Jan 28;43(D1):D447–52. Available from: http://dx.doi.org/10.1093/nar/gku1003

228. Guérin I, De Chastellier C. Pathogenic mycobacteria disrupt the macrophage actin filament network. Infect Immun. 2000;68(5):2655–62.

229. Small JV, Stradal T, Vignal E, Rottner K. The lamellipodium: Where motility begins. Trends Cell Biol. 2002;12(3):112–20.

230. Pollard TD, Borisy GG. Cellular motility driven by assembly and disassembly of actin filaments. Cell. 2003;112(4):453–65.

231. Liebl D, Griffiths G. Transient assembly of F-actin by phagosomes delays phagosome fusion with lysosomes in cargo-overloaded macrophages. J Cell Sci [Internet]. 2009;122(16):2935–45. Available from: http://jcs.biologists.org/cgi/doi/10.1242/jcs.048355

232. Aspenström P. The Rho GTPases Have Multiple Effects on the Actin Cytoskeleton. Exp Cell Res [Internet]. 1999;246(1):20–5. Available from: http://www.sciencedirect.com/science/article/pii/S0014482798943002

233. Aspenström P. Effectors for the Rho GTPases. Curr Opin Cell Biol [Internet]. 1999;11(1):95–102. Available from: http://www.sciencedirect.com/science/article/pii/S0955067499800118

234. Jaffe AB, Hall A. RHO GTPASES: Biochemistry and Biology. Annu Rev Cell Dev Biol [Internet]. 2005;21(1):247–69. Available from: http://www.annualreviews.org/doi/10.1146/annurev.cellbio.21.020604.150721

235. Aguilera M, Salinas R, Rosales E, Carminati S, Colombo MI, Berón W. Actin dynamics and Rho GTPases regulate the size and formation of parasitophorous vacuoles containing Coxiella burnetii. Infect Immun. 2009;77(10):4609–20.

236. BISHOP AL, HALL A. Rho GTPases and their effector proteins. Biochem J [Internet]. 2000 Jun 1;348(2):241 LP-255. Available from: http://www.biochemj.org/content/348/2/241.abstract

237. Schmidt A, Hall A. Guanine nucleotide exchange factors for Rho GTPases : turning on the switch. Gene Expr Patterns. 2002;16:1587–609.

238. Dovas A, Couchman JR. RhoGDI: multiple functions in the regulation of Rho family GTPase activities. Biochem J [Internet]. 2005;390(1):1–9. Available from: http://biochemj.org/lookup/doi/10.1042/BJ20050104

239. Rivero F, Illenberger D, Somesh BP, Dislich H, Adam N, Meyer A. Defects in cytokinesis, actin reorganization and the contractile vacuole in cells deficient in RhoGDI. EMBO J [Internet]. 2002 Sep 2;21(17):4539 LP-4549. Available from: http://emboj.embopress.org/content/21/17/4539.abstract

240. Leffers H, Nielsen MS, Andersen AH, Honoré B, Madsen P, Vandekerckhove J, et al. Identification of Two Human Rho GDP Dissociation Inhibitor Proteins Whose Overexpression Leads to Disruption of the Actin Cytoskeleton. Exp Cell Res [Internet]. 1993;209(2):165–74. Available from: http://www.sciencedirect.com/science/article/pii/S001448278371298X

241. Maeda M, Hasegawa H, Hyodo T, Ito S, Asano E, Yuang H, et al. ARHGAP18, a GTPase-activating protein for RhoA, controls cell shape, spreading, and motility. Mol Biol Cell [Internet]. 2011;22(20):3840–52. Available from: http://www.molbiolcell.org/cgi/doi/10.1091/mbc.E11-04-0364

242. Yeung CYC, Taylor SH, Garva R, Holmes DF, Zeef LA, Soininen R, et al. Arhgap28 is a rhoGAP that inactivates rhoA and downregulates stress fibers. PLoS One. 2014;9(9).

243. Prakash SK, Paylor R, Jenna S, Lamarche-Vane N, Armstrong DL, Xu B, et al. Functional analysis of ARHGAP6, a novel GTPase-activating protein for RhoA. Hum Mol Gen. 2000;9(4):477–88.

244. Lin Q, Fuji RN, Wannian Yang RAC. RhoGDI Is Required for Cdc42-Mediated Cellular Transformation. Curr Biol. 2003;13(2):1469–79.

245. Gee HY, Saisawat P, Ashraf S, Hurd TW, Vega-Warner V, Fang H, et al. ARHGDIA mutations cause nephrotic syndrome via defective RHO GTPase signaling. J Clin Invest. 2013;123(8):3243–53.

246. Gupta IR, Baldwin C, Auguste D, Ha KCH, El Andalousi J, Fahiminiya S, et al. ARHGDIA: A novel gene implicated in nephrotic syndrome. J Med Genet. 2013;50(5):330–8.

247. Joberty R, Perlungher RR, Macara IANG. The Borgs , a New Family of Cdc42 and TC10 GTPase-Interacting Proteins Downloaded from http://mcb.asm.org/ on March 10 , 2018 by UNIV OF CAPE TOWN LIBRARIES ELECTR JNLS ONLY. 1999;19(10):6585–97.

248. Farrugia AJ, Calvo F. The Borg family of Cdc42 effector proteins Cdc42EP1-5. Biochem Soc Trans [Internet]. 2016;44(6):1709–16. Available from: http://biochemsoctrans.org/cgi/doi/10.1042/BST20160219

249. Zhao X, Rotenberg SA. Phosphorylation of Cdc42 effector protein-4 (CEP4) by protein kinase C promotes motility of human breast cells. J Biol Chem. 2014;289(37):25844–54.

250. Patel NR, Bole M, Chen C, Hardin CC, Kho AT, Mih J, et al. Cell Elasticity Determines Macrophage Function. PLoS One. 2012;7(9):1–10.

251. Gaidano G, Bergui L, Schena M, Gaboli M, Cremona O, Marchisio PC, et al. Integrin distribution and cytoskeleton organization in normal and malignant monocytes. Leukemia [Internet]. 1990;4(10):682–7. Available from: http://europepmc.org/abstract/MED/1976870

252. Kim AS, Kakalis LT, Abdul-Manan N, Liu GA, Rosen MK. Autoinhibition and activation mechanisms of the Wiskott-Aldrich syndrome protein. Nature.

2000;404(6774):151–8.

253. Blundell MP, Bouma G, Metelo J, Worth A, Calle Y, Cowell L a, et al. Phosphorylation of WASp is a key regulator of activity and stability in vivo. Proc Natl Acad Sci U S A. 2009;106(37):15738–43.

254. Aplin a E, Howe a, Alahari SK, Juliano RL. Signal transduction and signal modulation by cell adhesion receptors: the role of integrins, cadherins, immunoglobulin-cell adhesion molecules, and selectins. Pharmacol Rev. 1998;50(2):197–263.

255. Steinberg F, Heesom KJ, Bass MD, Cullen PJ. SNX17 protects integrins from degradation by sorting between lysosomal and recycling pathways. J Cell Biol. 2012;197(2):219–30.

256. Cullen PJ. Endosomal sorting and signalling: an emerging role for sorting nexins. Nat Rev Mol Cell Biol [Internet]. 2008 Jun 4;9:574. Available from: http://dx.doi.org/10.1038/nrm2427

257. Böttcher RT, Stremmel C, Meves A, Meyer H, Widmaier M, Tseng H-Y, et al. Sorting nexin 17 prevents lysosomal degradation of β1 integrins by binding to the β1-integrin tail. Nat Cell Biol [Internet]. 2012 May 6;14:584. Available from: http://dx.doi.org/10.1038/ncb2501

258. Ghai R, Bugarcic A, Liu H, Norwood SJ, Skeldal S, Coulson EJ, et al. Structural basis for endosomal trafficking of diverse transmembrane cargos by PX-FERM proteins. Proc Natl Acad Sci U S A [Internet]. 2013 Feb 19;110(8):E643–52. Available from: http://www.ncbi.nlm.nih.gov/pmc/articles/PMC3581954/

259. Teasdale RD, Collins BM. Insights into the PX (phox-homology) domain and SNX (sorting nexin) protein families: structures, functions and roles in disease. Biochem J [Internet]. 2012 Jan 1;441(1):39 LP-59. Available from: http://www.biochemj.org/content/441/1/39.abstract

260. Czubayko M, Knauth P, Schlüter T, Florian V, Bohnensack R. Sorting nexin 17, a non-self-assembling and a PtdIns(3)P high class affinity protein, interacts with the cerebral cavernous malformation related protein KRIT1. Vol. 345, Biochemical and Biophysical Research Communications. 2006. 1264-1272 p.

261. Levin R, Grinstein S, Schlam D. Phosphoinositides in phagocytosis and macropinocytosis. Biochim Biophys Acta - Mol Cell Biol Lipids [Internet]. 2015;1851(6):805–23. Available from: http://dx.doi.org/10.1016/j.bbalip.2014.09.005

262. Simonsen A, Wurmser AE, Emr SD, Stenmark H. The role of phosphoinositides in membrane transport. Curr Opin Cell Biol. 2001;13(4):485–92.

263. Posor Y, Eichhorn-Grünig M, Haucke V. Phosphoinositides in endocytosis. Biochim Biophys Acta - Mol Cell Biol Lipids [Internet]. 2015;1851(6):794–804. Available from: http://dx.doi.org/10.1016/j.bbalip.2014.09.014

264. Mayinger P. Phosphoinositides and vesicular membrane traffic. Biochim Biophys Acta - Mol Cell Biol Lipids. 2012;1821(8):1104–13.

265. Araki N, Johnson MT, Swanson JA. A Role for Phosphoinositide 3-Kinase in the Completion of and Phagocytosis by Macrophages Macropinocytosis. J Cell Biol. 2012;135(5):1249–60.

266. Ghai R, Mobli M, Norwood SJ, Bugarcic A, Teasdale RD, King GF, et al. Phox homology band 4.1/ezrin/radixin/moesin-like proteins function as molecular scaffolds that interact with cargo receptors and Ras GTPases. Proc Natl Acad Sci [Internet]. 2011;108(19):7763–8. Available from: http://www.pnas.org/cgi/doi/10.1073/pnas.1017110108

267. Lo SH, Janmey PA, Hartwig JH, Chen LB. Interactions of tensin with actin and identification of its three distinct actin-binding domains. J Cell Biol [Internet]. 1994 Jun 1;125(5):1067 LP-1075. Available from: http://jcb.rupress.org/content/125/5/1067.abstract

268. Lo SH. Tensin. Int J Biochem Cell Biol. 2004;36(1):31–4.

269. Mouneimne G, Brugge JS. Tensins: A New Switch in Cell Migration. Dev Cell. 2007;13(3):317–9.

270. Popowicz GM, Schleicher M, Noegel AA, Holak TA. Filamins: promiscuous organizers of the cytoskeleton. Trends Biochem Sci. 2006;31(7):411–9.

271. Nakamura F, Stossel TP, Hartwig JH. The filamins: Organizers of cell structure and function. Cell Adhes Migr. 2011;5(2):160–9.

272. Stossel TP, Condeelis J, Cooley L, Hartwig JH, Noegel A, Schleicher M, et al.

Filamins as integrators of cell mechanics and signalling. Nat Rev Mol Cell Biol [Internet]. 2001 Feb 1;2:138. Available from: http://dx.doi.org/10.1038/35052082

273. Ciobanasu C, Faivre B, Le Clainche C. Integrating actin dynamics, mechanotransduction and integrin activation: The multiple functions of actin binding proteins in focal adhesions. Eur J Cell Biol [Internet]. 2013;92(10–11):339–48. Available from: http://dx.doi.org/10.1016/j.ejcb.2013.10.009

274. Kiema T, Lad Y, Jiang P, Oxley CL, Baldassarre M, Wegener KL, et al. The molecular basis of filamin binding to integrins and competition with talin. Mol Cell. 2006;21(3):337–47.

275. Ehrlicher AJ, Nakamura F, Hartwig JH, Weitz DA, Stossel TP. Mechanical strain in actin networks regulates FilGAP and integrin binding to filamin A. Nature [Internet]. 2011 Sep 18;478:260. Available from: http://dx.doi.org/10.1038/nature10430

276. Feng Y, Walsh CA. The many faces of filamin: A versatile molecular scaffold for cell motility and signalling. Nat Cell Biol. 2004;6(11):1034–8.

277. Bray D, Whe JG. D. bray. 1988;282(February).

278. Morone N, Fujiwara T, Murase K, Kasai RS, Ike H, Yuasa S, et al. Three-dimensional reconstruction of the membrane skeleton at the plasma membrane interface by electron tomography. J Cell Biol [Internet]. 2006 Sep 11;174(6):851–62. Available from: http://www.ncbi.nlm.nih.gov/pmc/articles/PMC2064339/

279. Svitkina TM, Verkhovsky AB, McQuade KM, Borisy GG. Analysis of the Actin–Myosin II System in Fish Epidermal Keratocytes: Mechanism of Cell Body Translocation . J Cell Biol [Internet]. 1997 Oct 20;139(2):397–415. Available from: http://www.ncbi.nlm.nih.gov/pmc/articles/PMC2139803/

280. Winklbauer R. Cell adhesion strength from cortical tension - an integration of concepts. J Cell Sci [Internet]. 2015;128(20):3687–93. Available from: http://jcs.biologists.org/cgi/doi/10.1242/jcs.174623

281. Ohashi T, Kiehart DP, Erickson HP. Dual labeling of the fibronectin matrix and actin cytoskeleton with green fluorescent protein variants. J Cell Sci.

2002;115(Pt 6):1221–9.

282. Porazinski S, Wang H, Asaoka Y, Behrndt M, Miyamoto T, Morita H, et al. YAP is essential for tissue tension to ensure vertebrate 3D body shape. Nature. 2015;521(7551):217–21.

283. Linder S, Hüfner K, Wintergerst U, Aepfelbacher M. Microtubule-dependent formation of podosomal adhesion structures in primary human macrophages. J Cell Sci [Internet]. 2000;113 Pt 23:4165–76. Available from: http://www.ncbi.nlm.nih.gov/pubmed/11069762

284. Galjart N, Perez F. A plus-end raft to control microtubule dynamics and function. Curr Opin Cell Biol. 2003;15(1):48–53.

285. Pierre P, Scheel J, Rickard JE, Kreis TE. CLIP-170 links endocytic vesicles to microtubules. Cell [Internet]. 1992;70(6):887–900. Available from: http://www.sciencedirect.com/science/article/pii/009286749290240D

286. Perez F, Diamantopoulos GS, Stalder R, Kreis TE. CLIP-170 highlights growing microtubule ends in vivo. Cell. 1999;96(4):517–27.

287. Diamantopoulos GS, Perez F, Goodson H V., Batelier G, Melki R, Kreis TE, et al. Dynamic localization of CLIP-170 to microtubule plus ends is coupled to microtubule assembly. J Cell Biol. 1999;144(1):99–112.

288. Rickard JE, Kreis TE. Binding of pp170 to microtubules is regulated by phosphorylation. J Biol Chem. 1991;266(26):17597–605.

289. Choi JH, Bertram PG, Drenan R, Carvalho J, Zhou HH, Zheng XFS. The FKBP12-rapamycin-associated protein (FRAP) is a CLIP-170 kinase. EMBO Rep. 2002;3(10):988–94.

290. Li H, Liu XS, Yang X, Wang Y, Wang Y, Turner JR, et al. Phosphorylation of CLIP-170 by Plk1 and CK2 promotes timely formation of kinetochore–microtubule attachments. EMBO J [Internet]. 2010 Sep 1;29(17):2953 LP-2965. Available from: http://emboj.embopress.org/content/29/17/2953.abstract

291. Brunner D, Nurse P. CLIP170-like tip1p spatially organizes microtubular dynamics in fission yeast. Cell. 2000;102(5):695–704.

292. Maia ARR, Garcia Z, Kabeche L, Barisic M, Maffini S, Macedo-Ribeiro S, et al. Cdk1 and Plk1 mediate a CLASP2 phospho-switch that stabilizes

kinetochore-microtubule attachments. J Cell Biol. 2012;199(2):285–301.

293. Sur S, Agrawal DK. Phosphatases and Kinases Regulating CDC25 Activity in the Cell Cycle: Clinical Implications of CDC25 Overexpression and Potential Treatment Strategies. Mol Cell Biochem [Internet]. 2016 May 2;416(1–2):33–46. Available from: http://www.ncbi.nlm.nih.gov/pmc/articles/PMC4862931/

294. Ham H, Huynh W, Schoon RA, Vale RD, Billadeau DD. HkRP3 is a Microtubule-Binding Protein Regulating Lytic Granule Clustering and NK Cell Killing. J Immunol [Internet]. 2015 Apr 15;194(8):3984–96. Available from: http://www.ncbi.nlm.nih.gov/pmc/articles/PMC4390494/

295. Cote J-F. Identification of an evolutionarily conserved superfamily of DOCK180-related proteins with guanine nucleotide exchange activity. J Cell Sci [Internet]. 2002;115(24):4901–13. Available from: http://jcs.biologists.org/cgi/doi/10.1242/jcs.00219

296. Shiraishi A, Uruno T, Sanematsu F, Ushijima M, Sakata D, Hara T, et al. DOCK8 protein regulates macrophage migration through Cdc42 protein activation and LRAP35a protein interaction. J Biol Chem. 2017;292(6):2191–202.

297. Mizesko MC, Banerjee PP, Monaco-Shawver L, Mace EM, Bernal WE, Sawalle-Belohradsky J, et al. Defective actin accumulation impairs human natural killer cell function in patients with dedicator of cytokinesis 8 deficiency. J Allergy Clin Immunol. 2013;131(3):840–8.

298. Ham H, Guerrier S, Kim J, Schoon RA, Anderson EL, Hamann MJ, et al. Dedicator of Cytokinesis 8 Interacts with Talin and Wiskott-Aldrich Syndrome Protein To Regulate NK Cell Cytotoxicity. J Immunol [Internet]. 2013;190(7):3661–9. Available from: http://www.jimmunol.org/cgi/doi/10.4049/jimmunol.1202792

299. Harada Y, Tanaka Y, Terasawa M, Pieczyk M, Habiro K, Katakai T, et al. DOCK8 is a Cdc42 activator critical for interstitial dendritic cell migration during immune responses. Blood. 2012;119(19):4451–61.

300. Mostowy S, Cossart P. Septins: The fourth component of the cytoskeleton. Nat Rev Mol Cell Biol [Internet]. 2012;13(3):183–94. Available from: http://dx.doi.org/10.1038/nrm3284

301. Kinoshita M, Noda M. Roles of septins in the mammalian cytokinesis machinery. Cell Struct Funct. 2001;26(6):667–70.

302. Low C, Macara IG. Structural analysis of septin 2, 6, and 7 complexes. J Biol Chem. 2006;281(41):30697–706.

303. Nagata KI, Asano T, Nozawa Y, Inagaki M. Biochemical and cell biological analyses of a mammalian septin complex, Sept7/9b/11. J Biol Chem. 2004;279(53):55895–904.

304. Hong W. SNAREs and traffic. Biochim Biophys Acta - Mol Cell Res [Internet]. 2005;1744(2):120–44. Available from: http://www.sciencedirect.com/science/article/pii/S0167488905000571

305. Jahn R, Scheller RH. SNAREs — engines for membrane fusion. Nat Rev Mol Cell Biol [Internet]. 2006 Aug 16;7:631. Available from: http://dx.doi.org/10.1038/nrm2002

306. Stow JL, Manderson AP, Murray RZ. SNAREing immunity: the role of SNAREs in the immune system. Nat Rev Immunol [Internet]. 2006 Dec 1;6:919. Available from: http://dx.doi.org/10.1038/nri1980

307. Pfeffer SR. TRANSPORT VESICLE DOCKING: SNAREs and Associates. Annu Rev Cell Dev Biol [Internet]. 1996;12(1):441–61. Available from: http://www.annualreviews.org/doi/10.1146/annurev.cellbio.12.1.441

308. Söllner T, Bennett MK, Whiteheart SW, Scheller RH, Rothman JE. A protein assembly-disassembly pathway in vitro that may correspond to sequential steps of synaptic vesicle docking, activation, and fusion. Cell [Internet]. 2018 Mar 19;75(3):409–18. Available from: http://dx.doi.org/10.1016/0092-8674(93)90376-2

309. Veale KJ, Offenhäuser C, Lei N, Stanley AC, Stow JL, Murray RZ. VAMP3 regulates podosome organisation in macrophages and together with Stx4/SNAP23 mediates adhesion, cell spreading and persistent migration. Exp Cell Res [Internet]. 2011;317(13):1817–29. Available from: http://dx.doi.org/10.1016/j.yexcr.2011.04.016

310. Kondo H, Rabouille C, Newman R, Levine TP, Pappin D, Freemont P, et al. p47 is a cofactor for p97-mediated membrane fusion. Nature [Internet]. 1997 Jul 3;388:75. Available from: http://dx.doi.org/10.1038/40411

311. Pawson T, Gish GD. SH2 and SH3 domains: From structure to function. Cell [Internet]. 2018 Feb 21;71(3):359–62. Available from: http://dx.doi.org/10.1016/0092-8674(92)90504-6

312. Rhee I, Davidson D, Souza CM, Vacher J, Veillette A. Macrophage Fusion Is Controlled by the Cytoplasmic Protein Tyrosine Phosphatase PTP-PEST/PTPN12. Mol Cell Biol [Internet]. 2013;33(12):2458–69. Available from: http://mcb.asm.org/cgi/doi/10.1128/MCB.00197-13

313. Rhee I, Zhong M-C, Reizis B, Cheong C, Veillette A. Control of Dendritic Cell Migration, T Cell-Dependent Immunity, and Autoimmunity by Protein Tyrosine Phosphatase PTPN12 Expressed in Dendritic Cells. Mol Cell Biol [Internet]. 2014;34(5):888–99. Available from: http://mcb.asm.org/lookup/doi/10.1128/MCB.01369-13

314. Lyons PD, Dunty JM, Schaefer EM, Schaller MD. Inhibition of the Catalytic Activity of Cell Adhesion Kinase β by Protein-tyrosine Phosphatase-PEST-mediated Dephosphorylation. J Biol Chem. 2001;276(26):24422–31.

315. Sal-man N, Isakov N. Pathogen Hijacking of Crk Adaptor Proteins and Crk-Regulated Signal Transduction Pathways. 2014;1(3):1–3.

316. Okigaki M, Davis C, Falasca M, Harroch S, Felsenfeld DP, Sheetz MP, et al. Pyk2 regulates multiple signaling events crucial for macrophage morphology and migration. Proc Natl Acad Sci [Internet]. 2003 Sep 16;100(19):10740 LP-10745. Available from: http://www.pnas.org/content/100/19/10740.abstract

317. Zheng C, Xing Z, Bian ZC, Guo C, Akbay a, Warner L, et al. Differential regulation of Pyk2 and focal adhesion kinase (FAK). The C-terminal domain of FAK confers response to cell adhesion. J Biol Chem. 1998;273(4):2384–9.

318. Gupta R, Chakrabarti P, Dikshit M, Dash D. Late signaling in the activated platelets upregulates tyrosine phosphatase SHP1 and impairs platelet adhesive functions: Regulation by calcium and Src kinase. Biochim Biophys Acta - Mol Cell Res. 2007;1773(2):131–40.

319. SACI A, LIU W-Q, VIDAL M, GARBAY C, RENDU F, BACHELOT-LOZA C. Differential effect of the inhibition of Grb2–SH3 interactions in platelet activation induced by thrombin and by Fc receptor engagement. Biochem J [Internet]. 2002 May 1;363(3):717 LP-725. Available from:

http://www.biochemj.org/content/363/3/717.abstract

320. Roach TI, Slater SE, White LS, Zhang X, Majerus PW, Brown EJ, et al. The protein tyrosine phosphatase SHP-1 regulates integrin-mediated adhesion of macrophages. Curr Biol [Internet]. 1998;8(18):1035–8. Available from: http://www.ncbi.nlm.nih.gov/pubmed/9740804

321. Kanwal Z, Zakrzewska A, den Hertog J, Spaink HP, Schaaf MJM, Meijer AH. Deficiency in Hematopoietic Phosphatase Ptpn6/Shp1 Hyperactivates the Innate Immune System and Impairs Control of Bacterial Infections in Zebrafish Embryos. J Immunol [Internet]. 2013;190(4):1631–45. Available from: http://www.jimmunol.org/cgi/doi/10.4049/jimmunol.1200551

322. Repaske R. Lysis of gram-negative bacteria by lysozyme. Biochim Biophys Acta [Internet]. 1956 Oct [cited 2015 Feb 2];22(1):189–91. Available from: http://www.sciencedirect.com/science/article/pii/0006300256902402

8. APPENDICES

Appendix I:

Bacterial Lysis buffer:

500mM Tris-HCl,

1% (w/v) SDS,

0.15% sodium deoxycolate,

1x protease inhibitor cocktail,

1x phosphatase inhibitor cocktail (Roche, Mannheim Germany)

50µg/ml lysozyme [322].

Appendix II:

Eukaryotic freezing media:

90% FCS/10% DMSO 1 ml per vial

Appendix III:

Eukaryotic lysis buffer:

50 mM Tris-HCl pH 7.4

150 mM NaCl

1 mM EDTA,

0.1% sodium deoxycholate.

1% (w/v) SDS

1x protease inhibitor cocktail,

1x phosphatase inhibitor cocktail (Roche, Mannheim Germany)